THE EFFECTS OF MOLECULAR ENCOUNTERS ON N.M.R. CHEMICAL SHIFTS.

A thesis

presented to the University of Aston in Birmingham for the degree of Doctor of Philosophy

by

Christopher Charles Percival B.Sc.

The Department of Chemistry

University of Aston in Birmingham

February 1981

The University of Aston in Birmingham

The Effects of Molecular Encounters on Nuclear Magnetic Resonance Chemical Shifts

A thesis presented for the degree of Doctor of Philosophy

by

Christopher Charles Percival

February 1981

Following suggestions in the literature, it is shown that intermolecular van der Waals dispersion forces can be considered to be described by two mechanisms. The first is due to the reaction field on the solute via the solvent and the second is due to a localized non-continuum 'buffetting' interaction essentially between the peripheral atoms of the solute and solvent.

It is shown that there is no necessity to introduce a site-factor into reaction field equations to calculate the nuclear screening constant in ^{1}H or ^{19}F nmr. The site-factor was probably only needed previously because of the neglect of the 'buffetting' interaction.

The 'buffetting' interaction produces a nuclear screening, $\sigma_{BI} = - BKr^{-6}(2\beta - \xi)^{2}$, that for a particular nucleus in the solute molecule is governed by the screening coefficient B which is a solute parameter, the constant K which is a solvent parameter, and β_T and ξ_T which are measures of the steric accessibility of the solute atom containing the resonant nucleus to encounters by the solvent molecule.

The characterization of σ_W on the above base is tested exhaustively on ^{1}H and ^{19}F chemical shifts of appropriate systems, through the evaluation of B - values that agree satisfactorily with literature values and of K for hydrogen - hydrogen interactions that agree with the theoretically derived value. Moreover it is shown that β_T and ξ_T can be calculated on a hard atom contact basis, implicitly neglecting repulsion forces.

The extended reaction field/continuum theory and 'buffetting' theory are utilized to calculate van der Waals a-values, heats of vaporization, and vibrational and electronic spectral intensity changes in passing from the gas phase to the liquid phase. All these non-nmr problems appear to be well accounted for on the basis of the theoretical interpretation presented.

The overall consistency of the approach suggests that β_T and ξ_T can be deduced reliably from experimental data and may therefore afford a method of elucidating molecular structures.

Nuclear Magnetic Resonance
Chemical Shifts
Van der Waals Dispersion Forces
Reaction field/Continuum models
Steric Contributions to Intermolecular Chemical Shifts

ACKNOWLEDGEMENTS

I should like to thank my supervisor, Dr. J. Homer, for his help and encouragement during the course of this work.

I am also grateful to Dr. A. V. Golton for his interest, Dr. M. C. Cooke for his assistance in compiling Chapter 2, and to my colleagues in the N.M.R. laboratory for their interesting comments.

Thanks are also due to Mrs. J. Tocker for her patience and skill in typing a difficult manuscript.

Finally, I should like to thank the Department of Chemistry for provision of the facilities and the Science Research Council for their financial support during the period 1977-1980.

A Note on Units

Although it is appreciated that S.I. units should be used whenever possible, the electrostatic units used in this thesis are cgsesu units (Gaussian system)*. The reason for this is to facilitate comparison with the past literature dealing with reaction field problems, especially with regard to nmr screening. Where necessary a conversion factor to S.I. is quoted in the text. Similarly some thermodynamic parameters are quoted in non-S.I. units.

One note of caution with respect to the esu units is that a linear, square or inverse electric field may all be quoted as esu. Therefore care must be exercised when converting to the more precisely defined S.I. units.

* W. J. DUFFIN "Electricity and Magnetism", 2nd Edn., McGraw-Hill (1973).
P. VIGOUREUX "Units and Standards of Electromagnetism", Wykeham (1971).

CONTENTS

CHAPTER 1

INTRODUCTION TO NUCLEAR MAGNETIC RESONANCE SPECTROSCOPY

	Page
1.1 Introduction	1
1.2 Nuclear Energy Levels in a Magnetic Field	2
1.3 The Classical Description of Nuclear Magnetic Resonance (N.M.R.)	3
1.4 The Population of Nuclear Spin States	6
1.5 Saturation	7
1.6 Magnetic Relaxation	8
1.6a Spin-Lattice Relaxation	8
1.6b Spin-Spin Relaxation	10
1.7 N.M.R. in a Macroscopic Sample	10
1.8 Factors Affecting Line Shape	13
1.8a Magnetic Dipole Interaction	13
1.8b Spin-Lattice Relaxation	13
1.8c Spin-Spin Relaxation	14
1.8d Miscellaneous Effects	14
1.9 Nuclear Screening and the Chemical Shift	15
1.9a General Aspects of Nuclear Screening	15
1.9b Some Specific Aspects of Nuclear Screening	17
1.10 Nuclear Spin-Spin Coupling	21

CHAPTER 2

THE OBSERVATION OF HIGH RESOLUTION N.M.R. SPECTRA

2.1 Introduction	24
2.2 Fourier Transform N.M.R. Spectroscopy	25
2.3 Continuous Wave N.M.R. Spectroscopy	26
2.3a The Magnet	26
2.3b Field Stabilization - Field/Frequency Locking	28
2.3c The Magnet Field Sweep	29
2.3d The Radiofrequency Oscillator	30
2.3e The Probe and Detection Systems	31

2.4 The Facilities Used 33

2.4a The Varian Associates HA100D N.M.R. Spectrometer 33

2.4b The Perkin-Elmer R12B N.M.R. Spectrometer 36

2.5 The Accurate Measurement of Chemical Shifts 39

CHAPTER 3

A CRITICAL RECONSIDERATION OF THE VAN DER WAALS SCREENING CONSTANT

3.1 Introduction 41

3.2 London Dispersion Forces and the Van der Waals Screening Constant, σ_W 41

3.3 The Models Used to Characterize σ_W 42

3.4 An Outline of the Continuum Model 44

3.5 A Review of Past Continuum Treatments 46

3.6 A Critique of the Rummens Site Factor 47

3.7 Past Literature Observations Regarding Continuum Treatments 50

3.8 An Outline of the Proposed Extension of Continuum Theory 54

CHAPTER 4

THE APPLICATION OF REACTION FIELD THEORY TO THE REFORMULATION OF THE VAN DER WAALS NUCLEAR SCREENING CONSTANT

4.1 Introduction 57

4.2 The Reaction Field of a Polarizable Point Dipole 58

4.3 A Critique of Van der Waals Forces Characterized by Reaction Fields 60

Page

4.4 The Primary Reaction Field, R_1, and its Contribution to σ_w 62

4.5 The Extra-Cavity 'Reaction Field' of the Solvent, R_2 64

4.6 The Expression for $\langle \mu^2 \rangle$ 69

4.7 Tests of the Reaction Field Equation 71

4.7a Gas-to-Solution ^1H Chemical Shifts of the Group IVB Tetramethyls 71

4.7b Van der Waals a-Values 75

4.7c Heats of Vaporization 79

CHAPTER 5

THE EFFECTS OF STERICALLY CONTROLLED MOLECULAR ENCOUNTERS ON THE VAN DER WAALS NUCLEAR SCREENING CONSTANT

5.1 Introduction 84

5.2 Electric Formulation of σ_{BI} 86

5.3 Geometrical Formulation of β and ξ 92

5.4 An Experimental Test of "Buffetting" 95

5.5 Consideration of Solvents with Peripheral Atom other than Hydrogen. 101

5.6 A Critique of the Molecular Encounter Theory 104

CHAPTER 6

APPLICATION OF MOLECULAR ENCOUNTER THEORY TO N.M.R.

6.1 Introduction 110

6.2 Gas-to-Solution ^1H Chemical Shifts in Relatively Simple Systems 110

6.2a The B-Value of Hydrogen in Methane 110

6.2bThe Q-Values of Chlorine and Bromine 111

6.2c σ_a of Cyclohexane and Benzene 111

6.2d The B-Value of Hydrogen in the Hydrogen Molecule 112

6.2e Consideration of the Molecules $Si(OCH_3)_4$, $Si(OCH_2CH_3)_4$ and $Si(CH_2CH_3)_4$ 116

6.2f Solute Size and σ_a Using the Anomalous Solvent, $C(NO_2)_4$ 118

6.3 Gas-to-Solution ^{19}F Chemical Shifts in Selected Systems 121

6.3a General 121

6.3b B-Values of Fluorine in CF_4 SiF_4 and SF_6 122

6.3c The B-Value of Fluorine in C_6F_6 128

Page

6.4 Some ^{1}H Chemical Shifts of Spheroidal Molecules 132

6.4a ^{1}H Chemical Shift Analysis of Benzene 132

6.4b Analysis of some other Spheroidal Molecules 135

6.5 An Examination of the Linear Reaction Field 139

6.6 Solvent Effects on Diastereotopic Chemical Shifts in Sulphinyl Chlorides 141

6.7 Conclusions 146

CHAPTER 7

SOME NON-N.M.R. ASPECTS OF MOLECULAR ENCOUNTER THEORY

7.1 Van der Waals a-Values 149

7.2 Heats of Vaporization 153

7.3 An Investigation of Some Vibrational and Electronic Spectral Line Intensities 155

7.3a Basic Theory 158

7.4 Conclusions 167

REFERENCES 169

TABLES

Table No.		Page
3.1	Value of Site-Factors for the Group $\overline{\text{IVB}}$ Tetramethyl Systems (eqn. 3.14)	51
3.2	Regression Analyses of $\sigma_w(\text{EXPT})$ on $(n_2^2-1)^2/(2n_2^2+1)^2\, S_{cont}$ for the Group $\overline{\text{IVB}}$ Tetramethyl Systems.	52
4.1	Data for the Group $\overline{\text{IVB}}$ Tetramethyls.	72
4.2	Values of $\sigma_w(\text{EXPT})$ and $\langle R_T^2 \rangle$ (eqn. 4.20) for the group $\overline{\text{IVB}}$ Tetramethyl Systems.	73
4.3	Linear Regression Analyses and Significance levels of $\sigma_w(\text{EXPT})$ on $\langle R_T^2 \rangle$ for the group $\overline{\text{IVB}}$ Tetramethyl systems.	74
4.4	Van der Waals a-Values - I.	80
4.5	Heats of Vaporization - II.	82
4.6	Physical Constants of some species considered ($\simeq 30^{\circ}C$)	83
5.1	Geometrical Results for the Group $\overline{\text{IVB}}$ Tetramethyls.	97
5.2	Values of K^H/r_{HH}^6 for the Group $\overline{\text{IVB}}$ Tetramethyls	98
5.3	Measurements for 1, 3, 5-Triisopropylbenzene in various solvents.	105
6.1	σ_a values for the solvent cyclohexane.	113
6.2	σ_a values for the solvent benzene.	114
6.3	Data for the Hydrogen molecule solute.	115
6.4	Data for the solutes $Si(OCH_3)_4$, $Si(OCH_2CH_3)_4$ and $Si(CH_2CH_3)_4$	119
6.5	Data for the systems involving $C(NO_2)_4$ as the solvent.	120

Table No.		Page
6.6	Data and results for the solute CF_4.	123
6.7	Data and results for the solute SiF_4.	125
6.8	Data and results for the solute SF_6.	126
6.9	Data and Analyses for the solute C_6F_6	131
6.10	Linear regression analysis for benzene.	133
6.11	Detailed β/ξ analyses of benzene.	136
6.12	Data and results for some spheroidal solutes.	137
6.13	Nuclear screening differences and linear reaction field differences for the ^1H nuclei A and Z in molecules I and II respectively.	142
6.14	Nuclear screening differences of the alpha Gem-dimethyl groups in sulphinyl chlorides.	144
6.15	Nuclear screening differences of the alpha gem-dimethyl groups in the sulphinyl chloride $Me\text{-}\overset{O}{\overset{\|}{C}}\text{-}C(Me)(Me)SOCl$.	147
7.1	Van der Waals a-values - I.	151
7.2	Heats of Vaporization - II.	156
7.3	Some gas phase values of (A_{ρ_1}/A_{ρ_2}) for methane at various pressures in He, Ar and N_2.	160 163
7.4	Some values of A_l/A_g for Certain systems.	
7.5	A continuation of the results from table 7.4.	165

ILLUSTRATIONS

Fig. No.		Page
1.1	The Relationship between the magnetic moment, μ, and the spin angular momentum, I.	5
1.2	Vectorial Representation of the classical Larmor precession.	5
1.3	Components of the transverse Macroscopic moment.	12
1.4	The absorption line shape (v-mode) and dispersion line shape (u-mode) of NMR.	12
2.1	Block Diagram of a typical NMR spectrometer.	32
4.1	A solute cavity in the solvent continuum.	66
4.2	Cone of influence for R_2 with solute and solvent cavities imagined to be in contact.	70
5.1	Space average situation of a solvent molecule average electric moment.	88
5.2	Time average electric fields with respect to directions parallel and perpendicular to the axis of the C-H bond.	89
5.3	Two dimensional representation of a methane molecule (hydrogen H and methyl group M) encountered by an isotropic solvent molecule(s).	94
5.4	Two dimensional representation of a group $\overline{IVB}$ tetramethyl molecule (hydrogen H and rest of molecule M) encountered by an isotropic solvent molecule(s) - I.	99
5.5	Two dimensional representation of a group $\overline{IVB}$ tetramethyl molecule (hydrogen H and rest of molecule M) encountered by an isotropic solvent molecule(s) - II.	100

Fig. No.		Page
5.6	Relationship between the Hartree-Fock calculated and experimental Q-values.	107
6.1	Two dimensional representation of the hydrogen molecule.	117
6.2	Two dimensional representation of a sulphur hexafluoride molecule (fluorine F and rest of molecule SF_5) encountered by an isotropic solvent(s)	124
6.3	Two dimensional representation of a hexafluorobenzene molecule (fluorine F) encountered by an isotropic solvent molecule(s) - I.	129
6.4	Two dimensional representation of a hexafluorobenzene molecule (fluorine F) encountered by an isotropic solvent molecule(s) - II.	130
7.1	Relationship between critical and field calculated van der Waals a-values.	154
7.2	Relationship between experimental and field calculated heats of vaporization.	157
7.3	Relationship between $(A_m/A_p)_{EXPT.}$ and ρ/M for the ν_3 -band of methane.	161

CHAPTER 1

INTRODUCTION TO NUCLEAR MAGNETIC RESONANCE SPECTROSCOPY

1:1 Introduction

The idea that certain atomic nuclei possessed magnetic moments was proposed to explain the hyperfine structure observed in optical atomic spectra.[1] It is now a well accepted fact that certain nuclei have magnetic moments. Advantage is taken of this phenomenon in nuclear magnetic resonance spectroscopy. (nmr).

When situated in an applied magnetic field, nuclear magnetic moments experience a couple and tend to adopt specific orientations with respect to the applied magnetic field direction. These orientations correspond to different energy levels of the nuclei. The quantization of the nuclear energy levels is governed by the nuclear angular momentum which may be expressed in terms of integral or half-integral multiples of $\hbar$, the reduced Planck's constant, $h/2\pi$, as $\hbar\,(I\,(I+1))^{\frac{1}{2}}$. The number of energy levels available to a particular nucleus in an applied magnetic field is given by $2I + 1$, where I is the nuclear spin quantum number. I may take half-integral or integral values.

It was shown in molecular beam experiments[2,3] that the measurable values of nuclear magnetic moments are discrete, corresponding to the space quantization of the nucleus when placed in a static magnetic field. When situated in a magnetic field, B, the energy levels of a nucleus with spin quantum number I are separated by $\mu B/I$, where μ is the maximum measurable value of the nuclear magnetic moment. Having determined magnetic moments using such molecular beam experiments it was found that if the molecular beam was subjected to a second magnetic field[4] oscillating through a range of frequencies, there was a reduction in the number of molecules reaching the detector when the frequency of the

oscillating magnetic field correspond with $\mu B/Ih$, due to an absorption of energy from the second oscillating magnetic field.

The observation of an nmr signal from other than a molecular beam was first shown using paraffin wax[5] and water[6]. With the advances in instrumentation and the theory of nmr the technique is an invaluable tool in chemistry and physics[7-9]. The intention of this introductory chapter is to present the basic theory of nmr with a particular emphasis towards intermolecular nuclear screening and especially the van der Waals screening constant which is the subject of this thesis.

1:2 Nuclear Energy Levels in a Magnetic Field

As indicated in section 1:1 the maximum measurable component of the nuclear angular momentum must be an integral or half-integral multiple of $\hbar$, and the component of the angular momentum along any direction has the 2I + 1 values $\hbar I$, $\hbar(I-1)$, ... $\hbar(-I+1)$, $\hbar(-I)$. The angular momentum and magnetic moment of a nucleus behave as parallel vectors (fig. 1.1) and may be expressed in terms of one another through the equation

$$\vec{\mu} = \gamma I \vec{\hbar} \qquad 1.1$$

where γ is a proportionality constant known as the magnetogyric ratio. From equation 1.1 (and fig.1.1) the observable values of the magnetic moment may be defined by $m\mu/I$, where m may assume the values I, I-1, ...-I + 1, -I. The nuclear energy levels are degenerate in the absence of an applied magnetic field, but this degeneracy is lifted when a magnetic field is applied to give the (2I + 1) energy levels. The energy of a nucleus in a uniform magnetic field, B_o, applied in the arbitrary reference direction, z, is given by

$$E_z = E_o - \mu_z B_o(Z) \qquad 1.2$$

where E_o is the intrinsic nuclear energy in the absence of a magnetic field and μ_z is the component of μ in the z- direction (fig. 1.1) μ_z may be written as $\mu\cos\theta$ such that $\cos\theta = m/I$ and then the allowed nuclear energy levels may be given by $E_o - m\mu B_o/I$. The difference between two adjacent energy levels is therefore $\mu B_o/I$.

The selection rule governing transitions between the nuclear energy levels is $\Delta m = \pm 1$. Therefore the fundamental condition for the nuclear energy level transitions in an nmr experiment is

$$\Delta E = h\nu = \mu B_o/I \qquad 1.3$$

and from equation 1.1, the resonant frequency is

$$\nu = \gamma B_o/2\pi \qquad 1.4$$

Equation 1.4 is the basic resonance equation for a nucleus in a uniform magnetic field.

In practice magnetic field strengths of the order 1 - 6 T are used which necessitates a frequency ν of 40 - 300 MHz (radiofrequencies) for the observation of ^1H and ^{19}F nmr.

1:3 The Classical Description of Nuclear Magnetic Resonance (NMR)

The magnetic moment, μ, and the angular momentum, p, of a nucleus in an external magnetic field may be related by

$$\vec{\mu} = \gamma\vec{p} \qquad 1.5$$

The equation of motion of the nucleus is written as

$$d\vec{\mu}/dt = \gamma(\vec{\mu} \times \vec{B}_o) \qquad 1.6$$

where $(\vec{\mu} \times \vec{B}_o)$ is the vector product of the magnetic moment with the magnetic field. If μ is rotated with an angular frequency, w , the rate of change of μ may be written as

$$d\vec{\mu}/dt = \vec{w} \times \vec{\mu} \qquad 1.7$$

from which it can be seen.that the angular frequency may be represented by

$$\vec{w} = -\gamma \vec{B}_o \qquad 1.8$$

That is, the effect of the magnetic field, B_o, is to cause a precession, or motion, of the magnetic moment (nucleus), μ, about the direction of the magnetic field, B_o. For a constant magnetic field, the magnetic moment is said to precess about the magnetic field direction with a frequency termed the Larmor frequency (fig. 1.2).

For convenience a co-ordinate system may be set up that rotates with the Larmor frequency. In the absence of any other perturbing influences the magnetic moment is then stationary with respect to the precessing reference frame. When another weaker magnetic field, B_1, is applied perpendicular to the original magnetic field, B_o, such that it rotates about the B_o direction, B_1 will also rotate within the co-ordinate system (fig. 1.2). This is, of course, providing that B_1 is not rotating at the frequency of the co-ordinate system (Larmor frequency). B_1 will tend to exert an extra couple, $\vec{\mu} \times \vec{B}_1$, on the magnetic moment tending to tip it toward the plane perpendicular to B_o. If B_1 is moving within the rotating frame the couple will vary rapidly and the resultant effect will be a slight wobbling of the steady precessional motion. If, however, B_1 is rotating at the Larmor frequency, and hence is stationary with respect to the rotating frame, it will provide a constant effect on the magnetic moment which will then tend to precess about the direction of the resultant field of B_1 and B_o.

In practice it is not convenient to apply a pure rotating magnetic field, B_1. Instead a linearly oscillating one is used because this may be regarded as the superposition of two magnetic fields rotating in opposite directions; the one having

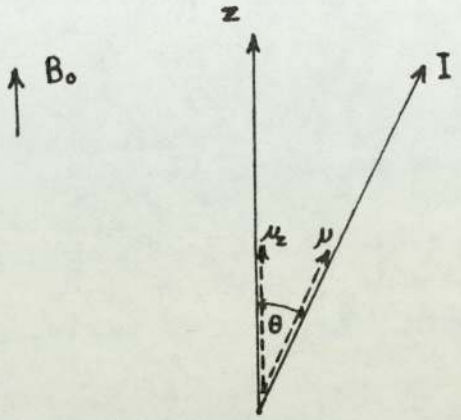

Fig. 1.1. The relationship between the magnetic moment μ and the spin angular momentum I.

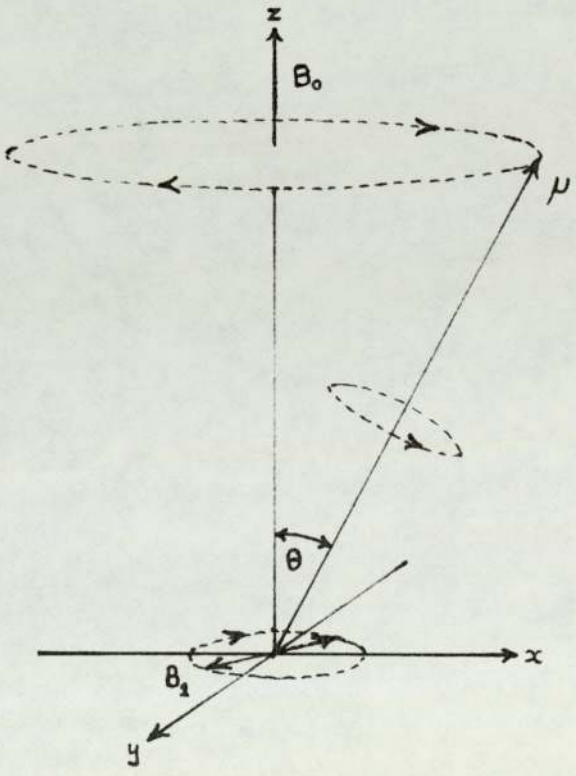

Fig. 1.2. Vectorial representation of the classical larmor precession

the correct sense with respect to the magnetic moment and applied magnetic field only having an effect.

1:4 The Population of Nuclear Spin States

The probability of absorption or stimulated emission of energy are equal, such that there is an equal probability of Δm being + 1 or - 1. In order to observe nuclear resonance signals there must be a nett change in the system governed by the distribution of nuclei between the various energy levels. For two energy levels, with N_1 and N_2 as the population numbers of the lower and upper energy levels respectively, the nett change in the system is given by

$$\Delta = P(N_1 - N_2) \qquad 1.9$$

where P is the probability of a transition occurring. In the absence of a secondary magnetic field, B_1, there will be a Boltzmann distribution of nuclei between the two energetically different nuclear levels. The probability of a nucleus occupying a particular energy level of magnetic quantum number m is given by

$$W = \frac{e^{m\mu Bo/IkT}}{2I+1} \qquad 1.10$$

or approximately, by series expansion of the exponential function,

$$W \simeq \frac{1 + m\mu Bo/IkT}{2I+1} \qquad 1.11$$

where k is Boltzmann's constant and T the absolute temperature.

Thus there is a distribution of nuclei favouring the lower energy state and for a nucleus of spin $I = \frac{1}{2}$, the probabilities of the nucleus being in the lower ($m = +\frac{1}{2}$) or upper ($m = -\frac{1}{2}$) energy level respectively are given by

$$W_1 = \tfrac{1}{2}\,(1 + \mu B/kT) \qquad 1.12a$$

$$W_2 = \tfrac{1}{2}\,(1 - \mu B/kT) \qquad 1.12b$$

From equations 1.12 a and b it is evident that the larger the magnetic field, B_o, applied to the nuclei the greater will be the excess population of nuclei in the lower energy state and the higher will be the sensitivity of the nuclear magnetic resonance experiment (equation 1.4). NMR is therefore possible because of the higher population of the lower energy levels.

In contrast to optical spectroscopy[10, 11], where a very rapid return is normally made from the excited state to the ground state after an energy absorption, the return or relaxation from the excited state to the ground state in nmr spectroscopy can take a considerable time. Also, nmr signals can weaken and disappear with increasing intensity of the magnetic field B_1, as the number of excess nuclei in the lower state tends to zero. This is a manifestation of the phenomenon of saturation.

1:5 Saturation

Continuous absorption of energy from a radiofrequency magnetic field tends to reduce the excess population in the lower energy state relative to that in the upper energy state, hence reducing the nett number of nuclei that would be available to absorb energy from the magnetic field, B_1. The reduction of the excess population in the lower energy level relative to the upper energy level will increase with the amplitude of the oscillating magnetic field and is referred to as saturation. Saturation not only reduces the overall magnitude of the signal intensity, but distorts the shape of the signal causing a broadening of the resonance line and, if the spectrum consists of several lines, non-uniform effects may occur because different relaxation rates can apply to different transitions. The condition of saturation may also produce transitions between nuclear energy levels that are nominally forbidden by the first order selection rules, with an absorption of two or more quanta of energy. These are termed multiple-quantum

transitions[12, 13].

1:6 Magnetic Relaxation

If the phenomenon of saturation was permanent, such that there is no mechanism to counter the effect, there would be severe limitations on the use of the technique of nuclear magnetic resonance experiments because a nett absorption would only be able to occur once in a given sample.

Mechanisms do exist, however, which restore the original distribution of nuclear energy levels after a resonant absorption. The removal of excess energy from an excited spin-state that allows the nucleus to return to a lower energy state is called a relaxation process. There are two principal types of relaxation processes; spin-lattice and spin-spin relaxation.

(a) Spin-Lattice Relaxation

A nuclear magnetic moment may experience rapidly fluctuating magnetic fields produced by other magnetic moments in the sample. If the motion of this nuclear magnetic moment happens to contain a frequency synchronous with the precessional frequency of a neighbouring nucleus, this nucleus will experience a magnetic field capable of inducing a transition. This field induces a stimulated emission (and absorption) of energy from the spin system in order to restore the equilibrium Boltzmann population distribution of the nuclear spins. Thus nett energy is transferred from the spin system to the surroundings. This is the mechanism of spin-lattice, or longitudinal, relaxation and is responsible for the achievement of a population distribution of nuclear spin states when the system is initially placed in a magnetic field.

The rate that a system returns to equilibrium after being perturbed is characterized by the spin-lattice relaxation time which is usually denoted by T_1. In order to study the mathematics

of the relaxation process it is convenient to define N_u and N_l as the number of nuclei in the upper and lower nuclear energy levels respectively, such that at equilibrium the excess number of nuclei in the lower energy level is:

$$N_{EX} = N_l - N_u \qquad 1.13$$

If W_1 and W_2 are the probabilities per unit time for a given nucleus to make an upward or downward transition by an interaction with the lattice around the nuclear moment, in the presence of a magnetic field, the number of upward transitions (per unit time) must at equilibrium be equal to the number of downward transitions (per unit time) as given by

$$N_l W_1 = N_u W_2 \qquad 1.14$$

The normal Boltzmann distribution for two energy states is given by

$$\frac{N_l}{N_u} = e^{2\mu Bo/kT} \simeq 1+2\mu Bo/kT \qquad 1.15$$

and thence

$$\frac{W_2}{W_1} \simeq 1+2uBo/kT \qquad 1.16$$

The rate of change of the number of excess nuclei, is given by

$$\frac{dN_{EX}}{dt} = 2N_u W_2 - 2N_l W_1 \qquad 1.17$$

where the factor of two arises from the fact that an upward transition decreases and a downward transition increases N_{EX} by two. Now,

$$\frac{dN_{EX}}{dt} = -2W\,(N_{EX} - N_{EQ}) \qquad 1.18$$

where $W = (W_1 + W_2)/2$ and $N_{EQ} = \frac{\mu Bo}{kT}\,(N_1 + N_2)$, the number of excess nuclei in the lower state at equilibirium. By integrating equation 1.18 and making the substitution $2W = 1/T_1$, it follows that

$$(N_{EX} - N_{EQ}) = (N_o - N_{EQ})\, e^{-t/T_1} \qquad 1.19$$

The rate by which the excess population reaches its equilibrium value is thus governed exponentially by T_1, the characteristic spin-lattice relaxation time.

(b) Spin-Spin Relaxation

The precessional motion of nuclear moments produce local magnetic fields at neighbouring nuclei and these fields may be thought to have oscillating and static components. A nucleus producing a magnetic field oscillating at its Larmor frequency, may induce a transition in a like neighbouring nucleus in a similar way to an applied oscillating magnetic field when used to observe resonance. This may lead to an interchange of energy between the pair of spins with the total energy of the nuclear system remaining unaltered. Thus there is no effect on the population distribution of nuclear spins.

The process is known as spin-spin relaxation and whilst it does not affect the distribution between spin-states after an energy absorption, the overall spin energy of the nuclei being unchanged, it influences the relationship between the motion of different spins. The characteristic spin-spin relaxation time is denoted by T_2.

1:7 N.M.R. in a Macroscopic Sample

So far the discussion has been based mainly on the magnetic properties of an isolated nucleus. The argument will now be developed to account for the observation of nuclear magnetic resonance in bulk samples. Bloch has treated this problem from a macroscopic viewpoint[14-16].

For an assembly of nuclei in an applied magnetic field, B_o, the various spin-states are occupied to different extents giving the sample a magnetic susceptibility. The magnetic moment per unit volume of the assembly of nuclei may be given by

$$M = \chi_o B_o \qquad 1.20$$

where χ_o is the static magnetic susceptibility of the sample. The so-called Bloch equations[14, 16], which are a set of phenomenological differential equations describing the interaction of the nuclear magnetization M with the radiofrequency magnetic field, may be written as,

$$dM_x/dt = \gamma(M_y B_o + M_z B_1 \sin\omega t) - M_x/T_2 \qquad 1.21a$$

$$dM_y/dt = \gamma(M_z B_1 \cos\omega t - M_x B_o) - M_y/T_2 \qquad 1.21b$$

$$dM_z/dt = -\gamma(M_x B_1 \sin\omega t + M_y B_1 \cos\omega t) - (M_z - M_o)/T_1 \qquad 1.21c$$

where M_x, M_y and M_z are the components of the magnetization vector $\vec{M}$ (fig. 1.3), w is the angular frequency of B_1 and t is the time. Obviously, $\vec{M}$ is analogous to $\vec{\mu}$, with the one difference that in the absence of an applied radiofrequency field $\vec{M}$ has only a z-component whereas $\vec{\mu}$ has x, y and z components.

viz. $M_z = \sum \mu_z$, $M_x = \sum \mu_x$ and $M_y = \sum \mu_y$

Assuming that resonance is passed through slowly - the slow passage approximation - the differentials with respect to time become zero, and the solutions of equations 1.21 a, b and c are

$$u = M_o \cdot \gamma B_1 T_2^2 (\omega_o - \omega) / D \qquad 1.22a$$

$$v = M_o \cdot \gamma B_1 T_2 / D \qquad 1.22b$$

$$M_z = M_o \cdot (1 + T_2^2(\omega_o - \omega)^2) / D \qquad 1.22c$$

where $D = 1 + T_2^2(\omega_o - \omega)^2 + \gamma^2 B_1 T_1 T_2$, M_o is the magnitude of the vector $\vec{M}$ in the absence of a radiofrequency magnetic field, B_1, u is the component of $\vec{M}$ that rotates in phase with B_1 and v is the component of $\vec{M}$ that rotates 90° out of phase with B_1. Depending on whether u or v is observed a dispersion or absorption curve respectively will be obtained (fig. 1.4). It should be noted that the equation for v (equation 1.22b) is almost a description of the Lorentzian curve[14, 17] which is the generally accepted absorption signal.

Mathematically the nmr signal would appear to be an infinitely sharp absorption line, but in practice absorption occurs over a

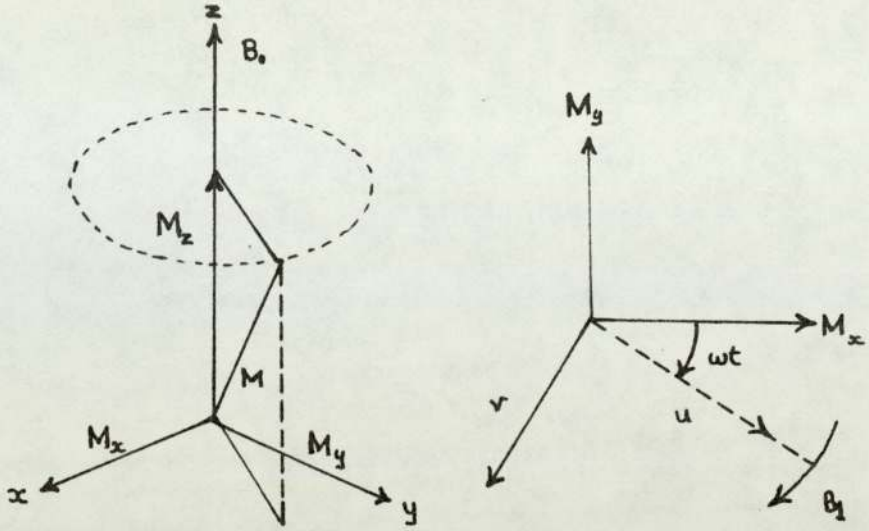

Fig. 1.3. Components of the transverse macroscopic moment.

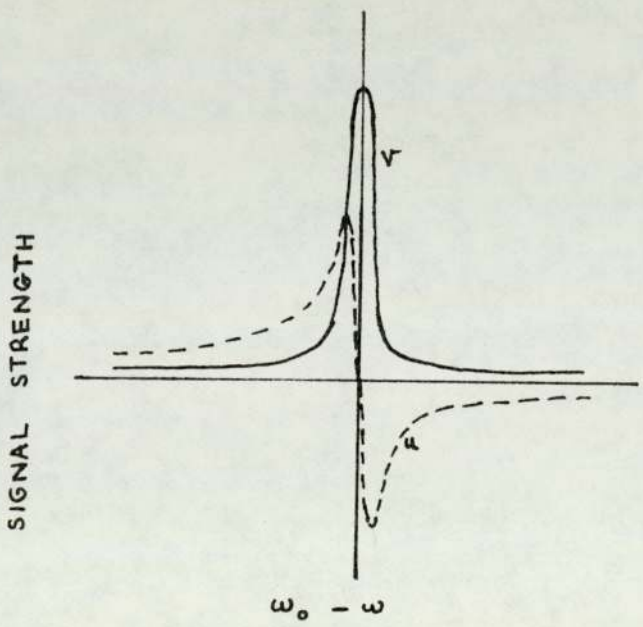

Fig. 1.4. The absorption line shape (V-mode) and dispersion line shape (U-mode) of NMR.

small but finite frequency range as a consequence of several different effects. Because, in practice, the v-mode (absorption) signal is displayed in preference to the u-mode (dispersion) signal, the factors affecting line shape will be discussed with the v-mode signal in mind.

1.8 Factors Affecting Line Shape

(a) Magnetic Dipole Interaction

The magnetic environment of a nucleus may be modified by fields due to magnetic moments of neighbouring nuclei.

In a solid or viscous liquid a nucleus at distance r from the nucleus being considered can produce a magnetic field at this nucleus of magnitude between $-\vec{\mu}/r^3$ and $+2\vec{\mu}/r^3$. The nucleus experiences not only the applied magnetic field B_o but extra magnetic fields over the range $+2\mu/r^3$ to $-\mu/r^3$ due to the effects of neighbouring nuclei. Magnetic resonance thence occurs over a range of frequencies and the line becomes broadened.

In freely tumbling liquids and gases where the molecules are allowed rapid random motion, the magnetic field at any one nucleus due to any neighbouring nuclei effectively averages to zero - the molecular correlation time being less than that required for the observation of a nuclear magnetic resonance signal. Magnetic dipole broadening is thus negligible in samples of liquids or gases which are used to produce high resolution nmr spectra.

(b) Spin-Lattice Relaxation

A nucleus will remain in a given energy state no longer than a factor of the spin-lattice relaxation time, T_1, and there is an uncertainty in the lifetime of that particular spin-state as governed by the Heisenberg uncertainty principle, such that

$$\Delta E . \Delta t \gtrsim \hbar . \qquad 1.23$$

ΔE may be represented by $h\Delta\nu$, $\Delta\nu$, being the uncertainty in frequency of the particular resonance line, and Δt may be set to the order of the uncertainty of the lifetime of the spin-

state ($\sim 2T_1$). Thus the uncertainty of the frequency may be written

$$\Delta\nu \gtrsim 1/4\pi T_1 \qquad 1.24$$

and the shorter the T_1 the broader will be the line.

(c) Spin-Spin Relaxation

In a similar way to that for spin-lattice relaxation, spin-spin relaxation may also cause an uncertainty in the frequency at which resonance will occur leading to the observation of resonance over a small range of frequencies causing line broadening. From the Lorentzian line equation the uncertainty of frequencies, or the line width, may be shown to be:

$$\Delta\nu = 1/\pi T_2 \qquad 1.25$$

Thus the shorter the T_2 the broader will be the line.

(d) Miscellaneous Effects

It has been mentioned previously (section 1.5) that if the magnitude of B_1 is so great that the signal intensity decreases, broadening of the line will be apparent as a result of saturation. Also, if paramagnetic species are present in the sample under scrutiny then T_1 is drastically shortened. This results in a line-broadening as is evident from equation 1.24.

The homogeneity of the magnetic field also plays an important part in the shape of a nmr line. If the magnetic field is not perfectly homogeneous, nuclei in different parts of the sample will experience different magnetic fields and hence resonate at slightly different frequencies. Thus if the magnetic field inhomogeneity is represented by ΔB, the uncertainty of the resonant frequency may be written by

$$\Delta\nu_1 = \gamma\Delta B/2\pi \qquad 1.26$$

By analogy with equation 1.25a time T_2' may be defined in terms of observed line width as,

$$\Delta\nu_1 = 1/\pi T_2' \qquad 1.27$$

T_2 includes contributions from the natural line width and magnetic field inhomogeneity and is given by

$$1/T_2' = 1/T_2 + \gamma \Delta B/2 \qquad 1.28$$

Finally, nuclei of spin I>1/2 possess a non-spherical nuclear charge distribution and there is a non-uniformity in the electric field at the nucleus that gives rise to a quadruple moment, q. Such non-uniformity about the nucleus can lead to a displacement of the nuclear magnetic energy levels by interaction with the quadrupolar electric field to promote relaxation and thence an uncertainty of the actual resonance position of the nmr line.

1.9 Nuclear Screening and the Chemical Shift

(a) General Aspects of Nuclear Screening

During experiments to compare nuclear magnetic moments of different isotopes in an applied magnetic field it was found that the exact resonance frequency of any isotopic-nucleus depended upon its chemical environment[18-20]. This phenomenon may be explained in terms of the screening from the applied magnetic field of the resonant nucleus by the extranuclear electrons. If the applied magnetic field is B_o, the actual magnetic field experienced by the resonant nucleus is given by $B_o(1 - \sigma)$ and the resonance equation (eqn. 1.4) may be rewritten as

$$\nu = \gamma B_o(1 - \sigma)/2\pi \qquad 1.29$$

where σ is the nuclear screening constant for the resonant nucleus in question. If two isotopically similar nuclei, in electronic environments i and j have shielding constants σ_i and σ_j respectively, another parameter known as the chemical shift may be defined as,

$$\delta_{ij} = \sigma_i - \sigma_j \qquad 1.30$$

The chemical shift is a more practical parameter than the fundamental shielding or screening parameter, because to measure an absolute screening parameter would require the reference measure-

ment of a nuclear species devoid of its extranuclear electrons. Chemical shifts are generally measured relative to a reference compound signal; for ^{1}H, ^{19}F, ^{31}P and ^{13}C nmr spectra some commonly used reference compounds are respectively, $Si(CH_3)_4$[21], $CFCl_3$[22], P_4O_6[23] and $CH_3{}^{13}COONa$[24]. These compounds are not used exclusively and any suitable material may be chosen as a reference for a particular measurement. For practical purposes the chemical shift may by comparison with equation 1.30, be expressed in terms of the magnetic fields experienced by two nuclei, as

$$\delta_{ij} \simeq \frac{B_i - B_j}{B_j} \qquad 1.31$$

for a fixed frequency experiment. Alternatively for a fixed field experiment the chemical shift may be written as

$$\delta_{ij} \simeq \frac{\nu_j - \nu_i}{\nu_{osc}} \qquad 1.32$$

where ν_{osc} is the oscillator frequency, viz. the frequency of the oscillating radiofrequency magnetic field.

For ^{1}H nmr spectra, using tetramethylsilane (T.M.S.) as a standard when mixed at low concentration in carbon tetrachloride, the position of the T.M.S. signal is denoted as 0δ, and signals to higher magnetic field, or of greater screening, than the T.M.S. signal have positive δ-values. This is not a desirable situation and another scale is commonly used, termed the τ-scale[25], which is related to the δ-scale through the equation,

$$\tau = \delta + 10 \qquad 1.33$$

With the τ-scale, the T.M.S. signal occurs at 10τ and the majority of ^{1}H spectra of organic compounds occur between 0 and 10τ. It has been pointed out that[26, 27], the τ-scale and the δ-scale have been much abused and many of the quoted values of chemical shifts must be treated with caution.

(b) Some Specific Aspects of Nuclear Screening

The significance of nuclear screening may be appreciated by consideration of a virial expression for the system being studied. In general, many observable parameters, X, may be represented in terms of the expansion

$$X = A + \frac{B}{V_m} + \frac{C}{V_m^2} + \ldots. \qquad 1.34$$

where A is the perfect gas value of X, B represents the effect of pairwise molecular interactions, C and higher terms represents the effects of multiple molecular interactions and V_m is the molar volume of the system. The nuclear screening, σ, may similarly be given in the terms of a virial expansion

$$o = \sigma_o + \frac{\sigma_1}{V_m} + \frac{\sigma_2}{V_m^2} + \ldots. \qquad 1.35$$

where σ_o is the absolute screening of the nucleus in an isolated molecule and σ_1, etc., represent the effects of pairwise, etc., molecular interactions on the screening. It has been shown[28-32] that there is a linear relationship between the chemical shift, $\sigma - \sigma_{ref.}$, and the bulk density of gases. This linearity tends to hold even into the liquid phase, indicating that a mechanism of screening operates on a similar basis in the gas phase and liquid phase. The implication is that terms higher than σ_1/V_m in equation 1.35 may be ignored and the nuclear screening constant may be written as two terms - the intramolecular screening constant (σ_o) and the (bimolecular) intermolecular screening constant (σ_s):

$$\sigma = \sigma_o + \sigma_s \qquad 1.36$$

General theoretical expressions[33, 34] have been proposed for σ_o following a quantum mechanical treatment of the intramolecular screening constant. The screening constant of a nucleus A in an isolated molecule may be written as[8]:

$$\sigma_o^A = \sigma_{DIA}^{AA} + \sigma_{PARA}^{AA} + \sum_{A \neq B} \sigma^{AB} + \sigma_{DEL}^{A} \qquad 1.37$$

where σ_{DIA}^{AA} is due to diamagnetic currents resulting from electronic motion about A. The term σ_{PARA}^{AA} depends on the mixing of ground and excited electronic states by the magnetic field which leads to induced paramagnetic currents about A. Induced currents in bonds or atoms other than that of A provide the anisotropic contributions σ^{AB}, and σ_{DEL}^{A} is due to the induced electronic motion of electrons delocalized in the molecular framework surrounding A.

From equation 1.37 it may be readily appreciated that intramolecular chemical shifts arise from different electronic densities at two different nuclei. They thus depend on electronic induction effects on the atom containing the resonant nucleus by other atoms in the molecule, static intramolecular electric fields, intramolecular van der Waals perturbations and spatial dispositions of the nuclei to the origins of the effects. In mathematical terms the intramolecular chemical shift may be written for two nuclei A and B; as

$$\Delta \sigma_o^{A-B} = \Delta\sigma_{DIA}^{AA-BB} + \Delta\sigma_{PARA}^{AA-BB} + \Delta\sigma^{AB-BA} + \Delta\sigma_{DEL}^{A-B} \qquad 1.38$$

From the point of view of this thesis no further attention will be devoted to intromolecular screening.

The intermolecular screening constant, or as it is sometimes called the solvent screening constant, σ_s, is generally formulated as[35, 36]

$$\sigma_s = \sigma_b + \sigma_w + \sigma_a + \sigma_E + \sigma_H \qquad 1.39$$

The various terms are due to the magnetic susceptibility of the sample (σ_b), the effects of van der Waals forces (σ_w), the effects of secondary magnetic fields produced by magnetically anisotropic solvent molecules (σ_a), the effects of electric fields arising from polar solvents and reaction fields within polar solute molecules (σ_E) and finally specific molecular interactions arising from, for example, hydrogen bonding and complexation (σ_H).

The magnetic susceptibility screening parameter, σ_b, has been firmly based and can be written[37]

$$\sigma_b = (\alpha - q - 4\pi/3)\chi_v \qquad 1.40$$

where α is a sample shape factor, q is a so called magnetic field interaction factor and χ_v is the volume magnetic susceptibility of the substance being considered. It is found[37] that to a first approximation q may be called zero, for coaxial cylindrical samples of lengths at least four times their diameters[38, 39], the classical susceptibility approach is valid and 2π represents the factor α.

To study screening parameters other than σ_b, it is necessary to account for changes in the latter which contribute to the chemical shift. This depends on the reference procedure adopted for the determination of the chemical shifts. A straightforward way of referencing is by mixing the reference substance with the sample. In this, the internal referencing procedure, the resonant nuclei in the molecule of interest and reference material experience the same susceptibility screening contribution, σ_b. It is possible to study solvent effects using an internal reference procedure providing care is taken in the choice of reference and the interpretation of resulting chemical shift data. Certainly, if care is not taken in measuring internally referenced chemical shifts erroneous results may be derived[40]. For routine analytical work, where internal referencing is used as a matter of course, a suitable reference compound depends on chosing a compound showing little shift dependence on the nature of solvents, exhibiting sharp absorptions so that only small amounts are needed, being stable and chemically inert, and which may be readily removed from the sample after study (section 1.9a). In principle, a more suitable referencing procedure is that of external referencing or pseudo-external referencing. The former case has until recently been relatively rare but there many spectrometers now

available with a built-in external reference. The latter case is more common, where the reference material is held in a capilliary or other suitable cell within the main sample tube. The theoretical implications of such an arrangement have been considered[41] by extending the approach of Dickinson[37]. The true chemical shift, δ^{T}_{BA} between the sample of interest, B, and the reference material, A, is given by the following equation:

$$\delta^{T}_{B-A} = \delta^{o}_{B-A} + \frac{2}{3}\pi (\chi_A - \chi_B) \qquad 1.41$$

when the sample tube is a long perfect cylinder.
The symbol δ^{o}_{B-A} represents the observed chemical shift between B and A and χ_A, χ_B are the volume magnetic susceptibilites of A and B respectively. If a spherical vessel is used to hold the reference material the observed and true chemical shift are equal because $\alpha = 4\pi/3$ and $\sigma_b = 0$ in equation 1.40; and thence no susceptibility correction is required. The disadvantage of external referencing, that are dependant on volume magnetic susceptibilites, is the uncertainty of the volume magnetic susceptibilites[42], especially in the case of mixtures[43]. Thus, studies of solvent effects on chemical shifts where conventional external referencing procedures are used can only be analysed quantitatively at a level consistent with the accuracy of the susceptibility correction[36].

If access to nmr spectrometers is available where the samples may be studied with the magnetic field applied lonitudinally to the axis of the nmr tube[44, 45] reference independent chemical shifts may be determined. However, many solvent chemical shifts continue to be measured by the classical referencing procedures.

Having accounted for σ_b and assuming that specific effects can be avoided (i.e. $\sigma_H = 0$) by studying solutions where the solute is taken at very low concentration (infinitely dilute), the basic problem is in accounting for σ_w, σ_a and σ_e; which in this order represent the relative ease of experimental access-

ibility. The most fundamental, though not yet fully understood, screening constant is σ_w with which the bulk of this thesis is concerned. In order to isolate σ_w it is necessary to measure the chemical shift of a nucleus within a solute molecule with respect to a suitable reference, first when the solute is in the gas phase (at zero density) to give $\sigma_o - \sigma_{ref.}$ and then at infinite diluation in a solvent to give $\sigma - \sigma_{ref.}$. Provided the solute and solvent are perfectly isotropic

$$\sigma = \sigma_o + \sigma_b + \sigma_w \qquad 1.42$$

and the difference between the susceptibility corrected[37] chemical shifts in the liquid phase relative to the gas phase will yeild σ_w:

$$\delta_{liq - gas} - \Delta\sigma_b = \sigma_w \qquad 1.43$$

The nuclear screening constant, σ_w, may be examined on an electric field effect basis, as indeed can σ_E. It is customary to write the nuclear screening due to electric field effects in terms of the well founded equation[35]

$$\sigma = -AE_z - BE^2 - \ldots. \qquad 1.44$$

where A and B are screening constant coefficients characteristic of the resonant nucleus being studied and the E terms are the linear, squared, etc. electric fields. It is now postulated that there has been an inherent inadequacy in some theoretical interpretations of σ_w and even possibily with regard to van der Waals dispersion forces in general. The search for this will be described in this thesis.

1.10 Nuclear Spin-Spin Coupling

On examination of spectra under conditions of high resolution it is often found that the chemically shifted absorptions are themselves composed of several lines. This added multiplicity is attributed to intramolecular interaction between the nuclear magnetic moments[46, 47]. These multiplets arise from the coupling interaction between neighbouring nuclear spins in an indirect way, via

the electrons in the molecules. A nuclear spin tends to orient the spins of the nearby electrons which in turn orientate the spins of other electrons and consequently spins of other nuclei. This electron spin mechanism is the most important contribution to spin-spin coupling although in general all magnetic interactions could contribute. In the simplest case the spacing between these multiplet lines are equal and the magnitude of this splitting is known as the coupling constant, represented by the symbol J(Hz).

Spin-spin interac tions exhibit several important features which help to distinguish them from chemical shifts. For example, coupling is not observed between groups of nuclei that have the same chemical shift and couple equally to all other resonant nuclei in the molecule and, when coupling is observed, the coupling constant is, to a good approximation, independent of the magnitude of B_o and of temperature. In general the size of the coupling constant decreases as the number of bonds separating the interacting nuclei increases, but increases with the atomic number of the interacting nuclei.

The complexity of the spin patterns is dependent on both the chemical shift difference between the interacting nuclei and the coupling constant. Nuclei with small shift separations, of the order of magnitude as the coupling constant ($\delta \simeq J$) are designated by letters close together in the alphabet, e.g. A, B, C ..... The symbols X, Y, Z are used to describe other groups of nuclei in the molecule which are chemically shifted with $\delta \gg J$, from the A, B, C group. Magnetic nuclei of the same chemical shift and coupling constant to other nuclei in the molecule are described by the same symbol and the number of such nuclei is indicated by a subscript. Such nuclei are usually termed magnetically equivalent nuclei.

If an absorption band arises from one set of identical nuclei, the number of peaks or lines constituting the absorption band arising from coupling may be predicted simply in cases where

$\delta \gg J$, viz. first order situations.

For a set of n_A equivalent nuclei of type A and n_X equivalent nuclei of type X a first order coupling treatment[48] will result in $2n_X I_X + 1$ peaks for the A band and $2n_A I_A + 1$ peaks for the X band. The relative intensities of the peaks comprising the multiplet structure are given by the 'n' - th binominal coefficient in the expansion of $(1 + x)^n$. In cases where $\delta \simeq J$, second-order spectra occur in which the above simple intensity and spacing rules no longer apply.

This feature of nmr spectroscopy has not been encountered in this work and will not be considered further.

CHAPTER 2

THE OBSERVATION OF HIGH RESOLUTION N.M.R. SPECTRA

2:1 Introduction

The fundamental requirement for the observation of nuclear magnetic resonance is that the resonance equation (eqn. 1.29) is obeyed:

$$\nu = \frac{\gamma B_o}{2\pi}(1 - \sigma) \qquad 2.1$$

where ν is the resonant frequency of the nucleus under study, B_o is the applied linear magnetic field strength, γ the magnetogyric ratio of the nucleus and σ is the screening of the nucleus. It follows that for any nucleus to be brought into resonance either B_o must be varied, by sweeping through a small range of B_o using sweepcoils, and keeping ν constant or vice versa. B_o may be obtained by using a permanent magnet, electromagnet or a superconducting solenoid. The frequency, ν is derived from the output of a radiofrequency oscillator and is the frequency at which the electric vector of the oscillating magnetic field rotates. The radiofrequency signal is passed through a coil surrounding the sample. In order to observe an nmr spectrum, a detection system is required of which there are two basic types: the single coil[49] and crossed coil[50] type.

Since the nmr work in this thesis employed continuous wave (cw) spectrometers, the emphasis of this chapter will be towards these. However, much of the nmr work published nowadays uses Fourier transform (F.T.) spectrometers and therefore a short section will be devoted to these initially. It would have been desirable to measure some gas phase chemical shifts using F.T. nmr spectroscopy during this work, had the facility been available. It was found to be impracticable to derive meaningful results from low density gas phase measurements on the cw spectrometers available.

2:2 Fourier Transform N.M.R. Spectroscopy[51-55]

Fourier transform nmr is becoming increasingly common in research and routine analysis. The basic difference between the standard continuous wave (cw) nmr technique and the F.T. nmr technique is that instead of using a steady radiofrequency field, the sample is irradiated with pulses of radiofrequency energy.

When the sample is irradiated with a pulse of radiofrequency energy all of the nuclei in the sample may be excited simultaneously. The width of the band of exciting energy depends on the pulse time which is usually of the order of 2-5 μs. After the pulse has finished the nuclei of the sample return to equilibrium depending on the relaxation times of the spins concerned. The decay signal of the spin systems is called a free induction decay pattern (F.I.D.). The F.I.D. contains all the relevant information present in a conventional cw spectrum but the F.I.D. can be observed in a much shorter time than a cw. spectrum.

The appearance of a F.I.D. is very complex and is what may be termed a time domain spectrum in contrast to the more conventional frequency domain spectrum. Time domain may be transformed into frequency domain by the mathematical technique of Fourier transformation, and this is achieved in practice by means of a program in a small dedicated computer.

The use of a single pulse F.T. nmr spectrum would be of no advantage over a cw. nmr spectrum. However, when the sample contains a low concentration of the nuclei to be studied, the true signal may be masked by noise. To overcome the poor inherent signal to noise, the spectrum is accumulated by repetitive pulsing such that the true signal increases with the number of pulses whereas the noise increases with only the square root of the number of pulses.

Among its many other applications F.T. nmr finds particular use in the investigation of low density gas phase samples and

natural abundance ^{13}C nmr spectra.

2:3 Continuous Wave N.M.R. Spectroscopy

The magnitudes of the chemical shifts measured and used in this thesis are relatively small. Therefore the magnet and its field stability must be given the utmost consideration in order to enable these chemical shifts to be measured with any confidence. The magnet and its field stability will therefore be discussed in some length, relative to the other instrumental features.

(a) The Magnet

The sensitivity of an nmr signal is theoretically proportional to B_o^2, although in practice this is closer to $B_o^{3/2}$ [8] and therefore the strongest field possible, in keeping with field homogeneity and magnet construction, must be employed. Permanent magnets, electromagnets and superconducting solenoids find application in nmr spectrometers and the usefulness of these in different applications depend on their different characteristics.

The advantage of the electromagnet is that it enables the field strength to be set in the typical range 0.1T to 2.5T, and given the flexibility in the oscillator frequency all magnetic nuclei may be studied at more than one frequency. This is a valuable asset when investigating complex spectra, especially where second order spectra are involved. The major drawbacks of the electromagnet are the high running costs and their relatively short lifetime.

The permanent magnet lacks the same flexibility of operation, but its chief assets are its high magnetic field resolution, stability and low running costs. On account of the fact that the magnetic field strength cannot be varied by more than ca 1% for a permanent magnet, different types of nuclei need different operating frequencies. The uniformity of field attainable by all types of magnet is comparable, being capable of giving homogeneity of a few parts in 10^9 of field.

For some time superconducting solenoid magnets have been used that can provide magnetic field strengths of 5T or more, with adequate homogeneity and stability for high resolution work[56]. As these soleoinds operate at liquid helium temperature (ca 10K) much auxiliary equipment is needed and the running costs are very high.

The upper limits of the magnetic field strengths quoted arise out of the need for field homogeneity over a volume of 0.5 cm^3. The required homogeneity calls for magnet pole faces of permanent magnets and electromagnets which are strictly parallel, free from machining marks and are optically flat[57]. The pole caps are usually chromium plated to resist corrosion. Homogeneity can be improved by attaching small coils (Golay coils) to the pole faces and generating shimming patterns by passing through the Golay coils small electric currents. Further improvement of the homogeneity of the magnetic field experienced by the nuclei being studied may be achieved by mechanical motion of the sample. The simplest way of doing this is to spin the sample, usually about the vertical axis of the nmr tube and perpendicular to the B_o field direction in permanent and electromagnets, at about 2000 r.p.m. by using an air turbine. In a superconducting solenoid the sample is spun along the axis of the B_o field direction. This helps to average out the effects of field gradients along the other two axes.

To enable accurate chemical shift measurements to be made a great deal of attention must be paid to field stability. Permanent magnets give rise to few problems in this respect since extensive and careful thermal control[58, 59] ensures absolute field stability and resolution. Ambient field disturbances can be minimised by μ-metal screening or by feedback devices. The stability of an electromagnet, however, depends

upon the stability of the current that passes through its coils. Some measure of current control is usually achieved by passing the magnet current through a small resistance and comparing the resultant voltage with a reference voltage. The difference in voltage is amplified and the error voltage then used for correction purposes.

Both electromagnets and permanent magnets are also provided with a field compensator[40], or flux stabiliser, which is a device employed to minimise the effects of external field variations. Whilst most magnets are designed so that the effect of external fields is almost negligible, fluctuations may still occur and are detected in coils situated near the magnet pole pieces or in a field node. The voltage induced by changes in the magnetic flux across the gap between the pole pieces are amplified and used to apply the necessary correction through an additional set of field coils wound around the pole pieces.

(b) Field Stabilization - Field/Frequency Locking

Spectrometers, particularly those employing an electromagnet, are often available with a field/frequency lock system in which the field (or frequency) is locked onto a particular resonance signal. External locking devices[61, 62] employ a control sample of high spin content (usually ^{2}H or ^{7}Li) built into the probe as close as possible to the experimental sample. The control sample is provided with its own nmr circuitry and gives rise to a resonance signal in the dispersion mode (u-mode). Any change in the intensity of this signal from zero, indicating a drift in the magnetic field strength, is used to actuate an electronic feedback loop which restores the field strength to its original value. In this way the field strength may be held constant to better than 1 in 10^{8} indefinitely. However changes in the field strength at the experimental sample are not exactly paralleled by changes at the control sample since the two samples are physically separated by a small distance. For this reason, internal locking systems

have been devised. In these[51], two separate audio frequencies, one the locking frequency and the other the observing frequency, are used to modulate the radio frequency. Thus the nmr spectrum consists of the normal spectrum (centreband) and side-bands to high and low field of the centreband shifted by amounts that depend on the modulation frequency. The magnetic field strength is then adjusted to a value that corresponds to one of the side-bands (at a frequency shifted from the centreband by the locking frequency) and to a sharp line in the spectrum of the sample being observed (in the dispersion mode). The output from the radio frequency detector is ultimately passed through a phase sensitive detector operating at the frequency of the sideband being used for the lock. The output from this phase sensitive detector is then used to actuate a control loop to the flux stabiliser, that maintains the necessary constant ratio of field strength to frequency. Other resonances from the sample can now be observed by varying the observing frequency through a suitable range and taking one half of the radiofrequency detector output through a second phase sensitive detector operating at the observing frequency. The output of this phase sensitive detector is then fed to the recorder or oscilloscope. The stability achieved depends upon the sharpness of the line chosen to provide the locking signal and upon the frequency stability of the audiofrequency oscillators.

The method described above, where the lock frequency is kept constant and the observing frequency varied is a true frequency sweep experiment. The converse, where the observing frequency is kept constant whilst the lock frequency varies, is a field sweep experiment.

(c) The Magnet Field Sweep

Commercial nmr spectrometers have available two types of magnetic field sweep; a recurrent sweep and a slow sweep. In the former case, the output of a saw tooth generator is amplified

and then fed to two small Helmholtz coils usually mounted close to the sample and having their axes in the same direction as the main magnetic field (B_o). The recurrent sweep allows oscillographic presentation of the signal by feeding the output of a linear sweep unit to the x-plates of the oscilloscope. The sweeps on the oscilloscope and the field are automatically synchronised and no phase shift device is required. By varying the time base and output of the saw tooth generator one can control both the rate of sweep and its amplitude. This linear sweep is brought into play when searching for the resonance of a nucleus and when making spectrometer adjustments.

A slow sweep unit is provided to enable the signal to be recorded under so called slow passage conditions in order to minimise line distortion. The slow sweep passage may be facilitated by using a motor driven recorder linked to a precision potentiometer, the output of which is applied to the sweep coils.

(d) The Radiofrequency Oscillator

The upper limit of the main magnetic field for conventional magnets is in the region of 2.5T, which sets the highest radiofrequency required at about 100MHz for ^{1}H and ^{19}F nuclei. However, with the advent of superconducting solenoid magnets with magnetic field strengths of 5T or more, radiofrequencies of 200MHz or more are required for ^{1}H and ^{19}F nuclei. A low power ($\sim$1W) source of radiofrequency energy, with a frequency stability of the same order of magnitude as the main magnet field stability viz. 1 in 10^{9}, is required. This is conventionally derived from a quartz crystal controlled oscillator. Some transmitters give different frequencies by controlling the extent of multiplication, through harmonics, of the power output from the crystal oscillator while others operate by substitution of different crystals. In addition to frequency stability the transmitter, that operates at a constant level, has its output modified by passing the signal through

variable attenuators before passing to the probe.

(e) The Probe and Detection Systems

The sample holder, or probe, is the assembly which carries the air turbine for sample spinning, the transmitter and receiver coils, the linear sweep coils, pre-amplifier and often the Golay coils. The probe position can usually be varied to enable the best position in the magnetic field to be found. The radiofrequency coil is wound on a precision glass former mounted vertically and perpendicular to B_o. The sample, in its cyclindrical glass tube, is inserted down the inside of the glass former and is usually supported at the top and bottom by bearings to facilitate even spinning.

Probes can be divided into two basic types; the single coil probe[49] and the double, or crossed, coil probe[50]. In the single coil arrangement energy from the radiofrequency power supply is fed to a coil (the sample coil), and this coil forms part of a radiofrequency bridge circuit. Energy absorption by the sample produces a change in the balance of the bridge which is detected by the receiver. For the double coil method use is made of two coils arranged with their axes perpendicular to one another and also to the magnetic field. Energy from the radiofrequency oscillator is fed to the sample via the transmitter coil. When the sample absorbs energy an emf is induced in the receiver or sample coil and this can be detected by the receiver. This is known as the nuclear induction method. Any lack of orthogonality between the coils will cause the transmitter to couple with the receiver coil and hence a leakage voltage is induced in the latter. A small amount of leakage is desirable since it serves as a source of carrier signal. Control of the leakage flux without moving the receiver coil is achieved by introducing semicircular sheets of metal (paddles) mounted at the end of the transmitter coil. Adjustment of these paddles gives a controlled finite leakage voltage enabling the receiver detector

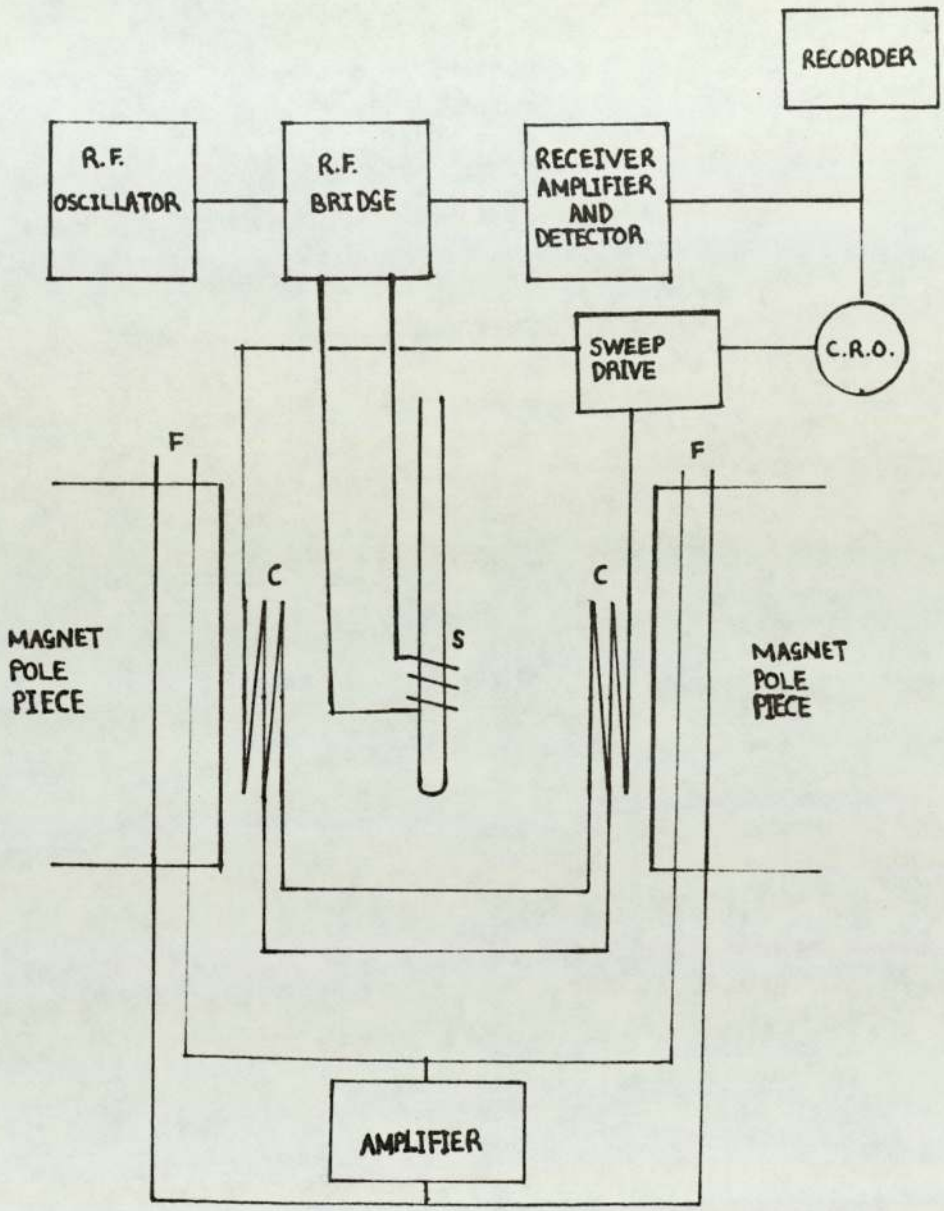

S - Sample and sample coils

C - Sweep, modulation and shim coils

F - Flux stabiliser coils

Fig. 2.1. Block diagram of a typical NMR spectrometer

to operate at an efficient level and also allowing the desired mode of complex nmr signal to be selected.

The signals to be detected are very weak and therefore the receiver must have a high sensitivity. Care is needed to reduce noise to a minimum. Noise may be the normal electrical noise that occurs in all circuits or it may be generated mechanically by, for example, the spinning of the sample. To obtain the best signal-to-noise ratio the first stage of amplification of the signal takes place in a pre-amplifier unit situated close to the probe. The transmitter and receiver are often built into a single unit with a control for the power output of the transmitter and a means of altering the gain of the receiver. The time constant of the output circuit of the receiver is usually variable so that it can be varied along with the sweep rate to obtain the most favourable signal-to-noise ratio for each sample. The receiver output is then fed to the recorder unit of the spectrometer.

2:4 The Facilities Used

Two spectrometers were used during the investigations reported in this thesis: a Varian Associates HA100D nmr spectrometer and a Perkin-Elmer R12B nmr spectrometer. Since the spectrometers received limited use only an outline of their specifications and operation will be reviewed. The choice of spectrometer was governed by its availability at the time it was required.

(a) The Varian Associates HA100D N.M.R. Spectrometer

This spectrometer[63] utilizes an electromagnet with an optimum magnetic field strength of 2.349T. The corresponding nominal frequency for ^{1}H resonance is 100MHz although signals are detected 2.5 kHz lower in the field sweep and 2.5 kHz higher in the frequency sweep HA mode. Current is supplied to the low impedence magnet through a comprehensive solid state power supply unit fed from a three phase mains power supply. The power supply

has a facility to protect against ± 10% variations in line voltage. The magnet current is variable and a fine field trimmer is provided to compensate for day to day change in magnetic field strength.

The magnet is mounted in a trunnion support yoke and the main coils are cooled with thermostatted water giving a constant temperature within the magnet pole pieces, normally in the range 300 - 309K. The whole magnet is contained in an insulating jacket to minimise the effects of ambient temperature changes on the magnetic field and the sample. A field compensator automatically corrects for any magnetic field drift and may be used as a sweep unit by reaction to a false error signal. Field homogeneity is improved by means of Golay coils contained in covers protecting the magnet pole pieces.

The probe is precision milled from aluminium and contains field sweep coils, modulation coils, a transmitter coil and a receiver coil. The probe is designed to accept, in general, sample tubes with 5 mm. outside diameters in conjunction with a turbine made of milled teflon. The turbine is fitted around the sample tube at the appropriate position and a compressed air supply causes the sample to spin about its long axis.

The detection system is of the crossed coil (or double coil) variety (section 2:3d). The absorption signal is isolated from the background radiofrequency signal by a geometric arrangement of the two coils, the v-mode being observed when the transmitter and receiver signals are out of phase by $\pi/2$ or 90°. The dispersion mode (u-mode) is studied by introducing a phase difference other than $\pi/2$ by means of a paddle or metal sheet, positioned in the radiofrequency field such that its rotation may cause an adjustment of the B_1 field.

A linear sweep unit allows variable sweep times and widths to be employed by using a sawtooth waveform derived from a phantastron oscillator. The sawtooth voltage modulates a

50kHz signal, applied from a separate oscillator circuit, and the modulated 50 kHz signal is amplified in two stages and mixed with an unmodulated 50kHz signal which is π out of phase. This provides a stable linear direct current sweep connected to the D.C. modulation coils on the probe to modify B_o.

The HA100D may be utilized in two distinct modes; the HR mode which provides a field sweep facility and the HA mode which uses the field-frequency lock system. In this thesis chemical shift measurements were made in the HA mode and it is this mode of operation that will be discussed in further detail.

In the HA mode of operation a reference material must be added to the sample under study so that the reference and sample are subject largely to the same conditions. The nmr signal from the reference is detected at the centre of the dispersion mode (u-mode) so that any movement of the signal gives rise to a finite voltage in the detector. The signal is amplified and applied to the field compensator or flux stabilizer and thus the instability is corrected. The sample signals are processed separately and the ultimately recorded. A detailed discussion of the field-frequency lock system can be found elsewhere[63-65]. Basically, the HA-mode of operation is controlled by the radiofrequency unit and the internal reference stabilization unit which adjusts B_o keeping the ratio of field and frequency in constant proportion.

The transmitter section comprises two audiofrequency oscillators; the sweep oscillator variable from 3500Hz to 2500Hz and a manual oscillator variable from 1500Hz to 3500Hz. The sweep oscillator frequency is controlled by movement of the recorder along its x-axis and the manual oscillator is controlled by a precision potentiometer. The oscillator circuits are identical Wien bridge sine wave generators, tuned for 50, 100, 250, 500 and 1000Hz and 1500-2500 and 2500-3500Hz sweep ranges. Selection

of either the lock signal, the sweep or manual oscillator frequencies, an external signal or the difference of the two oscillator frequencies is possible and may be presented on an oscilloscope or a Varian 4315A frequency counter.

Either oscillator may be used as the reference signal, depending on the sweep mode chosen. The two frequencies independently modulate the 100MHz radiofrequency carrier signal and the detected nmr signals are reduced to audiofrequency signals modulated with the components are detected by phase sensitive detectors after being suitably amplified and filtered.

The control signal is applied to the stabilization filter and passes the D.C. signal to the flux stabilizer to complete the loop. The nmr singal in the analytical channel is similarly detected and filtered in the integrator/decoupler before being applied to the recorder Y-axis circuits.

(b) The Perkin-Elmer R12B N.M.R. Spectrometer

This spectrometer[66] utilizes a permanent magnet with an optimum magnetic field strength of 1.492T equivalent to an observation frequency of 60MHz for ^{1}H nmr. The magnet is of a rigid barrel construction preventing any relative movement of the pole-pieces. Field stability is maintained both by passing air at a constant temperature around the magnet and by use of a μ-metal screen. The field stability achieved by means of the foregoing measures is such that short term variations are almost completely eliminated and long term drift is reduced to a very low level. Further stability may be ensured by field locking using a double resonance accessory.

Magnetic field homogeneity is improved by means of Golay coils fitted to the pole tips in the space between them. To reduce the effect on the resolution of any residual field variation, the

sample tube is spun about its long axis using a specially made plastic turbine fitted to the sample tube at the appropriate position. The spinning speed may be regulated by adjusting the rate of flow of air meeting the turbine.

Sweep and shift coils are wound on a coil former mounted on the magnet pole pieces. To scan the spectrum, the magnet field is swept through a small range by passing a sawtooth current through the sweep coils; the sweep range may be varied by changing the amplitude of the sawtooth. The sweep current is obtained from the oscilloscope X-deflection waveform or from a potentiometer driven by the pen recorder depending whether the spectrum is being observed on the cro or on the chart recorder. A 'fly-back' occurs while the pen is moving from one chart to the next. The part of the spectrum selected for study may be varied by means of field shift controls, adjustment of which changes the current through the shift coils.

The 60MHz irradiation field (B_1) is obtained from a highly stable crystal-controlled oscillator contained in a thermally regulated oven in the double resonance accessory when supplied; as in the case of the spectrometer used. The frequency stability of the oscillator is of the order of 2 parts in 10^9 per hour. A 6kHz signal, also obtained from a crystal-controlled oscillator, is applied to coils orthogonally located relative to the probe radiofrequency coil and aligned with the magnet axis, so that the magnetic field in the sample region is audiofrequency modulated. The B_1 field is controlled by means of a field modulation attenuator. At resonance the sample acts as a mixing device, and nmr sidebands are produced at field strengths corresponding to 59.994 and 60.006 MHz. Each sideband, when stimulated induces in the probe a 60MHz radiofrequency response, amplitude-modulated at 6kHz; the modulation contains information from the nmr signal.

The probe output is applied to a radiofrequency amplifier,

housed in the double resonance accessory when fitted, the output of which is detected to obtain the 6kHz signal. This signal is smplified and its phase is compared with a reference signal of adjustable phase derived from the 6kHz oscillator. The reference phase is adjustable so that the v-mode or u-mode component of the 60.006MHz sideband may be selected as required for observation and recording. As there is no audiofrequency detected in the absence of resonance, the spectrum baseline is extremely stable.

The nmr signal is filtered and may be applied to the cro for immediate observation, or to the chart recorder for a permanent record.

The double resonance accessory fitted to this R12B spectrometer was used in this thesis to stabilize the field-frequency ratio against field drift and effect a more accurate chemical shift measurement. This 'field locking' is achieved by introducing a small amount of a suitable reference material, such as tetramethyl silane, into the sample and using the resonance signal from this compound to maintain the required magnetic field value. The amplitude of the resonance signal may be controlled either automatically or manually.

In the locking modes (auto lock and manual lock) the radio-frequency levels are as required for normal operation. The locking signal level is similar to that of the observation frequency and is preset for auto lock but variable for the manual lock mode of operation. The second irradiation frequency is derived from a voltage-controlled oscillator operating between 9.6 and 14.4kHz, whose frequency is then halved. Thus the locking resonance is excited by a variable 4.8 - 7.2kHz signal that is combined with the normal 6kHz signal. The amplified output from the detection system passes through a 6kHz filter to select the 6kHz signal and then to the phase-sensitive locking detection system which selects the dispersion mode of the variable-frequency

signal and uses it to correct for any drift or disturbance to field.

The field correction is applied at two points, the 'fast lock' correction which gives a fast response to rapid changes in D.C. correction current via the field modulation coils, and the 'slow lock' correction together with a field shift applied to one of the field shift coils. Use of the two modes of correction enables a rapid response without instability. The slow lock system produces a field sweep via a small offset voltage that is used to search for the locking resonance. Once the locking resonance is sensed, its resonance swamps the offset voltage, and lock is established. The locking detection system also contains a detector for the absorption mode of the locking signal giving a D.C. output. This output is proportional to the level of the locking signal response in the sample when the double resonance accessory is in manual lock mode of operation. In auto lock mode this output is fed back to give automatic gain control in the input of the locking detection system. The functioning of the system is thereby made independent of the amplitude of the locking signal response from the sample thus enabling a range of locking material concentrations (1% - 10%) to be used.

2:5 The Accurate Measurements of Chemical Shifts

In normal continuous wave nmr spectrometry the absorptions are recorded on calibrated chart paper and approximate values for chemical shifts are deduced by measuring the separation between recorded lines. The investigations reported within this thesis, requiring accurate measurements of chemical shifts (0.1Hz or better), necessitate the careful control of conditions. For instance, it is necessary to use identical sweep speed and filter conditions because of possible response deficiencies. The spectra were drawn out in an expanded form (the minimum sweep width possible) several times. In the case of the HA100D spectrometer the position of each peak can be measured by placing the pen of the

recorder at a stationary position corresponding to the peak maximum and counting the sweep and manual oscillator frequencies of the Varian frequency counter. The difference between the two frequencies gives the chemical shift relative to the lock-signal. The degree of error is reduced further by taking the average of several values. In the case of the R12B spectrometer the chemical shifts are measured relative to precalibrated chart paper since no frequency counter was available. The spectra were drawn several times for the sample sample and the average chemical shift evaluated.

CHAPTER 3

A CRITICAL RECONSIDERATION OF THE VAN DER WAALS SCREENING CONSTANT

3:1 Introduction

The main research interest of this thesis is the characterization of the effects of solvents on the van der Waals screening constant, σ_W, in the liquid phase. This chapter is devoted to the background of past theoretical models - gas phase,[29, 67] cage[67] and continuum[68-83] - used in the characterization of σ_W. Most of the attention will be given to the inadequacies of continuum models in accounting for σ_W because they have been used in this work. Also, because σ_W stems from a van der Waals interaction, van der Waals dispersion forces[70, 71] are considered, in their own right, from a classical point of view. The many literature quotations that strongly suggest that there is something missing in past characterizations of continuum models, especially with regard to σ_W, are highlighted and these provide a background to the modified version of the characterization of σ_W presented in later chapters of this thesis.

3:2 London Dispersion Forces and the Van der Waals Screening Constant σ_W

The van der Waals forces between molecules may be described in terms of London dispersion forces and repulsion forces so that σ_W must have a contribution from both. It is generally accepted that at intermolecular distances (contact separations) it maybe reasonable to neglect repulsion forces. Indeed, significant contributions to the repulsive part of σ_W only occur if there is considerable overlap of the molecular orbitals of the interacting molecules. Therefore a theoretical characterization of σ_W need, to a first approximation, only reply on a theory concerning the attractive dispersion-type forces.

From the point of view of a continuum treatment the solute molecule is thought of as being a point non-polarizable dipole at the centre of a spherical cavity surrounded by solvent continuum[68]. The oscillations of the solute electrons produce transient electric dipole moments which in turn produce instantaneous inhomogeneous polarizations of the solvent continuum. These polarizations lead

to "reaction fields" within the solute cavity that are uniform throughout the cavity and in the direction of the transient electric dipole[69]. This interaction is essentially between a pair of electronic oscillators which may be considered to be the solute and the 'solvent continuum'. London's treatment of van der Waals dispersion forces between simple harmonic oscillators[70, 71], demonstrated that these forces arise from all the second order terms in the energy of the interacting oscillators. These second order terms always tend to displace the unperturbed oscillator energy levels downwards thus leading to attractive forces between the oscillators. The London dispersion energy[70, 71], for a pair of hydrogen atoms of polarizability α separated by a distance r, is

$$\Delta U = -3\nu_0 \alpha^2/4r^6 \qquad 3.1$$

where $h\nu$ is a transition energy between the energy levels of the interacting oscillators (hydrogen atoms), and may be related to the ionization energy of the species. It is well accepted[70, 71] that dispersion forces and thence energies are directly additive. The basis of London's argument outlined above is equivalent to saying that van der Waals dispersion forces arise from all square field effects (the linear field, or first order, effects averaging to zero). Thus the van der Waals dispersion screening may be written in terms of square fields only, such that (section 1:9b, equation 1.56)

$$\sigma_w = - B \sum E^2 \qquad 3.2$$

For non-polar isotropic systems one of these square fields will be the mean square reaction field in the solute cavity[69].

3:3 The Models Used to Characterize σ_w

Following the discourse given in section 1:9b it is necessary to compare the gas-to-liquid chemical shift of an isotropic solute, involving an isotropic solvent, (section 1:9b, equation 1.55) with an appropriate theoretical function in order to test the adequacy of the relevant theory relating to σ_w. The theoretical function relating to σ_w depends on the model used to characterize it and

of these there are basically three; namely continuum, gas phase and cage models.

The gas phase model[29, 67] of the liquid specifically depends on bimolecular interactions and the calculation of two centre potentials. Although the virial expansion of nuclear screening (section 1:9b, equation 1.34) suggests that only pairwise collisions between molecules, possibly even in liquids, need be considered, a characterization of a dense gas or liquid should involve more than one pairwise collision at any given time. This requires an extension of the simple bimolecular approach and the setting up of equations to represent the potential energy of the system. The solution of the problem would necessarily imply the use of many approximations.

With the cage model[67], only the first solvent shell around the solute molecule is considered. Consequently, the average effect of one solvent molecule on the nuclear screening of the nucleus of the solute molecule is predicted and the total screening is obtained by summing the individual pair interactions. The cage model therefore necessarily involves some empiricism. Both the gas and cage models have been developed mainly by Rummens et al[67] and although the results obtained give a more or less semiquantitative description of σ_w, reliable results depend on the approximations taken in evaluating the potential energy functions and the availability of intimate measurements on molecules rather than the more easily accessible bulk properties of molecules.

The preferred model in this thesis is the continuum model because bulk properties of molecules are only required and this description is a closer representation of the liquid phase than the two previously described models. Following Onsager,[68] the treatment of σ_w on a continuum basis requires that the solute molecule is singled out and treated as being a point species at the centre

of a cavity surrounded by a continuum representing the solvent. In following the continuum model approach, it is also realized that the presently accepted continuum model may itself be inadequate in accounting for σ_w and dispersion forces in general; evidence for the former inadequacy will be presented later in the thesis. Consequently, the classical continuum model will be extended and based on a model with additional features reminiscent of both cage and gas models. Before proceeding, however, past characterizations of σ_w on a continuum basis will be discussed along with some justification of how continuum models may be extended to give an approximate description of dispersion forces.

3:4 An Outline of the Continuum Model

Following the lead taken by Bell[84] in initiating the use of a continuum model in calculating electrostatic energies of dipole molecules, Onsager[68] published his classical paper on electric dipole moments of molecules in liquids. The treatment was applied to polar molecules although it was implied that there should be no real difference between this and the treatment of non-polar molecules. The argument of Onsager,[68] for the case where there is no applied electric field, is essentially as follows.

In the absence of a solvent medium the potential at a point with co-ordinates r, θ, produced by a point dipole of moment μ lying at the origin and with its axis directed along the reference co-ordinate, is given by $\phi = \mu\cos\theta/r^2$. When such a dipole is at the centre of a spherical cavity of radius a in an initially unpolarized medium the field within the cavity is modified by the reaction field set up by the dipole. Although the evaluation of this effect requires the consideration of spherical harmonics (see chapter 4), only the results obtained will be presented. For the potential in the cavity[68]

$$\phi_1 = \mu\cos\theta/r^2 - Rr\cos\theta \qquad 3.3$$

where

$$\vec{R} = \frac{2(\epsilon_2 - 1)}{(2\epsilon_2 + 1)} \frac{\vec{\mu}_3}{\bar{a}} \qquad 3.4$$

is the reaction field and is in the same direction as that of the dipole producing it and therefore dependent on the instantaneous orientation of the dipole. The symbol ϵ_2 represents the dielectric constant of the solvent medium. The field outside the cavity is modified and the electric potential outside the cavity becomes

$$\phi_2 = \mu^* \cos\theta / r^2 \qquad 3.5$$

where μ^* is the apparent dipole moment of the solute as observed from outside the cavity and given by

$$\vec{\mu}^* = \frac{3\epsilon_2}{(2\epsilon_2 + 1)} \vec{\mu} \qquad 3.6$$

The only field that acts on a spherical molecule in a polarized dielectric is therefore the reaction field, $\vec{R}$, because the dipole field cannot act upon the molecule producing it. The dipole moment $\vec{\mu}$, is the dipole moment of the molecule in vacuo, $\vec{\mu}_o$, plus the dipole moments induced in the molecule by the reaction field acting upon it. Thus $\vec{\mu}$ may be written as

$$\vec{\mu} = \vec{\mu}_o (1 + \alpha_1 g + (\alpha_1 g)^2 + (\alpha_1 g)^3 + \ldots) \qquad 3.7$$

where α_1 is the solute polarizability (mean) and g is the reaction field factor, $2(\epsilon_2 - 1)/(2\epsilon_2 + 1)a^3$. The infinite series in $\alpha_1 g$ (equation 3.7) is converging, since $\alpha_1 g \ll 1$, and may be written as $(1 - \alpha_1 g)^{-1}$. Thus the liquid phase solute dipole moment is

$$\vec{\mu} = \vec{\mu}_o (1 - \alpha_1 g)^{-1} \qquad 3.8$$

The solute reaction field is thence given by

$$\vec{R}_1 = g \vec{\mu}_o (1 - \alpha_1 g)^{-1} \qquad 3.9$$

and for a non-polar molecule the all important square reaction field is

$$\langle R_1^2 \rangle = g^2 \langle \mu_o^2 \rangle (1 - \alpha g)^{-2} \qquad 3.10$$

The reaction field and continuum treatment will be considered in more detail in Chapter 4, although the above equation 3.10 is presently accepted to be the entire mean square reaction field in accounting for σ_w.

3:5 A Review of Past Continuum Treatments

The presently accepted general equation for σ_w is

$$\sigma_w = -B \langle R_1^2 \rangle \qquad 3.11$$

where $\langle R_1^2 \rangle$ is the mean square reaction field in the solute cavity. Various workers[35, 72, 73] have attempted to characterize σ_w on a continuum basis and presented various equations to this end. The earliest attempts suggested that the equation[72, 73]

$$\sigma_w = -\frac{3}{4} B h g \left[\frac{\nu_1 \nu_2}{\nu_1+\nu_2}\right] \qquad 3.12$$

should be applicable, based on calculations on energies of vaporization of non-electrolytes. The sumbol g is called the reaction field factor that will be precisely defined in the next chapter, and ν_1 and ν_2 are mean absorption frequencies of the solute (1(and solvent (2) molecules. However insufficient data on suitable solvents were used to test the approach in this case. Other workers[74, 75] have studied the continuum model and used it to correct observed shifts in polar systems to obtain information about linear electric field effects on nuclear screening. The conclusions reached were not convincing in respect of the model or the equation used for σ_w.

De Montgolfier[76-79] conducted extensive investigations of σ_w characterized by continuum theories. He concluded that σ_w may be characterized through the equation

$$\sigma_w = -6 \left[\frac{(n^2 - 1)^4}{(2n^2 + 1)^2(n^2 + 2)^2}\right]_{\text{soln.}} \left[\frac{k_1 B \Delta E_1}{\alpha_1}\right]_{\text{solute}} \qquad 3.13$$

where n is the D-line Na refractive index of the energy (essentially the solvent), ΔE, is a complex transition energy of the solute molecule, α_1 is the mean polarizability of the solute molecule and k_1 is effectively a site-factor dependent on the geometry of the solute molecule. Of the theories published to date on the characterization of σ_w, de Montgolfier provided the most consistent explanation of the variation of σ_w with solvent. This is notwithstanding

the efforts of Rummens[80-83] who effectively reiterated the ideas of de Montgolfier[76-79], but rejected the site factor k_1 as having no place in a continuum model. However, Rummens later reintroduced a site factor that appears again to be out of place in a continuum model. The Rummens equation for σ_w is given as[83]

$$\sigma_w = -\frac{6KB\alpha_1 I_1}{a_1^6}\frac{(n_2^2-1)^2}{(2n_2^2+1)^2} S \qquad 3.14$$

where S is the Rummens site factor, I_1 is the ionization energy of the solute molecule, α_1 the mean polarizability of the solute molecule, a_1 the solute cavity radius, n_2 the D-line Na refractive index of the solvent and K a reaction field/site factor constant. Equation 3.14 is probably the most widely accepted continuum equation for σ_w, but it is felt that there are very strong objections to the use of a site factor, such as S, in continuum theory. This contention will be expanded in the next section.

Another important point is that the solute molecule has been treated as being non-polarizable by previous workers, but with polarizability introduced at a later stage of the treatment. It is intended in this thesis to treat the solute as being polarizable ab initio for the sake of consistency in the theoretical treatment.

3:6 A Critique of the Rummens Site Factor

Rummens[83] discounted the site factor of de Montgolfier[77, 79] on the basis that it has no place in a theory dependent on a uniformly polarized cavity surrounding a non-polarizable solute that is considered as a point dipole. Similarly, it is difficult to reconcile Rummens' site factor[83], which accounts for the site of a resonant nucleus in a solute, with the reaction field treatment of a point dipole solute. This observation aside, it appears additionally that there are several oversights in Rummens' approach. Basically, Rummens takes the correctly defined site factor for a pair of molecules in the gas phase, Spair[85, 86], and transposes

this to the liquid phase. The site factor for a pair of molecules is given by[85, 86]

$$S_{pair} = \frac{1 + q^2}{(1 - q^2)^4} \qquad 3.15$$

where $q = d/r$, with d being the distance of the resonant nucleus form the centre of mass of the solute molecule and r is the distance between the centres of masses of the solute and solvent molecules. The above equation 3.15 can be arrived at in two ways. First, it may be derived by averaging the inverse sixth power of the distance between a resonant nucleus and a fixed point in the continuum while the solute freely rotates in its cavity. Second, the equation may equally well be derived by averaging the inverse sixth power of the distance between the nucleus, in a static molecule, and a spherical surface of continuum at a fixed radius from the centre of the solute molecule. Rummens extends this gas phase site factor for a continuum, S_{cont}, by further averaging the inverse sixth power of the distance over the continuum from a distance of the sum of the radii of the solute and solvent (r_{12}) to a distance of infinity (∞). This is correct from a mathematical point of view but Rummens appears to take the average over all shells of continuum from r_{12} to ∞. This is tantamount to averaging over five dimensions, or at least two dimensions twice. Certainly in the derivation[85] of S_{pair} two dimensions are accounted for in considering the shell of the solvent molecule centre about the solute molecule. Thus in the evaluation of S_{cont} it should only be necessary to extend S_{pair} in the remaining radial dimension, viz. into the continuum. In the derivation given by Rummens, S_{cont}, is found to be

$$S_{cont} = \frac{1}{(1 - q^2)^3} \qquad 3.16$$

where q is d/r_{12}.

It is considered here that the derivation of S_{cont} should follow the method described below. The continuum site-factor

$$S_{cont} = \frac{\int_{r_{12}}^{\infty} S_{pair}\, r^{-6} dr}{\int_{r_{12}}^{\infty} r^{-6} dr} \qquad 3.17$$

which is an average over r^{-6} of S_{pair} (equation 3.15) from r_{12} throughout the continuum (to effectively ∞). From equation 3.15 equation 3.17 may be written as

$$S_{cont} = 5r_{12}^5 \int_{r_{12}}^{\infty} \frac{r^2 + d^2}{(r^2 - d^2)^4}\, dr \qquad 3.18$$

Evaluation of this integral[87] (by parts and partial fractions) gives

$$S_{cont} = \frac{5}{6}\left(\frac{1 + q^2}{(1 - q^2)^3} + \frac{3 - 2q^2}{2q^4 (1-q^2)}\right) + \frac{5}{8q^5} \ln\left(\frac{1-q}{1+q}\right) \qquad 3.19$$

For simple systems q varies between 0.2 and 0.4 so that the site factor defined by equation 3.16 varies from 1.13 to 1.69 whereas that defined by equation 3.17 varies from 1.20 to 1.90. It was suggested that the most rigorous test of equation 3.16 (and now perhaps equation 3.16) is the interpretation of the gas-to-infinite dilution chemical shifts of the totally isotropic systems, the group IVB tetramethyls. It was stated[83]

> "... the plots of experimental van der Waals shifts vs. $(n_2^2 - 1)^2/(2n_2^2 + 1)^2$ (the reaction field term) result in approximately parallel straight lines, none of which goes through the origin. Introduction of the site factor (S_{cont} in equation 3.14) makes these plots go through the origin, all with correlation coefficients of about, 0.993..."

By reference to Table 3.1 it is evident that the site factors for

the group IVB tetramethyl systems, as given by equation 3.16, are roughly constant for a given solute molecule. It must also be emphasized that if each of the abscissa values of a linear regression are multiplied by a constant then neither the intercept nor the correlation coefficient will be changed. Consequently, in the present case, it is impossible for these site factors (either from equation 3.16 or equation 3.19) to change the correlations of σ_W vs. f(n) - reaction field term - significantly or, moreover, the intercepts, which must remain finite (Table 3.2). It appears that the use of site factors, both from equations 3.14 and 3.19 in no way improves the characterization of σ_W.

This must throw into question the validity of the currently accepted characterization of σ_W[83]. It may further be argued that the concept of a site-factor is incompatible with a reaction-field theory where the field within the cavity containing the solute molecule must be homogeneous. This has also been pointed out by Foreman[88]. It would appear that the use of a site factor in a reaction field characterization of σ_W appears to be conceptually, mathematically and physically incorrect.

3:7 Past Literature Observations Regarding Continuum Treatments

If the widely accepted treatment of σ_W is in fact incorrect there could be hitherto unrecognised shortcomings in basic continuum theory. In fact such shortcomings have been pointed out in the literature. The intention now is to draw the various observations together in an attempt to more clearly identify the route to improving continuum theory.

Although Onsager's reaction field theory[68] is essentially for polar solute molecules, the theory is assumed to be capable of extension to transient dipole moments and thence non-polar solute molecules and is therefore of fundamental relevance. The conclusion reached by Onsager in his discussion is that his treatment is an incomplete description of continuum theory. It is quoted[68]:

TABLE 3.1 VALUES OF SITE-FACTORS FOR THE GROUP IVB TETRAMETHYL SYSTEMS (EQ. 3.16)

	SOLUTE				
	CMe_4	$SiMe_4$	$GeMe_4$	$SnMe_4$	$PbMe_4$
SOLVENTS					
CMe_4	1.309	1.426	1.452	1.536	1.597
$SiMe_4$	1.294	1.407	1.429	1.509	1.567
$GeMe_4$	1.297	1.410	1.432	1.513	1.571
$SnMe_4$	1.294	1.407	1.429	1.509	1.567
$PbMe_4$	1.299	1.413	1.436	1.517	1.576

TABLE 3.2 REGRESSION ANALYSES OF $-\sigma_M^{30°C}$(KPT) ON $(n_2^2 - 1)^2 / (2n_2^2 + 1)^2$. ^{S}CONT (EQN. 3.19) FOR THE GROUP IVB TETRAMETHYL SYSTEMS

SOLUTE*	CORRELATION COEFFICIENT	INTERCEPT/ppm
CMe_4	0.885	0.100
$SiMe_4$	0.923	0.135
$GeMe_4$	0.918	0.134
$SnMe_4$	0.930	0.148
$PbMe_4$	0.936	0.152

* at infinite dilution in all five group IVB tetramethyl solvents

> "... The present development of the theory is by no means complete... Nevertheless, it appears that the development of the theory...will involve careful consideration of molecular arrangements, and probably some arbitary exercise of judgement..."

Certainly, other researchers such as Kirkwood[89] and Prock and McCankey[90] have agreed with Onsager that continuum/reaction field theory is incomplete. It is stated in the book by Prock and McCankey[90] that

> "...Not taken into account in the Onsager equation are those short range forces, chemical in nature, that exist between molecules in condensed media..."

It has been pointed out by Pullman[91] that there are two principal methods of studying environmental effects in liquids - continuum models and discrete models - both of which have their individual shortcomings.

In papers dealing with nmr and especially in connection with σ_w, the most significant indication of an inadequacy of the continuum model has been given by Buckingham et al[35]:

> "...Two effects may contribute to σ_w:... Interaction between the solute and solvent in its equilibrium configuration...(and)...Departures from the equilibrium solvent configurations will lead to a 'buffetting' of the solute and hence to a time dependent distortion of the electronic structure..."

It will be seen later that this is the general theme of the characterization of σ_w in this thesis.

From some excellent work on medium effects on nuclear screening by Raza and Raynes[92] it was concluded that:

> "...the tentative, but physically reasonable, conclusion that the magnitude of σ_w depended primarily upon the amount of 'exposure' to the solvent experienced by the solute proton..."

which indicate that something more than a simple reaction field approach is required. When reporting on a factor analysis on a group of data with respect to solvent effects on nuclear screening, Bacon and Maciel[93] stated that:

> "...a factor was missing and that a re-examination of the premises on which solvent effect contributions, particularly dispersion shifts, are based is required..."

It has been concluded also by Buckingham[94], in consideration of σ_E, that the resonant hydrogen nuclei, which are generally on or close to the periphery of the molecule, are:

> "...therefore exposed to direct contact with the surrounding molecules,..."

In fact it has been suggested by Lumbroso-Bader et al[95] that neighbouring solvent molecules must be included in a reaction field characterization of nuclear screening such that the influence of the solvent medium should be considered in terms of a continuum approach and the electrical part of solvent effects as due to a specific solute-solvent interaction.

A paper that directly throws into doubt the state of reaction field theories with respect to nmr screening is by Laszlo[40, 96] and Musher[96] who concluded that:

> "...the reaction-field is not adequately given by $R = [(n^2 - 1) / 3\alpha] [(\epsilon - 1) / (\epsilon + n^2/2)] \mu$ or by expressions from other presently available theories..."

Of interest is the suggestion by Coulson[97] in a general overview of dielectrics approaches to intermolecular forces that:

> "...near neighbour solvent molecules must be treated differently (to the remaining solvent)..."

The above literature quotations, suggesting that continuum theory is probably incomplete, are by no means exhaustive. However, the few examples shown here are sufficient to stimulate the need founded.

3:8 An Outline of the Proposed Extension of Continuum Theory

In view of the analysis of the interacting isotropic oscillators[70, 71] (section 3.2) as desribed by London, it is evident that the square field describing dispersion forces, and thence van der Waals dispersion screening, σ_W, (equation 3.2) may be thought as being made up of two parts. One part being made up from the sums of the mean square reaction fields from the solvent and acting upon the solute molecule: this does not involve any solvent-solute distances in the analysis. The other part is made up from the solvent dipoles creating a square field at the solute

molecule. This latter contribution involves a solvent-solute distance and, unlike the first part, that is of a continuum nature, relies on the discrete nature of the solute and solvent molecules. Thus, even on the approach of London[70, 71], the basic Onsager[68] model appears to be inadequate. On this basis, and with the evidence presented in section 3.7, an outline of the extended continuum approach to be used in this thesis to describe σ_w will be given.

It is proposed that the reaction field contribution must be made up of two parts. These are the classical reaction field of the solute molecule described generally in the way of past workers[68, 69] and a further reaction field from the nearest neighbour solvent molecules. It must be accepted that since van der Waals dispersion forces are being considered, with their inherent r^{-7} dependence, the nearest 'continuum molecules' to the central solute must have a greater effect than the remainder of the continuum. Indeed, these nearest neighbour solvent molecules will be anything but continuum[83, 85, 86] and it is probably not unreasonable to treat these solvents as occupying cavities themselves. If this is so it may be argued that their extra-cavity electric fields may augment the reaction - field of the solute cavity. This continuum-cage type of approach, to accommodate these fields, may be regarded to be an equilibrium type of situation where the configuration of the molecules with respect to the rest of the continuum is taken to be static, other than electron oscillations.

It will be shown that there is a need for yet another square field term to describe the more discrete solute-solvent encounters. This discrete part of the square field effect will be considered from the point of view of solute-solvent peripheral atom encounters with the molecules having a finite shape and size, rather than being

treated as point dipoles. Such a non-equilibrium situation may be thought of as being a molecular "buffetting" interaction between the solvent and solute peripheral atoms. The idea of a non-equilibrium "buffetting" effect was expressed by Buckingham et al,[35] at the early stages of the application of continuum models to σ_w, although in a different sense to that presented in this thesis.

Bases on the proposals expressed for σ_w in terms of square field effects (equation 3.2) may be assumed to be written as

$$\sigma_w = -B(\langle R_1^2 \rangle + \langle E_2^2 \rangle + \overline{E}_{B1}^2) \qquad 3.18$$

where $\langle R_1^2 \rangle$ is the mean square solute reaction field, $\langle E_2^2 \rangle$ is the extra cavity square field of the solvent molecules surrounding the solute molecule and $\overline{E}_{B1}^2$ is the square of the "buffetting" field due to the solvent-solute non equilibrium encounters.

The application of reaction field theory to σ_w will now be developed and the effects of more specific molecular encounters on σ_w will be attempted on a somewhat classical basis.

CHAPTER 4

THE APPLICATION OF REACTION FIELD THEORY TO THE REFORMULATION OF THE VAN DER WAALS NUCLEAR SCREENING CONSTANT

4:1 Introduction

The reaction field concept outlined in section 3.4 will now be considered in more detail and then extended in an effort to more completely describe σ_w. To facilitate this the historical back ground to the development of reaction field theory and continuum models will be discussed initially and the philosophy behind the approach undertaken in the work will be presented in outline.

The consequences of treating a molecule as a point dipole at the centre of a cavity surrounded by continuum were investigated initially[98] by using a model of an ion treated as a charged conducting sphere surrounded by a continuous dielectric. Such a model facilitated considerable progress in the theory of electrolytes but is inappropriate for electric moments. A vast improvement was achieved[84] in the latter connection by considering an ideal non-polarizable electric dipole moment at the centre of a spherical cavity in a continuum. It is this approach that has provided the basis of many of the continuum models used to investigate dielectric properties. The basic approach has been adapted with varying degrees of rigour[69, 99-103] including treating the dipole as eccentric and considering the cavity as being ellipsoidal.

Although the type of extensions of the basic model mentioned above can lead to some mathematically elegant and interesting results, the basic model will be adopted herein to afford an adequate treatment of the reaction field/continuum model. This will keep the ensuing mathematical treatment as simple as possible and may provide as accurate a description of the system as might

anything more elegant in view of the approximations that will be encountered later on in the treatment. Perhaps the only significant extension of the basic model is that the dipole will be eventually considered as polarizable.

4:2 The Reaction Field of a Polarizable Point Dipole[69, 101]

As a preliminary to extending conventional reaction field theory the formulation of basic reaction fields will be considered. Attention will be focussed on an electric dipole moment at the centre of a spherical cavity that is surrounded by a continuum medium of solvent. The electric dipole moment polarizes the continuum and this polarization produces an electric field in the spherical cavity that is proportional to the magnitude of the electric dipole moment. This electric field is called the reaction field. To calculate the reaction field, the potential within the cavity due to the dipole itself and due to the interaction of the dipole with the continuum must be known.

If the centre of the dipole is chosen as the origin of a co-ordinate system in which the direction of the z-axis is taken as being along the dipole vector, there is symmetry about the z-axis (fig. 4.1). Because there are no charges present inside or outside the cavity the electric potentials must satisfy Laplace's equation[69], $\nabla^2\phi = 0$. The general solution of Laplace's equation is developed into a series of spherical harmonics, but the axial symmetry of the present system permits the general solution to be written as

$$\phi = -\left(\frac{A}{r^2} + Br\right)\cos\theta \qquad 4.1$$

where A and B are integration constants which have different values inside and outside the cavity, r is the radial distance from the origin and θ is the angle between the radial vector and the z-axis.

The following boundary conditions are appropriate for the solution of this problem; the subscripts 1 and 2 refer to inside and outside the cavity, respectively:

1. ϕ is continuous, viz. $\phi_1(a) = \phi_2(a)$

2. All tangential components of the electric fields produced in the system are continuous, viz. $E_{\theta 1}(a) = E_{\theta 2}(a)$. Since $E_\theta = -(1/r)(\partial\phi/\partial\theta)$ it follows that $\partial\phi_1(a)/\partial\theta = \partial\phi_2(a)/\partial\theta$

3. All normal components of the dielectric displacement are continuous, viz. $D_{r1}(a) = D_{r2}(a)$. Since $D_r = -\epsilon(\partial\phi/\partial r)$ or ϵE_r, it follows that $\epsilon_1(\partial\phi_1(a)/\partial r = \epsilon_2(\partial\phi_2(a)/\partial r)$.

4. As $r \to 0$, or equivalently $a \to \infty$, the field of a dipole in a medium of dielectric constant ϵ_1 is obtained whose potential is defined as $\phi_1(r \to 0) = \mu\cos\theta/\epsilon_1 r^2$

5. Because there is no externally applied electric field, then $\phi_2(r \to \infty) = 0$.

From condition 5 it follows that $B_2 = 0$ and from 4, $A_1 = \mu/\epsilon_1$. Hence the potentials inside and outside the cavity may be written respectively as

$$\phi_1 = \left(\frac{\mu}{\epsilon_1 r^2} - B_1\right)\cos\theta \qquad 4.2a$$

$$\phi_2 = -\frac{A_2}{r^2}\cos\theta \qquad 4.2b$$

From conditions 2 and 3 the values of B_1 and A_2 may be obtained and the more complete expressions for the potentials become:

$$\phi_1 = \left(\frac{1}{\epsilon_1 r^2} - \frac{2(\epsilon_2 - \epsilon_1)}{\epsilon_1(2\epsilon_2 + \epsilon_1)}\frac{r}{a^3}\right)\mu\cos\theta\,, \qquad 4.3a$$

$$\phi_2 = \frac{3\mu\cos\theta}{(2\epsilon_2+\epsilon_1)r^2} \qquad 4.3b$$

The tangential electric fields and radial electric displacements with respect to the radial vector, may be written

$$E_{\theta 1} = -\frac{1}{r}\left(\frac{\partial\phi_1}{\partial\theta}\right) = \left(\frac{1}{\epsilon_1 r^3} - \frac{2(\epsilon_2 - \epsilon_1)}{\epsilon_1(2\epsilon_2+\epsilon_1)a^3}\right)\mu\sin\theta \qquad 4.4a$$

$$E_{\theta 2} = \frac{-1}{r}\left(\frac{\partial \phi_2}{\partial \theta}\right) = \frac{3\,\mu \sin\theta}{(2\epsilon_2 + \epsilon_1)\, r^3} \qquad 4.4b$$

$$D_{r1} = -\epsilon_2 \left(\frac{\partial \phi_1}{\partial r}\right) = \left(\frac{2}{r^3} + \frac{2(\epsilon_2 - \epsilon_1)}{(2\epsilon_2 + \epsilon_1)a^3}\right)\mu\cos\theta \qquad 4.4c$$

$$D_{r2} = \epsilon_2 \left(\frac{\partial \phi_2}{\partial r}\right) = \frac{6\epsilon_2\,\mu\cos\theta}{(2\epsilon_2 + \epsilon_1)\, r^3} \qquad 4.4d$$

It is clear from the above equations (especially 4.4a and b) that the angle θ can only be zero for there to be a constant reaction field in the cavity that is single valued and thus it must be coaxial with the generating dipole. The reaction field, R_1, is therefore

$$R_1 = \frac{2(\epsilon_2 - \epsilon_1)}{(2\epsilon_2 + \epsilon_1)} \frac{\mu}{a^3} \qquad 4.5$$

It has been shown in chapter 3 that equations of the type 4.5, even with site factor modifications, are unable to characterize van der Waals dispersion screening. The reason for this will now be investigated.

4:3 A Critique of Van der Waals Forces Characterized by Reaction Fields

In his treatment of van der Waals dispersion forces, London[70, 71] described the mutual dipolar interaction of two molecules, i.e. the forces are treated as being caused by dipolar electric fields only. This approach requires the values of the dipole moments of the interacting molecules derived from a description of coupled electron oscillators. Essentially, this treatment of van der Waals dispersion interactions is based on a discrete dipole - dipole interaction model. It is noticeable that induced dipole effects were not described in the London[70, 71] treatment probably because the effect may be very small.

An alternative description of van der Waals dispersion forces is through a reaction field (continuum) model. The continuum model

does not recognize the effects of individual molecules other than that in the central cavity represented by the point dipole under study. There is thus no part in continuum theory for the direct effects of the dipolar fields of solvent molecules. It is these effects that London characterized, and if they were included in reaction field approaches they would be treated twice, their effects having already been accommodated in the reaction field. Kirkwoods[89] approach was consistent with these contentions because, even though he considered the moments of nearest neighbour solvent molecules, these were only added to the solute moment in an enlarged cavity and not considered to enhance the moment of the solute material. It is clear that in continuum theory, only reaction fields have to be considered and not primary dipolar fields, although secondary dipolar fields that could originate from the effects of the reaction field may have to be dealt with.

In view of the above contentions it appears, at least superficially, that there is little scope for improving conventional reaction field approaches. However, it does appear that Onsager[68] based approaches may be incomplete for the following reasons. In a pure liquid all molecules must on average have the same properties. Therefore, if one molecule is single out in a cavity, and characterised, every other molecule individually can be treated in the same way. It is important to determine the effects of this. Referring to equations 4.4b and 4.4d, it can be seen that because the electric potentials ϕ_1 and ϕ_2 are continuous at the cavity surface and the former leads to discrete dipolar and reaction fields, these fields must have identities outside the cavity. Equations 4.4b and 4.4d can therefore be rewritten as

$$E_{\theta 2} = \frac{\mu \sin\theta}{r^3} - \frac{Ra^3 \sin\theta}{2r^3} \qquad 4.6a$$

$$D_{r2} = \frac{2\mu \cos\theta}{r^3} + \frac{Ra^3 \cos\theta}{r^3} \qquad 4.6b$$

As has just been emphasised continuum theory is not concerned with

dipolar fields but merely with reaction fields. In reference to these it has been argued that θ must be zero. In consequence the only effect of concern is

$$D_{r2} = \frac{Ra^3}{r^3} \qquad 4.7$$

When the selected solvent cavity is remote from the solute molecule, now considered a constituent of the continuum, D_{r2} is vanishingly small. However, the situation is different when the solvent cavity contacts the solute molecule. In this situation $D_{r2} = R/8$ ($D_{r2}^2 = R^2/64$) at the centre of the solute and its polarizing influence on the molecular (point) dipole can be ignored. However, at the periphery of the solute, where atoms are usually located for which chemical shifts may be studied, $D_{r2} \simeq R$ and the influence of the solvent molecule must be considered. Therefore a term, designated R_2, must be included with R_1 in a continuum treatment of the solute molecule.

If solvent molecules polarize the peripheral atoms of a solute molecule, so must the solute molecule polarize the peripheral atoms of the solvent molecules. The polarization of the solvent atoms generates local dipoles (stemming from reaction field considerations and not inherent) that will cause a perturbation of the adjacent atoms of the solute. It is evident, therefore, that this, a third effect, must be included with R_1 and R_2. The intention now is to consider R_1 and R_2 and leave the third (second order) effect until chapter 5.

4:4 The Primary Reaction Field, R_1, and its Contribution to σ_w

In the Onsager model[68], the cavity is treated as being evacuated such that $\epsilon_1 = 1$ and the expression 4.5 for R_1 becomes

$$R_1 = \frac{2(\epsilon_2 - 1)}{(2\epsilon_2 + 1)} \frac{\mu}{a^3} \qquad 4.8$$

The formula $2(\epsilon - 1)/(2\epsilon_2 + 1)a^3$ is called the reaction field factor and represented by g. Thus for brevity

$$R_1 = g\mu \qquad 4.9$$

This reaction field, produced by the dipole moment μ, will induce further electric moments in the cavity that are proportional to the reaction field, as shown by equations 3.7 and 3.8. Thus the true reaction field must be given by

$$R_1 = g\mu(1 - \alpha_1 g)^{-1} \qquad 4.10$$

where α_1 is the solute mean polarizability.

Because the present treatment relates to non-polar molecules the only relevant dipole moment is a transient one. Although the conventional theory is strictly for a permanent dipole moment, it will be assumed that the theory is directly transposable to transient dipole moments. Because σ_w is governed by square electric dipole moments

$$\langle R_1^2 \rangle = g^2 (1 - \alpha g)^{-2} \langle \mu^2 \rangle \qquad 4.11$$

or written in terms of dielectric constants and refractive indices

$$\langle R_1^2 \rangle = \frac{4(n_1^2 + 2)^2 (\epsilon_2 - 1)^2}{9(2\epsilon_2 + n_1^2)^2} \frac{\langle \mu^2 \rangle}{a^6} \qquad 4.12$$

by employing the expression[68] $(n_1^2 - 1)/(n_1^2 + 2) = \alpha_1/a^3$ and the formula for g. Inherent in this is the acceptance of the cavity radius, being given by the approximate expression

$$4\pi Na^3/3 = 1 \qquad 4.13$$

where N is the number of solute molecules per unit volume and identical to L/V_m, where L is Avogadro's number and V_m the molar volume of the solute. The choice of a has been contentious; Bell[34] suggested that a should be the kinetic radius of the molecule and Kirkwood[89] along with Frölich[69] suggested that a should be an order of magnitude greater than the molecular radius. The Onsager cavity radius (equation 4.3) is between the above mentioned two suggestions and is consistent with the theory being used.

Thus, the mean square reaction field of a polarizable point dipole, may be written

$$\langle R_1^2 \rangle = \left(\frac{8\pi L}{9V_m}\right)^2 \frac{(n_1^2 + 2)^2 (n_1^2 - 1)^2}{(2n_2^2 + n_1^2)^2} \langle \mu_i^2 \rangle \qquad 4.14$$

where n_2^2 has been substituted for the dielectric constant ϵ_2 of the isotropic solvent (strictly only true at infinite frequency).

It must be stressed once again that the above treatment is based on an oversimplified model because in reality a molecule is not a point and there is no such thing as a microscopically indivisible continuum; also, no account is taken of fields produced by higher electric moments of the solute molecule.

4:5 The Extra-Cavity 'Reaction Field' of the Solvent, R_2

The earlier suggestion (section 4:3) that near neighbour solvent molecules should be treated differently to the rest of the continuum is consistent with the implications of the quotations from the literature given previously in section 3:7. Rummens[83] considered this as justification for the introduction of a site-factor[83] to account for deficiencies in the fundamental approach. The present contention is that this is necessary and that R_2 has to be included in reaction field theory.

At this stage it is interesting to observe Kirkwood's[89] modification of the Onsager[68] treatment of polar molecules in an external field. His treatment resulted in a specific effect from the solute molecule and its nearest neighbours. This bears some similarity to the proposed inclusion of R_2 with R_1. Kirkwood related the dipole moment, μ, of a single molecule and the total moment, $\bar{\mu}$, of that molecule and its Z nearest neighbours through the following equation:

$$\mu\bar{\mu} = \mu^2(1 + Z\overline{\cos}\,\gamma) \qquad 4.15$$

where $\overline{\cos}\,\gamma$ is the average value of the energy weighted cosines of the angles between the dipole moment of the central molecule and those of its near neighbours. In the present context interest is focussed on $\langle \mu^2 \rangle$ and it would be interesting to entertain an

adaptation of equation 4.15 for this. However, this would create several fundamental problems. If Z was equated to twelve, corresponding to close packing[36], and $\overline{\cos}\ \gamma$ to $1/\sqrt{3}$ for the average orientation of the dipoles, the values of $\langle R^2 \rangle$ evaluated by the unacceptably high factor of about eight. Additionally, the dimensions of the effective cavity would be unclear[89]. Nevertheless, there is an attraction to the Kirkwood[89] approach, the success of which suggests, along with a comparison of equation 4.14 and 4.15, that the total mean square reaction field may best be described by a sum of two terms; one similar to equation 4.14 and an additional one from the effect of the nearest neighbours. It is now proposed that this may be achieved by a simple extension of the Onsager approach without recourse to the Kirkwood principles.

When considering the effect of R_1 on nuclear screening it would appear necessary to evaluate the time average effect of $\langle R_1^2 \rangle$ directly at the relevant nucleus. However, reference to equations 4.4a and 4.4c and the accepted formula

$$\bar{R} = \bar{\mu} g\ (1 - \alpha g)^{-1} \qquad 4.16$$

reveals that not only are R and μ directly proportional but co-linear. Therefore referring to figure 4.1, if a molecule is considered to contain a peripheral resonant nucleus this would have to be considered to not always experience the effect of $\langle R_1^2 \rangle$ and on time average some absurdly small factor of this. This apparent paradox is avoided by evaluating the square field $\langle R_1^2 \rangle$ that is responsible for the van der Waals force[69, 72] on the whole molecule. Because this solute molecule is considered to be uniformly polarizable it follows that any atom anywhere within it is subject to $\langle R_1^2 \rangle$ and that this may be used in the evaluation of the screening of individual nuclei. The treatment of $\langle R_2^2 \rangle$ must conform with the underlying principle.

In view of the above contentions it is necessary to evaluate the total square field function of R_2 that causes the van der Waals

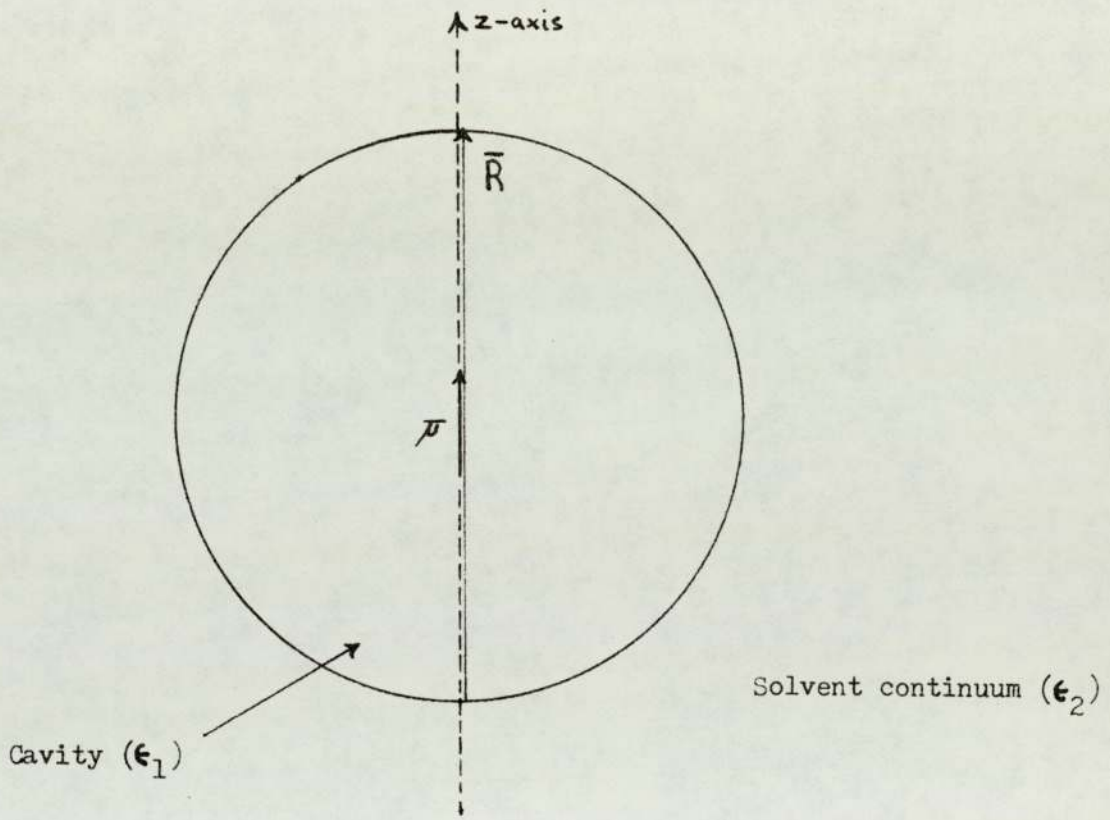

Fig. 4.1 A solute cavity in the solvent continuum.

force on molecule 1 and assume that this is responsible for screening the relevant nuclei. As shown earlier $\langle R_2^2 \rangle$ is only effective at peripheral atoms but these must be considered purely as part of the uniformly polarizable solute molecule. Therefore, if there are Z_2 nearest neighbour solvent molecules there must be Z_2 pairwise interactions. The initial problem is to determine how to treat these.

London[71], in describing the dispersion forces between molecules, considered the force between a pair of molecules on a coupled electron oscillator basis and concluded that when considering a many body interaction each pair effect is approximately additive to give the total effect of the interaction. So from the point of view of the model under consideration the R_2 on molecule 1 is the sum of the individual pair effects over all time. Any attempt to argue that the solvent fields are effective at different times is tantamount to saying that the pairwise interactions are not additive and this would be contrary to London's conclusions[71].

If a molecule 1 has one near neighbours of type 2, R_2 may be considered to affect molecule 1 through a cone subtended by the periphery of molecule 1 at the centre of 2, where its dipole is located. This is equivalent to saying that molecule 1 may be considered to be approximately subject to $\langle R_2^2 \rangle$ for $1/Z_1$ of all time (the space between molecules being ignored because electrons cannot couple with nothing) where Z_1 are the number of molecules 1 that can surround a molecule 2. There are however two such cones that can have an influence on molecule 1 - when the moment of 2 is essentially towards molecule 1 and also when away from molecule 1. The pair interaction is thus equivalent to $2/Z_1 \times \langle R_2^2 \rangle$. Because there are Z_2 such pairwise interactions the total effect on molecule 1 is $Z_2 \times 2/Z_1 \langle R_2^2 \rangle$ which becomes $2\langle R_2^2 \rangle$ when $Z_1 = Z_2$. Whilst $\langle R_2^2 \rangle$ is only effective at the periphery of the solute molecule, this molecule has to be considered a uniformly polarizable cavity and the force acting on the whole molecule, considered

due to $\langle R_2^2 \rangle$, which is the field causing the screening of atoms within the molecule. Because its magnitude is evaluated for peripheral atoms it might be argued that it is only really applicable to peripheral atoms and that other values of $\langle R_2^2 \rangle$ would be operative for differently sited nuclei; this point requires further elucidation.

Consistent with the assumption that van der Waals forces between molecules are approximately additive[70, 71], molecules in cavities of the type 2 can only affect the properties of the molecule filling cavity 1, through $2\langle R_2^2 \rangle$ for a pure liquid or at least for molecules of the same size. In the present context, therefore, any property arising from van der Waals forces must depend on $\langle R_1^2 \rangle + 2\langle R_2^2 \rangle$ for a molecule in the bulk of a pure liquid. Therefore when molecule 1 is surrounded by twelve molecules (approximately for a pure liquid) it follows from equation 4.14 that the total mean square reaction field $\langle R_T^2 \rangle$ is given by

$$\langle R_T^2 \rangle = \left(\frac{8\pi L}{9V_m} \right)^2 \frac{(n^2 - 1)^2 (n^2 + 2)^2}{9n^4} \left(\langle \mu^2 \rangle + 2 \langle \mu^2 \rangle \right) \qquad 4.17$$

This is arranged in the form of equation 4.15 to demonstrate the similarity between the outcome of this approach and that of Kirkwood[89].

In the case of solutions of compound 1 very dilute in a different solvent 2 the relevant square reaction field is given by

$$\langle R_T^2 \rangle = \frac{64\pi^2}{81} \left\{ \frac{\langle \mu_1^2 \rangle}{V_1^2} \frac{(n_1^2 + 2)^2 (n_1^2 - 1)^2}{(2n_2^2 + n_1^2)^2} + \right.$$

$$\left. \frac{f\langle \mu_2^2 \rangle}{V_2^2} \frac{(n_2^2 + 2)^2 (n_2^2 - 1)^2}{9n_2^4} \right\} \qquad 4.18$$

where $f = Z_2 \times 2/Z_1$. It can be shown, by consideration of the formula for the close packing of spheres[36], that

$$Z_1 = \pi((r_1 + r_2)/r_1)^2$$

and thence f becomes $Z_2 \times 2 \sin^2 (\theta/2)/\pi$ where θ is the angle subtended by the periphery of 1 at the centre of 2 where 1 and 2

are considered as spherical cavities, in contact. This is illustrated in figure 4.2. For molecules whose radii (calculated from equation 4.13) are not too dissimilar, as in the case of the molecules (solutes and solvents) considered in this thesis, it can be shown that the value of $\sin^2(\theta/2)$ is about the same as the value of $\theta/4$, with θ measured in radians. Replacing $\sin^2(\theta/2)$ by $\theta/4$, for convenience, the expression for f in equation 4.18 maybe written as $Z_2\theta/2\pi$.

To summarize therefore, it is proposed that the total reaction field effect can be written as the sum of two terms (equation 4.18):

$$\langle R_T^2 \rangle = \langle R_1^2 \rangle + \langle E_2^2 \rangle \qquad 4.20$$

where $\langle R_1^2 \rangle$ is defined by equation 4.14 and $\langle E_2^2 \rangle$ by

$$\langle E_2^2 \rangle = f\langle R_2^2 \rangle \qquad 4.21$$

Thus the van der Waals screening, which is also taken to be directly additive,[104-106] in terms of reaction fields is

$$\sigma_{RF} = -B\langle R_T^2 \rangle \qquad 4.22$$

where B is the square field screening coefficient.

In order to test the validity of the reaction field theory as proposed above it is necessary to formulate an explicit expression for the mean square dipole moment $\langle \mu^2 \rangle$ and this will be outlined in the next section. Then, by judicious choice of the appropriate systems, that are compatible with the inherent theoretical principles, equations 4.18 and 4.22 will be tested using the appropriate data (table 4.6).

4:6 The Expression for $\langle \mu^2 \rangle$

Both the direct and indirect square reaction fields depend on the value chosen for $\langle \mu^2 \rangle$. Methods of obtaining $\langle \mu^2 \rangle$ include the use of Slater screening parameters[107], diamagnetic susceptibilities[108], and polarizability measurements[109] and the expression for a quantum mechanical oscillator[70, 71]. The values of $\langle \mu^2 \rangle$ obtained from the expression for a quantum mechanical oscillator,

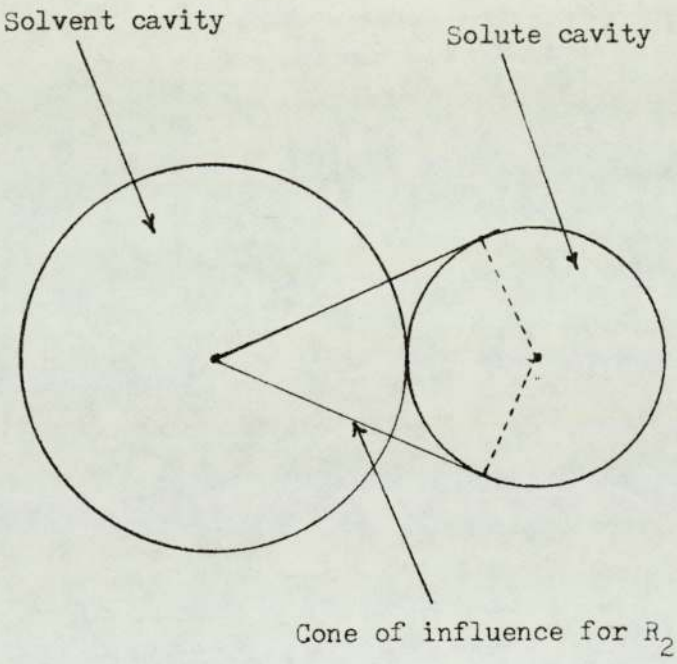

Fig. 4.2 Cone of influence for R_2 with solute and solvent cavities imagined to be in contact.

$$\langle \mu^2 \rangle = 3\alpha h\nu / 2 \qquad 4.23$$

and polarizability measurements agree quite well, but differ from those obtained from diamagnetic susceptibility measurements and Slater screening parameters.

The quantum mechanical oscillator expression will be used because of its relative simplicity and its direct relevance to the foundation of the London dispersion forces[70, 71] which form the very basis of this thesis. In the quantum mechanical oscillator expression, $h\nu$ is set to twice the value of the ionization energy[110], I, of the molecule concerned. Equation 4.23 is rewritten as

$$\langle \mu^2 \rangle = 3\alpha I \qquad 4.24$$

The idea that $h\nu = 2I$[110] is still a matter of contention, though it will be used in this work.

4:7 Tests of the Reaction Field Equation

4:7a Gas-to-Solution ^{1}H Chemical Shifts of the Group IVB Tetramethyls

The most suitable systems with which to test the reaction field screening as described by equation 4.22, are perfectly isotropic systems. Systems that fall into this category are probably the group IVB tetramethyls. Each of the five compounds can be taken in turn as solutes in each of the five solvents. The zero density gas-to-infinite dilution chemical shifts of these systems have been measured[78] and the relevant data are tabulated in tables 4.1 and 4.2. For each solute molecule in the five solvents a linear regression analysis of the gas-to-solution ^{1}H chemical shift on $\langle R_T^2 \rangle$ is performed and the significance of the correlation is determined using Spearman's correlation test[111]. The results are given in table 4.3.

If equation 4.22 is a totally accurate description of σ_w, the linear regression analysis should give a correlation coefficient of unity, a gradient equal to the screening coefficient, B, which

TABLE 4.1 DATA FOR THE GROUP IVB TETRAMETHYLS

	$\alpha^{67}/10^{-24}CM^3$	$I^{67}/10^{-12}erg$	V_M^{67}/CM^3	$n^{2\ 81}$
CMe_4	10.2	16.6	124.6	1.7902
$SiMe_4$	11.9	15.7	139.5	1.8266
$GeMe_4$	12.8	14.7	138.2	1.9088
$SnMe_4$	14.4	13.2	139.5	2.0541
$PbMe_4$	15.9	15.7	135.9	2.2644

TABLE 4.2 VALUES OF $-\sigma_{w\,(EXPT)}^{30^{\circ}C}$ 67 AND $\langle R_T^2 \rangle$ (EQUATION 4.18) FOR THE GROUP IVB TETRAMETHYL SYSTEMS

SOLUTE	CMe_4		$SiMe_4$		$GeMe_4$		$SnMe_4$		$PbMe_4$	
SOLVENTS	$-\sigma_w$/ppm	$10^{-12}\langle R_T^2\rangle$/esu	$-\sigma_w$/ppm	$10^{-12}\langle R_T^2\rangle$/esu	$-\sigma_w$/ppm	$10^{-12}\langle R_T^2\rangle$/esu	$-\sigma_w$/ppm	$10^{-12}\langle R_T^2\rangle$/esu	$-\sigma_w$/ppm	$10^{-12}\langle R_T^2\rangle$/esu
CMe_4	0.217	0.089	0.255	0.086	0.260	0.087	0.280	0.088	0.285	0.092
$SiMe_4$	0.185	0.088	0.228	0.084	0.228	0.085	0.250	0.086	0.258	0.091
$GeMe_4$	0.215	0.102	0.262	0.098	0.260	0.100	0.280	0.101	0.287	0.106
$SnMe_4$	0.222	0.127	0.270	0.122	0.257	0.124	0.297	0.125	0.302	0.133
$PbMe_4$	0.277	0.181	0.322	0.175	0.325	0.178	0.350	0.178	0.358	0.188

TABLE 4.3 LINEAR REGRESSION ANALYSES AND SIGNIFICANCE LEVELS OF $-\sigma_w^{30^\circ C}$ (EXPT) ON $\langle R_T^2 \rangle$ FOR THE GROUP IVB TETRAMETHYL SYSTEMS

SOLUTE *	CORRELATION COEFFICIENT	SIGNIFICANCE LEVEL	GRADIENT $= 10^{-18}$ B/esu	INTERCEPT /ppm
CMe_4	0.933	$5\% < P < 10\%$	0.81	0.128
$SiMe_4$	0.953	$P < 1\%$	0.87	0.169
$GeMe_4$	0.950	$P = 5\%$	0.87	0.170
$SnMe_4$	0.960	$P = 5\%$	0.92	0.185
$PbMe_4$	0.966	$P < 1\%$	0.88	0.190

* solute at infinite dilution in all five group IVB tetramethyls as solvents.

for the hydrogen atom is[90, 112, 113] between 0.74×10^{-18} esu and 1×10^{-18} esu, and a zero intercept. It can be seen from table 4.3 that the regressions are very good and are significant. The B-values obtained (average of 0.87×10^{-18} esu) are within the range expected[90, 112, 113] but there is a non-zero intercept that is unaccounted for in equation 4.24. It would appear, therefore, that the reaction field description described in this chapter is, as expected, an incomplete one and there is an additional effect still to be characterized.

4:7b Van der Waals a-Values

A more exacting test of reaction field theory than its application to nmr chemical shifts, would be to calculate a very fundamental van der Waals parameter. Such a parameter is the a-value in the van der Waals equation of state[114, 115], and this will now be considered.

In a liquid (or gas) the molecules will experience balanced forces from molecules on all sides. However, the molecules near the surface will be pulled in toward the interior of the liquid by the unbalanced attractions of their neighbours below the surface. The total force on one surface molecule will be proportional to the number of molecules that pull it downwards and thence the density of the fluid. The total force on all the surface molecules will also be proportional to the density and the force on each molecule Thus the force on the surface molecules may be written in terms of the proportionality

$$F \propto \left(\frac{N}{V}\right)^2 \qquad 4.25$$

where N is the number of molecules per volume, V. The force on the molecules in a unit of surface area is termed the internal pressure and given by

$$P_{INT} = a\left(\frac{N}{V}\right)^2 \qquad 4.26$$

where a is a proportionality constant characteristic of the liquid or gas being considered.

For gases at high density or for liquids the volume at the disposal of a molecule of the gas or liquid is less than the bulk volume of the fluid by Nb, where b is the effective volume of one molecule. With the corrections involving a and b the perfect gas equation

$$PV = NkT \qquad 4.27$$

for a system of N molecules must be amended to the classical van der Waals equation of state, which, to some extent, is accepted to be applicable to liquids[114] as well as gases;

$$\left(P + a\left(\frac{N}{V}\right)^2\right)\left(V - Nb\right) = NkT \qquad 4.28$$

It appears therefore that a serves as the most fundamental measure of intermolecular foces, especially dispersion forces, between molecules and should be amenable to characterization by reaction field theory.

For a molecule i in a continuum made up from molecules of type j, the pairwise potential energy may be expressed by u_{ij}. The total potential energy of the molecule may, to a first approximation, be written as the sum of the pair potential energies:

$$U_i = \sum_{i<j} u_{ij} \qquad 4.29$$

For a continuum the sum may be replaced by an integral over the volume of the continuum and thus equation 4.29 becomes:

$$U_i = N_j \int_{\sigma}^{\infty} u_{ij} d^3r \Big/ \int_{\sigma}^{\infty} d^3r \qquad 4.30$$

where N_j is the number of molecules j, $d^3r = 4\pi r^2 dr$ the volume element of continuum a distance r from i, and σ is the effective radius of molecule i. If $j \gg 1$, $N_j = N$ and it may be written that

$$U_i = \frac{N}{V_N} \int_o^a u_{ij} d^3r \qquad 4.31$$

where $V_N \approx \int_\sigma^\infty d^3r$, the volume of the system. At the wall or surface of the fluid there is only a nett force into the medium and thus

$$U_i\,(\text{WALL}) = \frac{1}{2} U_i \qquad 4.32$$

or,

$$U_i\,(\text{WALL}) = \frac{N}{2V_N} \int_\sigma^\infty u_{ij} d^3r \qquad 4.33$$

The energy of molecule i in terms of a reaction field may be given by[69, 75] the expression

$$U_i = -\frac{1}{2} \alpha_i \langle R_T^2 \rangle \qquad 4.34$$

where α_i is the polarizability of molecule i. Therefore $U_i(\text{WALL})$ may be written as

$$U_i\,(\text{WALL}) = -\frac{1}{2} \alpha_i \langle R_{SUR}^2 \rangle \qquad 4.35$$

The expression for a, in terms of pair potentials,[115] is

$$a = -\frac{1}{2} \int_\sigma^\infty u_{ij} d^3r \qquad 4.36$$

and thence from equations 4.33, 4.35, and 4.36

$$a = \frac{1}{2} \alpha_i \langle R_{SUR}^2 \rangle V_i \qquad 4.37$$

where $V_i = V_N/N$, the molecular volume. Van der Waals a-values (and b-values) are generally quoted in a molar rather than molecular sense in order to be directly comparable to the more conventionally written van der Waals equation of state[115]:

$$\left(P + \frac{a}{V^2}\right)(V - b) = LkT \qquad 4.38$$

where a in equation 4.38 is the a of equation 4.28 times L^2 ($L \simeq 6.023 \times 10^{23}$ molecules mol^{-1}). Rewriting equation 4.37, therefore, in order to be compatable with equation 4.38 rather than equation 4.28, leads to:

$$a = \frac{L}{2} \alpha_i \langle R^2_{SUR} \rangle V_M \qquad 4.39$$

where V_M is the molar volume of the fluid ($=LV_i$).

The reaction field and its effect on a surface molecule is different to the reaction field and its effect on a molecule in the interior of a liquid. A non-polar molecule in a cavity, 1, at the surface of a liquid will only be surrounded by continuum for one half of the cavity surface. Because reaction fields may be imagined to arise from the apparent charges at the interface of the cavity and continuum it is envisaged that the cavity potential will be halved at the surface compared to the bulk of the liquid. This is equivalent to the modification of equation 4.31 to 4.32. Thence the reaction field in a surface cavity is only half of that for a cavity in the bulk ($R_1/2$). The all important mean square reaction field in a surface cavity is therefore $\langle R^2_1 \rangle /4$ and this would be the total square field using Onsager's theory[68]. However, the effect of the reaction field extension from neighbouring molecules must also be considered.

In the surface of a liquid there is also an imbalance of the forces stemming from $\langle R^2_2 \rangle$, acting on the surface molecules due to the removal of neighbouring molecules immediately above the surface. Thus the imbalance must be considered from the point of view of the effect of R_2 on molecule 1 from the diametrical molecules immediately below the surface; the effects of 'in-surface' molecules 2 are ineffective in contributing to the internal pressure. The force on molecule 1 due to these three, for a pure liquid, 'subsurface' molecules is thus $3 \times 2 \langle R^2_2 \rangle / z_1$, or $\langle R^2_2 \rangle /2$, assuming that there are twelve near neighbour molecules about any given molecule in the bulk. This is consistent with the argument in section 4.5. Therefore, the total square field contributing to the forces on a molecule 1 in the surface of a

liquid is $\langle R_1^2 \rangle /4 + \langle R_2^2 \rangle /2$, which for a pure liquid becomes

$$\langle R_{SUR}^2 \rangle = 3\langle R_1^2 \rangle /4 \qquad 4.40$$

Effectively equation 4.39 may be written, for a pure liquid, as

$$a = \frac{3}{8} L \alpha_i \langle R_1^2 \rangle V_M \qquad 4.41$$

If α_i is in the units of cm^3 molecule^{-1}, V_M in cm^3 mol^{-1} and the reaction field in cgs esu units, a will be in cm^3 erg mol^{-2}. However, because the reference values used[116] for comparison with the values calculated e#press a in the units of l^2 atmmol^{-2} these latter units will be adhered to in this thesis. This necessitates the modification of equation 4.41 to

$$a\ (l^2\ atm mol^{-2}) = 2.229.10^{11} \alpha_i \langle R_1^2 \rangle V_M \qquad 4.42$$

with the units of α_i, V_M and $\langle R_1^2 \rangle$ as suggested above.

Table 4.4 gives the calculated (equation 4.42), using data from table 4.6, and tabulated[116] values of a. It can be seen that although in many instances the values predicted using equation 4.42 are low, the agreement between these and the literature values is better than would be expected using the value of $\langle R_{SUR}^2 \rangle$ based on a Onsager-only approach, where $\langle R_{SUR}^2 \rangle$ would be $\frac{1}{4}\langle R_1^2 \rangle$. Although it must be accepted that a is a gas phase parameter evaluated using a liquid phase theory and that there is probably a temperature effect on van der Waals a-values[114, 116], that might explain the discrepancy between literature and calculated values it could also be concluded that reaction field theory does not completely describe the fields responsible for van der Waals forces. This work, on van der Waals a-values, will be extended in chapter 7.

4:7c Heats of Vaporization

Linder[73] stated that the potential energy of a liquid should be approximately equal to the negative of the energy of vaporization, although this assums that the rotation, translation and vibration of each molecule is the same in the liquid and gas phase.

TABLE 4.4 VAN DER WAALS a-VALUES-I

SPECIES	a-VALUE/l^2 atm mol^{-2} TABULATED[115]	CALCULATED (EQN. 4.42)
Ar	1.345	0.77
Kr	2.3	1.23
Xe	4.194	3.99
CH_4	2.253	2.56
CMe_4	16.49*	8.16
$SiMe_4$	18.07*	10.05
C_6H_{12}	22.81	15.03
1, 3, 5 $(CH_3)_3$ C_6H_3	34.39	26.95
C_6H_6	18.	17.64
C_2H_2	4.39	2.58
C_2H_4	4.472	7.42
C_2H_6	5.489	7.92
H_2	0.241	0.05
SiF_4	4.195	1.21
CCl_4	20.39	20.57

* calculated from critical data

$l l^2$ atm mol^{-2} = 0.1013 Jm^3 mol^{-2}

This latter assumption is seldom satisfied and there is no assurance that the energy of vaporization would correctly give the interaction potential. However, for the purposes of this thesis it will be accepted, at least initially, that the potential energy of a liquid and its negative energy of vaporization are the same.

Adopting the expression[69, 72] for the potential energy of a non-polar molecule in a static electric field for the case of a reaction field and the above assumption that the potential energy and the negative of the energy of vaporization are equal, the energy of vaporization, E^{VAP}, may be written, in molar terms, as

$$E^{VAP} = \alpha_L \langle R^2 \rangle / 2 \qquad 4.43$$

At low vapour pressures, the vapour, in equilibrium with its liquid, is essentially ideal, and the negative energy of vaporization, $-E^{VAP}$, defined as the energy in taking a molecule from the liquid to the gas at zero pressure, may be replaced[117] by ΔE^{VAP}. ΔE^{VAP} is the difference in energy between the vapour phase and the liquid phase and may in turn be replaced[117] by $\Delta H^{VAP} - LkT$, where ΔH^{VAP} is the enthalpy or heat of vaporization.

Because vaporization takes place from the surface of a liquid it is porposed that the reaction field expression should be appropriate for the surface of a liquid and the expression for ΔH^{VAP} is

$$\Delta H^{VAP} = \alpha_L \langle R^2_{SUR} \rangle / 2 + LkT \qquad 4.44$$

It is shown in table 4.5 that the calculated ΔH^{VAP} (equation 4.44), using the data in table 4.6, does not correspond with the literature value[116] of ΔH^{VAP}, although it is better than would be found on the basis of an Onsager reaction field treatment alone. However, more will be done towards the characterization of ΔH^{VAP} in chapter 7 when the shortcomings of this treatment will also be discussed.

TABLE 4.5 HEATS OF VAPORIZATION -I

SPECIES	Temp. Range	ΔH^{VAP}_{EXP} [116] (kJ mol^{-1})	ΔH^{VAP}_{CALC} (Eqn. 4.44)* (kJ mol^{-1})
Ne	16 - 43	2.047	0.36
Ar	55 - 148	7.273	3.70
Kr	73 - 207	10.283	4.47
Xe	105 - 165	15.843	9.91
CH_4	67 - 187	8.898	11.01
CMe_4	171 - 425	23.611	9.32
$SiMe_4$	191 - 451	26.916	10.19
$SnMe_4$	222 - 351	33.013	15.95
$PbMe_4$	244 - 383	36.967	26.96
C_6H_{12}	228 - 530	32.733	17.63
C_6H_6	236 - 563	34.052	24.07
CCl_4	223 - 549	31.888	25.38
C_2H_2	130 - 308	19.503	8.60
C_2H_4	105 - 282	14.436	20.98
C_2H_6	113 - 297	15.631	20.95
1, 3, 5 $(CH_3)_3$ C_6H_3	283 - 438	43.960	23.48
SiF_4	129 - 252	22.113	3.60
H_2	10 - 31	1.048	0.33

* LkT taken as the average over the temperature range quoted with ΔH^{VAP}_{EXP}

TABLE 4.6 PHYSICAL CONSTANTS OF SOME SPECIES CONSIDERED ($\simeq 30^{\circ}C$)

SPECIES	$\alpha/10^{-24}cm^3$	$I/10^{-12}erg$	V_m/cm^3mol^{-1}	n^2
Ne	0.396[73]	34.5[73]	16.7[118]	1.1908[a]
Ar	1.644[73]	25.2[73]	28[118]	1.5215[a]
Kr	2.486[73]	22.4[73]	38.9[118]	1.5765[a]
Xe	4.021[73]	19.5[73]	47.5[118]	1.8149[a]
CH_4	2.55[119]	20.9[116]	$\simeq 30$[67]	1.8187[a]
C_6H_{12}	10.9[67]	15.7[67]	108.5[67]	2.0264[116]
C_6H_6	9.87[119]	14.8[116]	88.9[67]	2.2420[116]
1, 3, 5 $(CH_3)_3C_6H_3$	15.4[119]	13.5[116]	138.9[116]	2.2482[116]
C_2H_2	3.33[119]	18.3[116]	42.3[115]	1.7453[a]
C_2H_4	4.26[119]	16.8[116]	40[67]	2.1023[a]
C_2H_6	4.47[119]	18.4[116]	43[67]	2.0667[a]
$CH_3C{=}CCH_3$	7.15[b]	15.9[116]	78.3[116]	1.9380[116]
$(CH_3)_2C{=}C(CH_3)_2$	11.68[b]	13.3[116]	118.9[116]	1.9943[116]
$Si(OCH_3)_u$	12.9[a]	14.8[c]	150.3[121]	1.8301[116]
$Si(CH_2CH_3)_4$	19.2[67]	15.7[67]	190.2[67]	2.0295[81]
$Si(OCH_2CH_3)_4$	20.41[a]	14.8[c]	224.0[67]	1.8961[116]
$C(NO_2)_4$	8.96[b]	17.5[116]	120[121]	2.0690[116]
H_2	0.81[119]	24.72[116]	28.8[116]	1.2293[a]
CF_4	2.89[32]	28.5[32]	66.8[120]	1.3248[a]
SiF_4	3.33[32]	27.1[32]	62.7[120]	1.4642[a]
SF_6	4.53[32]	30.9[32]	77.7[120]	1.5174[a]
C_6F_6	10.1[119]	15.0[116]	117.4[120]	1.8312[a]
CCl_4	10.5[67]	18.3[67]	97.0[67]	2.1144[81]
CBr_4 ($\simeq 100^{\circ}C$)	15.2[b]	16.8[c]	112.7[115]	2.5568[116]
1, 4 $C_4H_8O_2$	8.73[67]	15.2[67]	86.2[67]	2.0296[a]

a. Estimated from the Lorentz-Lorenz formula[90].

b. Estimated from data in ref. 119.

c. Estimated from data on similar compounds.

CHAPTER 5

THE EFFECT OF STERICALLY CONTROLLED MOLECULAR ENCOUNTERS ON THE VAN DER WAALS NUCLEAR SCREENING CONSTANT

5:1 Introduction

It was proposed in the last chapter that there is a further contribution, yet to be taken into account, in the characterization of σ_W besides the reaction field contribution. The suggestion was that this originates with the polarization of peripheral solvent atoms by the equivalent of R_2. Therefore it was not surprising to find that there was some factor missing in the analysis of the results in section 4.6. However, the statistical significance and excellent correlation found in the regressions of σ_W on $\langle R_T^2 \rangle$ indicate that this further effect may be approximately the same in similar systems. Before attempting to characterize this, secondary, non-reaction field, effect it is interesting to look into some past indications, both experimental and speculative, of the possibility of a localized specific type of contribution to σ_W. Hopefully these indications will help towards the eventual characterization of this non-reaction field effect.

An 'exposure' factor was advocated[92] in order to explain ^1H chemical shifts in compounds such as $Si(CH_2CH_3)_4$. The concept of an 'exposure' factor suggests that the continuum model should be inadequate, as has been found, and that a model requiring a more intimate knowledge of molecular encounters is required to describe σ_W. Additionally, it has been shown[122] that the benzene induced ^1H shifts in but-1-en-3-one show an unusual dependence on the composition of mixtures containing these compounds. Normally, ratios of induced ^1H shifts for different positions in a given molecule should be independent of concentration. In the case mentioned above it was found that the alkenic hydrogen adjacent to the carbonyl function showed an anomalous shift. This anomaly

can be explained only on the basis of a short-range interaction between the relevant hydrogen atom and benzene. This remaining localized contribution to σ'_W will be termed a "buffetting" effect in recognition of Buckingham's original realization[35] that non-equilibrium effects should be characterized, although in fact he was probably referring to an effect equivalent to that of $\langle R_2^2 \rangle$ characterized herein.

The present hypothesis is that the reaction field concept of a point solute molecule at the centre of a cavity is unreal, and that an additional effect due to discrete pair-wise 'collisions' of solute and solvent molecules must be acknowledged in order to accommodate the dipolar effects of the reaction field polarized peripheral atoms and thence complete the characterization of the dispersion forces involved. If such pairwise encounters are important their effect should be analagous to that of bimolecular encounters in the gas phase, where the primary dipolar fields may be thought to cause a similar effect to R_2. At the outset, therefore, it is wise to seek some justification for this assumption from known parameters applicable to the gas phase. Using the gas phase value of $\partial\sigma/\partial\rho = -7.7$ ppm cm^3 mol^{-1} reported[123] for CH_4, the pair-wise collisions of methane molecules in the liquid phase should, based purely on the density dependence produce a contribution of - 0.26 ppm to the gas-to-liquid shift in addition to the normal reaction field contributions. This additional contribution is similar to the values of the intercepts quoted in table 4.2.

Although the above comparisons are by no means rigorous the numerical compatibility is sufficiently satisfactory to indicate some justification for evaluating the hypothesis in detail.

Continuing with the assumption that van der Waals force effects are additive[70, 71, 104-106] and electric field screenings

may be written as[35]

$$\sigma = -AE_2 - BE^2 - B\langle E^2 \rangle \ldots . \qquad 5.1$$

it is proposed that σ_w should be characterized by

$$\sigma_w = \sigma_{RF} + \sigma_{BI} \qquad 5.2$$

where σ_{RF} is characterized by equation 4.22 and σ_{BI} is a new screening constant yet to be characterized. If σ_{BI} arises from the dipolar fields due to polarized atoms at the periphery of solvent molecules it must be remembered that the polarization is caused by R_1. Because the direction of R_1 is unique at a given instant of time and is effective only over a distance $r \simeq a$ it is evident that σ_{BI} must essentially be characterized by pairwise solute-solvent interactions.

5:2 Electric Field Formulation of σ_{BI}

The polarization at the centre of the solute molecule by R_2 is very small because of the significant attenuation of R_2 over an additional cavity (solute), or molecular, radius. However R_2 is considered to be almost the same at the periphery of the solute cavity as in the solvent cavity of origin. Therefore the polarization of the periphery of the solute molecule is significant. A similar polarization of the periphery of a solvent molecule will occur and the electric fields of the induced dipoles can affect the screening of nuclei at the periphery of a solute molecule. σ_{BI} will therefore be considered on the basis of a perturbation of the peripheral solute atoms by electric fields originating at the periphery of the solvent. For simplicity a hydrogen atom hydrogen atom dipolar interaction will be considered from the point of view of encounters between the peripheral atoms of solvent and solute. The reference for considering these encounters will be a right hand triple based on the solute hydrogen atom with the z-axis colinear with the bond to that atom.

The electric field, $\vec{E}$, produced at the solute atom containing

the resonant nucleus of interest by a point solvent atom electric moment, $\vec{m}$, when the two are separated by a distance r is given by:[69]

$$\vec{E} = \frac{3(\vec{m}.\vec{r})\,\vec{r}}{r^5} - \frac{\vec{m}}{r^3} \qquad 5.3$$

If there is no restriction on the spatial position of the solvent atom with respect to the solute atom, the time average linear electric field over all space will be zero but the mean square value may be finite. It is therefore necessary to evaluate the square of the instantaneous electric field at the resonant nucleus. The problem may be simplified by considering the time averaged behaviour of the solvent atom and its moment in order to obtain the resulting mean electric field. The instanteous value of the time-averaged electric field, that is averaged to zero, can be deduced by considering the situation in one octant about the solute hydrogen atom of interest. On time-average the appropriate solvent atom can be considered to reside on a radius vector at an angle of $54^{\circ}\ 44'$ to each of the three co-ordinate axes based on the solute atom, and the solvent moment $\vec{m}$ can be characterized by considering the solvent electron moments in one octant about the solvent atom.

By considering the electron oscillations in one octant about the solvent atom, the electric fields, at the solute hydrogen atom that are parallel and perpendicular to the bond containing the resonant nucleus (fig. 5.2) may be written as:

$$\vec{E}_x = \frac{2\vec{m}_{x'}}{r^3} - \frac{\vec{m}_{y'}}{r^3} - \frac{\vec{m}_{z'}}{r^3} \qquad 5.4$$

$$\vec{E}_y = \frac{2\vec{m}_{y'}}{r^3} - \frac{\vec{m}_{x'}}{r^3} - \frac{\vec{m}_{z'}}{r^3} \qquad 5.5$$

$$\vec{E}_z = \frac{2\vec{m}_{z'}}{r^3} - \frac{\vec{m}_{x'}}{r^3} - \frac{\vec{m}_{y'}}{r^3} \qquad 5.6$$

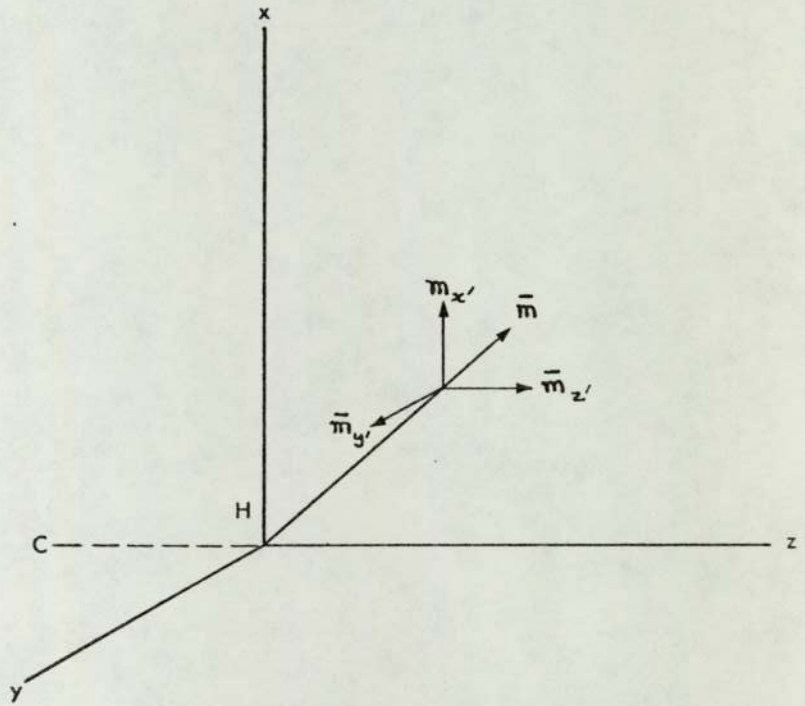

Fig. 5.1. Space average situation of a solvent molecule average electric moment.

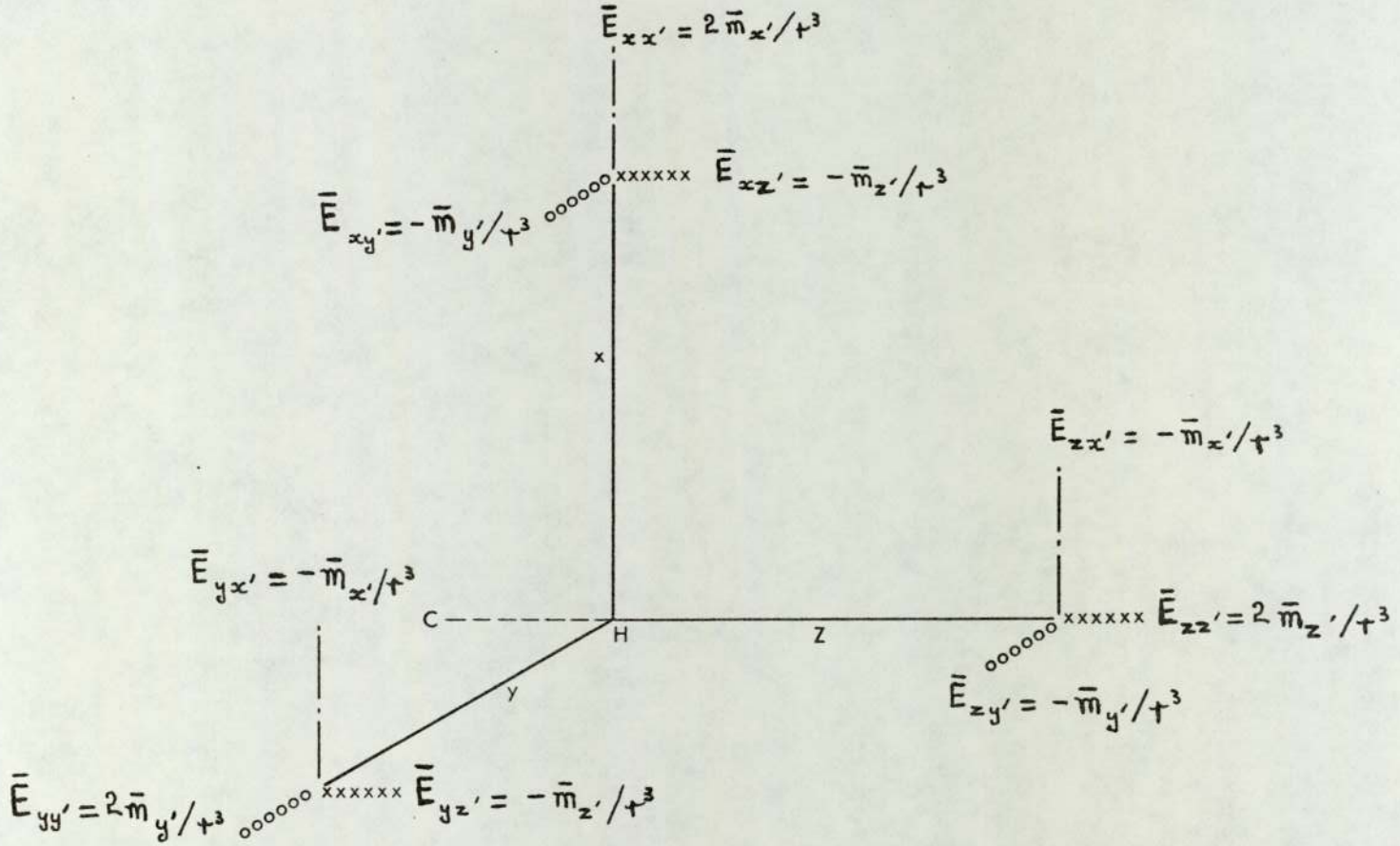

Fig. 5.2. Time average electric fields with respect to directions parallel and perpendicular to the axis of the C-H bond.

The average position of the solvent atom may be considered to reside successively for equal times on each solute axis. Therefore each of moments $\vec{m}_{x'}$, $\vec{m}_{y'}$, and $\vec{m}_{z'}$, are effective at the same time on each solute axis for $\frac{1}{3}$ of time in one octant. In this isotropic situation the total field will be zero. However if there is some constraint on the approach of the solvent atom to the solute atom the fields given by equations 5.4 - 5.6, may be modulated. Assuming that such a constraint can be described by modulation factors applicable to $\vec{E}_z$, $\vec{E}_x$ and $\vec{E}_y$ in the octant it is convenient to consider these to be defined by $o \leq \beta \leq 1$, $o \leq \alpha \leq 1$ and $o \leq \alpha' \leq 1$. The factors β, α and α' are taken to be measures of the anisotropy of the approach, or steric hindrance, of the solvent to the solute atom containing the resonant nucleus. The fields in question may now be rewritten as

$$\vec{E}_x = \alpha (2\vec{m}_{x'} - \vec{m}_{y'} - \vec{m}_{z'}) r^{-3} \qquad 5.8$$

$$\vec{E}_y = \alpha' (2\vec{m}_{y'} - \vec{m}_{x'} - \vec{m}_{z'}) r^{-3} \qquad 5.9$$

$$\vec{E}_z = \beta (2\vec{m}_{z'} - \vec{m}_{x'} - \vec{m}_{y'}) r^{-3} \qquad 5.10$$

If, as in the case of many C-H bonds and C-F bonds, there is axial symmetry about the solute z-axis it is possible, to a good approximation, to put $\alpha = \alpha'$. The average electric field in one octant over all time may be written as the average of equations 5.8 - 5.10 such that

$$\vec{E}_{AV} = \frac{(2\beta - 2\alpha)}{6r^3} (2\vec{m}_{z'} - \vec{m}_{x'} - \vec{m}_{y'}) \qquad 5.11$$

In the context of σ_{BI} the most meaningful electric field would be the square of the linear electric field (or more precisely the scalar product) over the four octants away from the bond containing the atom of interest. In this case β and α would have upper limits of 4 instead of 1 as defined for one octant. For this four octant definition it is necessary to express the effect in terms of four

pairwise potentials[70, 71]. Thus, the total square field in the four octants as defined above, keeping the upper level of β and α as unity and for convenience putting $2\alpha = \xi$ (or $\alpha + \alpha' = \xi$), may be written as,

$$\bar{E}^2_{TOT} = \frac{4}{36r^6} (4\bar{m}^2_{z'} + \bar{m}^2_{x'} + \bar{m}^2_{y'}) (4.2\beta - 4.\xi)^2 \qquad 5.12$$

Any cross terms in the electric moments will be zero because of the cartesian coördinates chosen. Expressing each moment in terms of mean electron charge displacements such as

$$\bar{m}^2_x = e^2 \langle x^2 \rangle \qquad 5.13$$

and assuming that the mean displacement in the x, y and z directions on the solvent hydrogen atom are the same, the square field may be written as

$$\bar{E}^2_{TOT} = \frac{64e^2 \langle x^2 \rangle (2\beta - \xi)^2}{6r^6} \qquad 5.14$$

The value of $\langle x^2 \rangle$ may, to a reasonable approximation[135], be written as the mean square value of the radial distribution function of the 1s arbital in the free hydrogen atom. The radial distribution function for the 1s arbital of the hydrogen atom is[124]

$$R = \frac{2}{a_o^{3/2}} \exp\left(\frac{-q}{a_o}\right) \qquad 5.15$$

and thence

$$\langle x^2 \rangle = \frac{\int_0^\infty q^2 \cdot R \cdot dr}{\int_0^\infty R \cdot dr} \qquad 5.16$$

where a_o is the Bohr radius ($=0.529 \times 10^{-10}$ m)[116] and q is the variable radial distance from the hydrogen nucleus. Evaluating the integral gives

$$\langle x^2 \rangle = 2 a_o^2 \qquad 5.17$$

and the square field is then given by

$$\bar{E}^2 = \frac{64\, e^2 a_o^2}{3r^6} (2\beta - \xi)^2 \qquad 5.18$$

Putting the electron charge in terms of esu. units (4.802 x 10^{-10} Franklin)

$$\bar{E}^2 = \frac{K}{r^6} (2\beta - \xi)^2 \qquad 5.19$$

where

$$K = 1.377 \times 10^{-34} \text{ esu} \qquad 5.20$$

In keeping with the general philosophy of square field screening[35], σ_B may be written as,

$$\sigma_{BI} = \frac{-BK}{r^6} (2\beta - \xi)^2 \qquad 5.21$$

The usefulness of equations 5.19 and 5.21 can only emerge if there is some way of assigning values to β and ξ on a steric basis but that is consistent with the aforegone discourse. A geometrical basis for β and ξ will now be presented.

5:3 Geometrical Formulation of β and ξ

The parameters of β and ξ describe the total effective accessibility of a solute atom to the solvent atom as a result of pairwise encounters in one octant. The solvent atom is contained on the periphery of the solvent molecule which is assumed to be spherical. The pairwise encounters within a particular octant on the solute atom are considered to act successively and need not involve the same solute atom or solvent molecule. If the model is correct then the square field of equation 5.19 must be considered to be operative for any one of the solute peripheral atoms. With this in mind the values of β and ξ will be based on a geometrical accessibility where the encountering species are rigid and passive. For most solute molecules the solvent encounters of significance will be ineffective within the four octants of space around the solute atom that embraces the bond to that atom. This is because

the remainder of the solute molecule occupies most of this space preventing the solvent molecule approaching the solute and makes the solute atom-solvent atom distance, r, so large as to render the field effect insignificantly small. Consequently the encounters in the other four octants only need be considered. A hypothetical solvent-solute encounter situation is depicted in figure 5.3 on a two-dimensional basis. However, each molecular situation needs to be considered individually.

From figure 5.3, if the centres of the peripheral solvent atoms can adopt all positions on an arc of radius r_c from the centre of the solute atom in the octant of interest, $\beta = 1$ and $\alpha = 1$ ($\xi = 2$). If contact is broken from the solvent atoms and solute atom, β and α will be less than unity. If the two dimensional angle θ is the angle of the radius vector with the so-called α-axis which happens to be the angle of non-contact in this case the following values of β and α for contact will apply (fig. 5.3):

$$\beta_c = 1 \text{ and } \alpha_c = \left(\frac{45^\circ - \theta^\circ}{45^\circ}\right) \text{ if } \theta^\circ \leq 45^\circ \qquad 5.22$$

or

$$\alpha_c = 0 \text{ and } \beta_c = \left(\frac{90^\circ - \theta^\circ}{45^\circ}\right) \text{ if } \theta^\circ \geq 45^\circ \qquad 5.23$$

The remaining part of β and α from unity, $(1 - \beta_c)$ and $(1 - \alpha_c)$ must operate on a distance modulated basis. It is proposed that the modulation should be on inverse sixth power of distance basis because of the van der Waals dispersion nature of the square field effect. If r' is the solute atom-solvent atom distance at the α-axis, viz. the extreme point in the octant of interest where direct atom-atom contact is prevented by steric hindrance, r_c is the solute atom-solvent atom distance at contact and assuming a

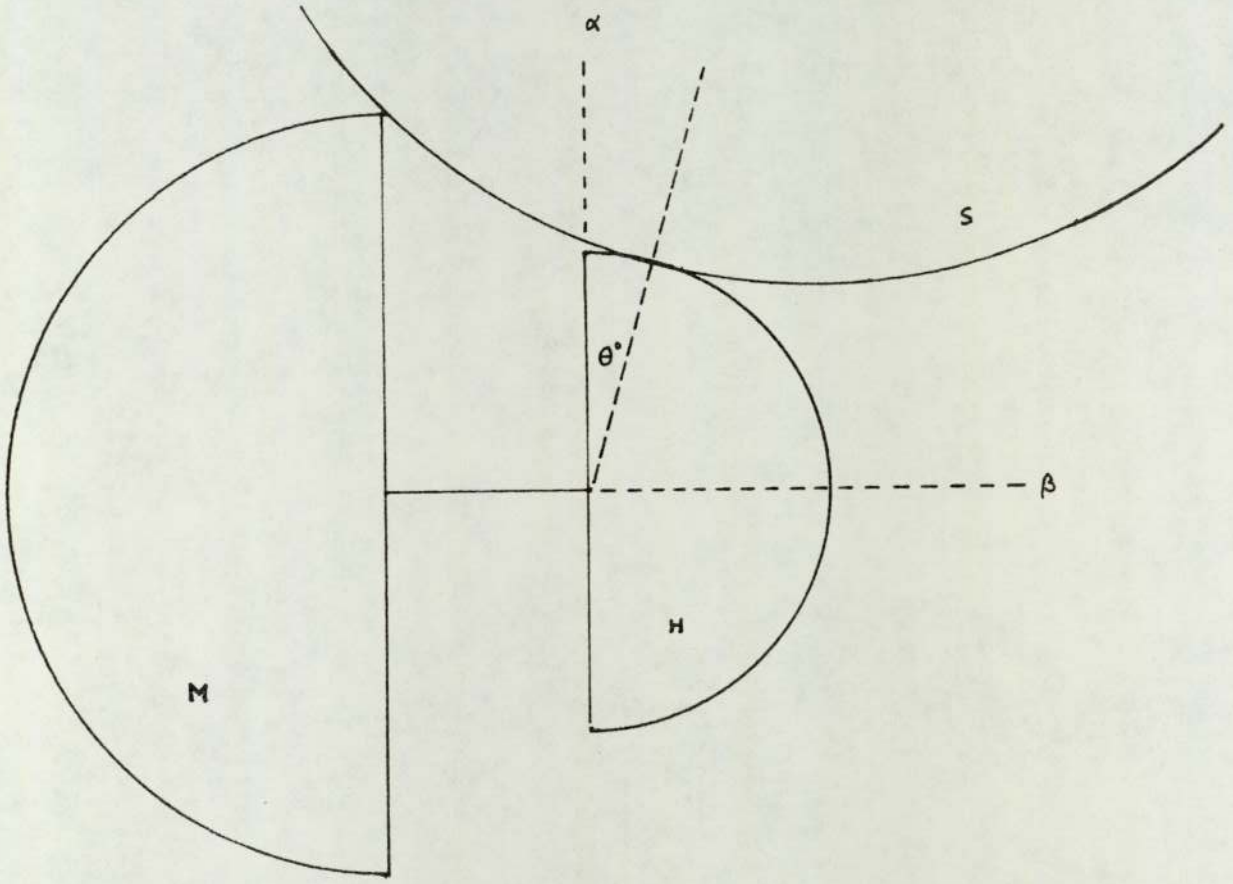

Fig. 5.3. Two dimensional representation of a methane molecule (hydrogen H and methyl group M) encountered by an isotropic solvent molecule(S).

continuous change in distance from contact, r_c, to the point at a distance r', the average inverse sixth power of the distance used in the modulation of β and ξ will be

$$\langle r^{-6} \rangle = \frac{\int_{r_c}^{r'} r^{-6}\, dr}{\int_{r_c}^{r'} dr} = \frac{(r_c^{-5} - r'^{-5})}{5(r - r_c)} \qquad 5.24$$

The total value of β and α would then be given by

$$\beta_T = \beta_c + (1 - \beta_c)\, r_c^6 \langle r^{-6} \rangle \qquad 5.25$$

and

$$\alpha_T = \alpha_c + (1 - \alpha_c)\, r_c^6 \langle r^{-6} \rangle \qquad 5.26$$

or

$$\xi_T = \xi_c + (2 - \xi_c)\, r_c^6 \langle r^{-6} \rangle \qquad 5.27$$

for the appropriate situations. In the above treatment, where hydrogen atom-hydrogen atom encounters have been considered the value of r_c may conveniently be set to the sum of the van der Waals radii of the two atoms[116] (for two hydrogen atoms this is 2.4×10^{-8} cm.). The general theory will now be tested fron an nmr point of view and extended to take account of solvent atoms other than hydrogen using the above-mentioned molecular model to evaluate β and ξ geometrically.

5:4 An Experimental Test of "Buffetting"

The first step in assessing the validity of "buffetting" theory is to demonstrate that a reliable and extensively viable value of K for H - H interactions is available. For this purpose the systems referred to in table 4.2 are considered. Calculations of $(2\beta_T - \xi_T)^2$ reveal that this parameter is sensitive to the dimensions of the solute but not the solvents. It is for this reason that the good

linear regressions demonstrated in table 4.3 were obtained and the intercepts but not the slopes of these are influenced by equation 5.21; the values of B thus remain valid. Table 5.1 presents the values of $(2\beta_T - \xi_T)^2$ calculated for the group IVB tetramethyls on a geometrical basis. The basis of the geometrical model for a group of IVB tetramethyl solute molecule is a 'hard' hydrogen atom hemisphere bonded to the rest of the molecule treated as 'hard' hemispherical methyl groups bonded to the central atom.

The solvent, considered as a sphere of the appropriate size with the solvent hydrogen atoms around the periphery, is envisaged to encounter the solute hydrogen atom of interest from two different aspects with equal probability. The two encounter aspects are depicted in figures 5.4 and 5.5, with the total β and ξ values calculated in terms of one octant, consistent with the theory in section 5.2. The values of K^H/r_{HH}^6 deduced from equation 5.21 are presented in table 5.2, using the steric parameters calculated on the above basis and $\sigma_w - \sigma_{RF}$ from table 4.2 From these 20 similar values of K^H/r_{HH}^6 a mean value of 0.7133×10^{12} esu (SD = 0.05×10^{12} esu) is obtained. If r_{HH} is taken[116] to be 2.4×10^{-8} cm, the sum of two van der Waals radii of hydrogen, K is found to be 1.363×10^{-34} esu, in close agreement with the theoretically calculated value in section 5.2 of 1.377×10^{-34} esu. This certainly gives confidence to the theory behind the formulation of σ_{BI} in equation 5.21 and the geometrical formulation of β_T and ξ_T. Neopentane as solute has been isolated to demonstrate that the mean value of $K^H/r_{HH}^6 = 0.7133 \times 10^{12}$ esu found experimentally can be used with equation 5.21 using $\beta = 0.66$ and $B = 0.81 \times 10^{-18}$ esu to evaluate the value of ξ_T of 0.85 (SD = 0.02) in good agreement with

TABLE 5.1 GEOMETRICAL RESULTS FOR THE GROUP IVB TETRAMETHYLS

SOLUTE	*GEOMETRICALLY DETERMINED $(2\beta_T - \xi_T)^2$	M - C BOND LENGTH[116] / 10^{-10} M
CMe_4	0.230	1.54
$SiMe_4$	0.270	1.87
$GeMe_4$	0.275	1.98
$SnMe_4$	0.295	2.14
$PbMe_4$	0.300	2.83

* for the solute in all five group IVB tetramethyl solvents.

TABLE 5.2 VALUES OF K^H/r_{HH}^6 ($\times 10^{-12}$ esu^{-1}) FOR THE GROUP IVB TETRAMETHYLS

$10^{18}B$/esu	SOLUTE SOLVENT	CMe_4	$SiMe_4$	$GeMe_4$	$SnMe_4$	$PbMe_4$
0.87	$SiMe_4$	0.7706	0.6598	0.7534	0.6982	0.7279
0.87	$GeMe_4$	0.7690	0.6437	0.7231	0.6928	0.7105
0.92	$SnMe_4$	0.7332	0.6301	0.6927	0.6707	0.6853
0.82	$PbMe_4$	0.8713	0.6705	0.7311	0.7008	0.7273

AVERAGE K^H/r_{HH}^6 = 0.7133 x 10^{12} esu ($\pm$ 0.05 x 10^{12} esu)

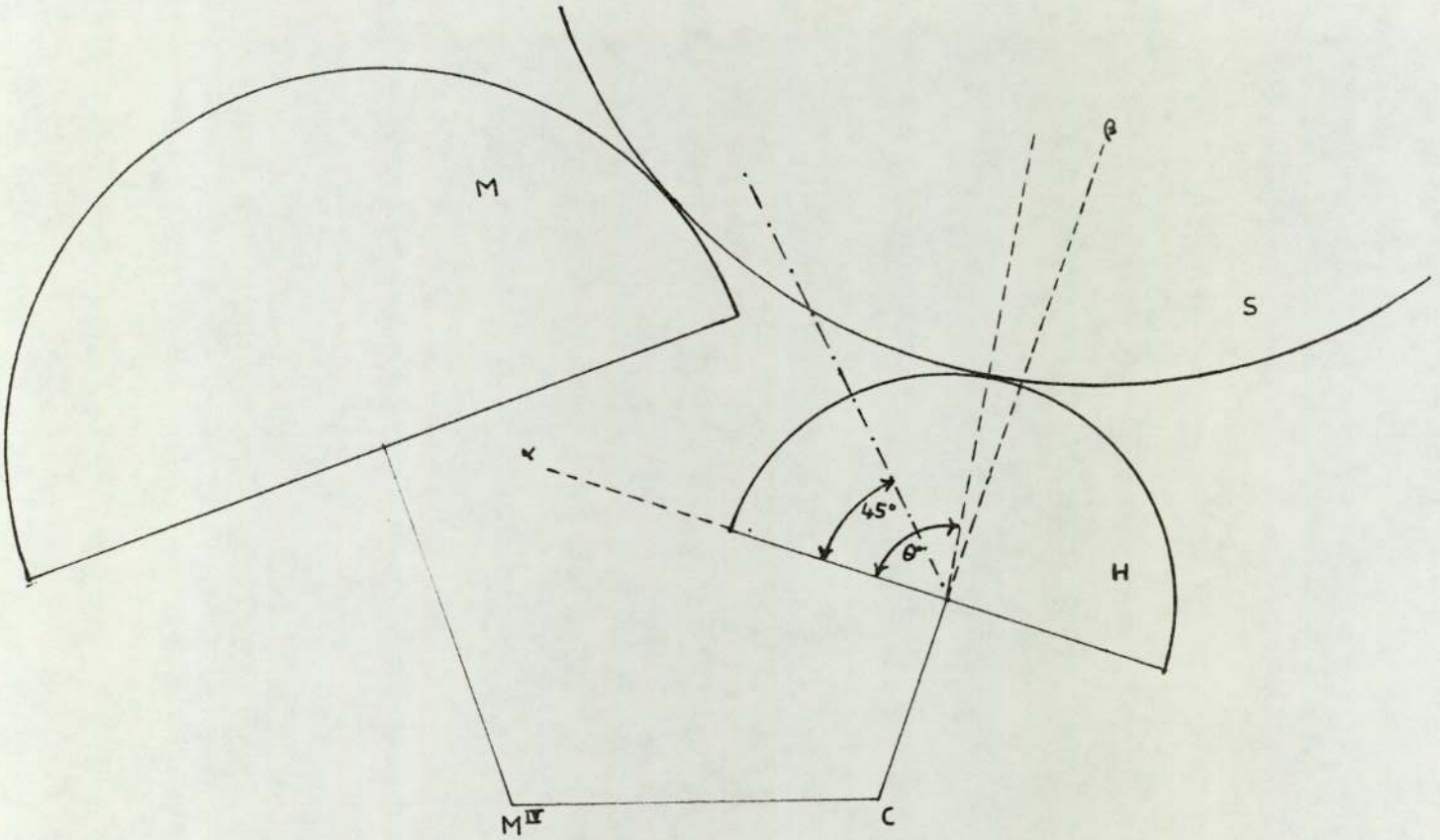

Fig. 5.4. Two dimensional repesentation of a group IV B tetramethyl molecule (hydrogen H and rest of molecule M) encountered by an isotropic solvent molecule(S)-I.

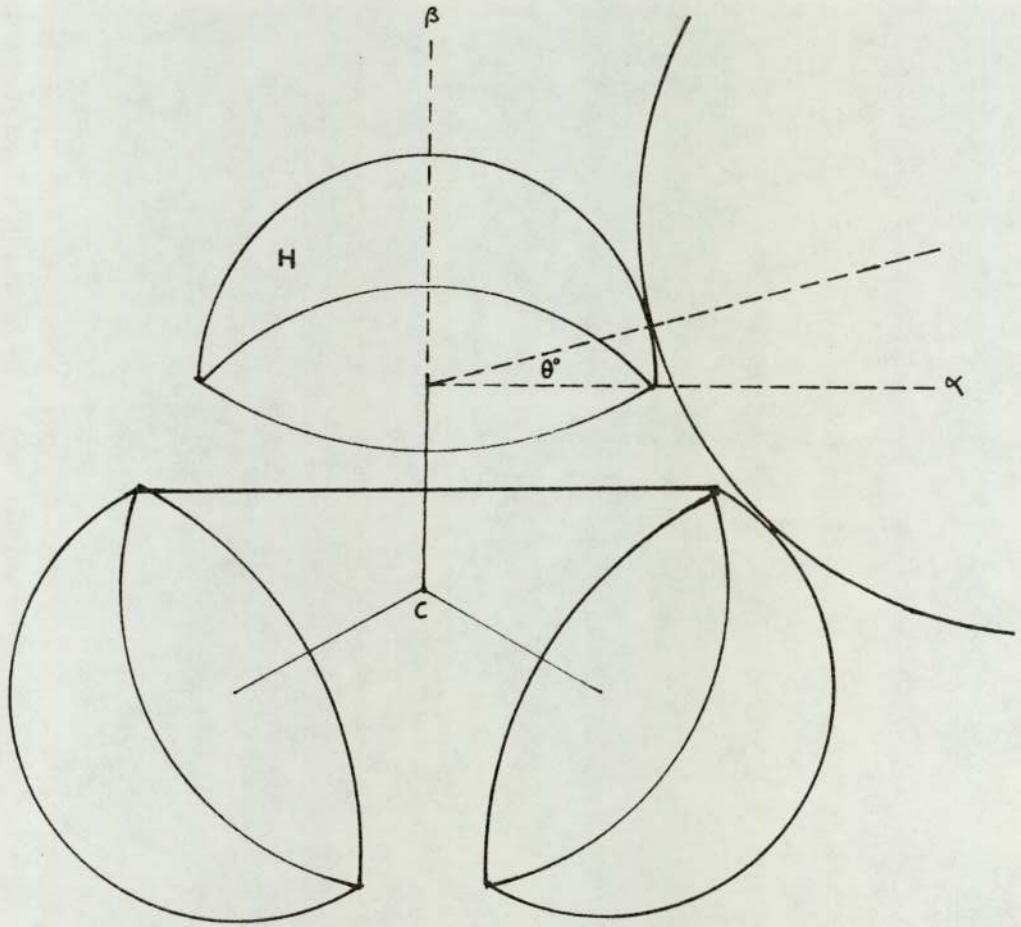

Fig. 5.5. Two dimensional representation of a group IV B tetramethyl molecule (hydrogen H and rest of molecule M) encountered by an isotropic solvent molecule(S)-II.

that calculated on a geometric basis (0.84).

Having established some degree of confidence in the theory regarding H - H encounters, it would be prudent to test the theory in the consideration of encounters with solvents containing peripheral atoms other than hydrogen.

5:5 Consideration of Solvents with Peripheral Atoms other than Hydrogen

If the so-called "buffetting" solvent atom is changed from hydrogen to an atom with more electrons (chlorine for example) it may be expected[112, 125] that the effect of "buffetting" will be greater. However, the general theory of section 5.2 is built up around a theory of hydrogen atom - hydrogen atom encounters and such an extension to other situations on an ab initio basis would be a formidable task on account of the increased number of electrons. Yonemoto[126] suggested a Hartree-Fock scaling factor, Q, which is equal to unity for a hydrogen atom and is replaced by $Q = \langle \sum x_i^2 \rangle / a_o^2$ for atoms such as the halogens. These values of Q can be multiplied into equations 5.19 and 5.21 to obtain the "buffetting" effect of a non-hydrogen atom. However, the value of Q must be distance modulated by the sums of the van der Waals radii of the intereacting atoms in the appropriate way. So, modifying equations 5.19 and 5.21 in more general terms leads to,

$$\overline{E^2} = \frac{K^H}{r_{HH}^6} (2\beta_T - \xi_T)^2 \; Q^X \left(\frac{r_{HH}}{r_{HX}}\right)^6 \qquad 5.28$$

and

$$\sigma_{BI} = \frac{-BK^H}{r_{HH}^6} (2\beta_T - \xi_T)^2 \; Q^X \left(\frac{r_{HH}}{r_{HX}}\right)^6 \qquad 5.29$$

where X refers to the interacting solvent atom.

In order to test the validity of equation 5.29 the intramolecular chemical shifts between two non-equivalent hydrogen atoms

in an appropriate solute molecule at low concentration in various solvents were studied. The solute molecule considered was 1, 3, 5-triisopropylbenzene and the chemical shift between the methyl hydrogen resonance (doublet) and the methine hydrogen resonance (septet) was measured in the solvents tetramethylsilane (H), carbon tetrachloride (cl), tetranitromethane (O), 1, 4 dioxan (H/O), carbon tetrabromide dissolved in tetramethylsilane (Br/H), and decafluorocyclohexene (F), using the Varian Associates HAIOOD spectrometer.

The β and ξ values for the methine and methyl hydrogen atoms were very difficult to calculate and the most reliable way of predicting β and ξ was found to be by the use of a 'Courtauld Atomic Model' of the solute molecule and spheres of the appropriate size[116] for the encountering solvent molecule. The β and ξ's estimated in this way are probably not too accurate but thought to be a reasonably good estimate for the purpose of this study. Therefore, if the chemical shift of the methyl group in a given solvent is taken to be δ_{CH_3} and for the methine group δ_{CH}, their difference may be written as

$$\Delta\delta_{CH_3-CH} = \delta_{CH_3} - \delta_{CH} \qquad 5.30$$

and since the absolute δ's depend on,

$$\delta = \sigma_{RF} + \sigma_{BI} - \sigma_{REF} \qquad 5.31$$

it follows that

$$\Delta\delta_{CH_3-CH} = \sigma_{BI}^{CH_3} - \sigma_{BI}^{CH} \qquad 5.32$$

assuming the reaction field to be the same at both hydrogens (no site factor). It is necessary to use one solvent as a basis for the rest of the measurements and calculations; tetramethylsilane was chosen for this purpose, having a periphery of hydrogen atoms. The Q-value for hydrogen is taken to be unity ($Q^H = 1$), as

mentioned previously. The intramolecular chemical shift difference measured between the solvent under study with its periphery of atoms X is related to that in tetramethylsilane (H) by

$$\Delta^{X-H}_{CH_3-CH} = (\sigma^{CH_3}_{BI}(X) - \sigma^{CH}_{BI}(X)) - (\sigma^{CH_3}_{BI}(H) - \sigma^{CH}_{BZ}(H)) \qquad 5.33$$

Written more explicitly using equation 5.29 and rearranging, equation 5.33 becomes

$$Q^X = \left(\frac{\Delta^H (2\beta_T - \xi_T)^2_{CH_3 - CH}}{\Delta^X (2\beta_T - \xi_T)^2_{CH_3 - CH}} - \frac{\Delta^{X-H}_{CH_3 - CH}}{\frac{BK^H}{6}_{r_{HH}} \Delta^X (2\beta_T - \xi_T)} \right) \left(\frac{r_{HX}}{r_{HH}} \right)^6 \qquad 5.34$$

where $\Delta^X (2\beta_T - \xi_T)^2_{CH_3 - CH} = (2\beta_T - \xi_T)^2_{CH_x(X)} - (2\beta_T - \xi_T)^2_{CH(X)}$.

It is appropriate to discuss the case of 1,4 dioxan and carbon tetrabromide dissolved in tetramethylsilane in more detail. The distances r_{HX} are based on an average solute atom van der Waals radius. For 1,4 dioxan there are eight hydrogen atoms and two oxygen atoms on the periphery of the solute molecule. The van der Waals radius[116] of hydrogen is 1.2×10^{-8} cm and of oxygen is 1.4×10^{-8} cm and thence the average H/O van der Waals radius in 1,4 dioxan is 1.24×10^{-8} cm. In the case of carbon tetrachloride in tetramethylsilane the situation is even more complex. The ratio of tetramethylsilane to carbon tetrabromide used was 5.6 molecules to 1 molecule respectively. Since the van der Waals radius of bromine[116] is 1.95×10^{-8} cm the average H/Br van der Waals radius in the $CBr_4/SiMe_4$ system used is 1.31×10^{-8} cm. With this value the average of $\Delta(2\beta_T - \xi_T)^2_{CH_3 - CH}$ can be shown to be 0.175. Because one oxygen atom replaced two hydrogen atoms, in the case of 1,4 dioxan, the value of Q^O is related to the calculated value of $Q^{H/O}$ by the formula

$$Q^{H/O} = \frac{8Q^{H} + 2Q^{O}}{10} \qquad 5.35$$

However, in the case of $CBr_4/SiMe_4$, in unit volume the solute may be "buffetted" by 5.6 x 12 H and 4 Br atoms. On account of the differing volumes of each solvent molecule the probability of H-buffetting is 5.6 x 12 x V^{TMS}/V^{CBr_4} times that of the 4Br atoms. Consequently the experimental value of $Q^{H/Br}$ in the mixture will be given by

$$Q^{H/Br} = \frac{83.2Q^{H} + 4Q^{Br}}{87.2} \qquad 5.36$$

from which Q^{Br} can be found.

The results and measurements with 1, 3, 5 triisopropylbenzene are shown in table 5.3 and it can be seen that, although there is not absolute agreement between the values of Q calculated here and those derived from Hartree-Fock calculations,[126] there is a definite correlation between them as shown by figure 5.6 (correlation coefficient = 0.98; significance level $\leq$ 1%). The source of the discrepancy may be due to inaccuracies in the determination of β and ξ from a molecular model that may not be precisely to scale, and also to the fact that the screening constant coefficient, B, may not be the same for the methine and methyl hydrogens.

The evidence of this particular piece of research gives credence to the idea that the theory introduced in this chapter may be extended to 'non-protic' solvents. Further evidence will be presented in subsequent chapters which will both complement and supplement the ideas presented so far throughout this thesis.

5:6 A Critque of the Molecular Encounter Theory

The presence of some other term in the characterization of σ_W besides the reaction field terms in σ_{RF} is probably correct in view of the evidence presented herein and from the numerous examples

TABLE 5.3 MEASUREMENTS FOR 1, 3, 5 TRIISOPROPYLBENZENE IN VARIOUS SOLVENTS

X	SOLVENT	$r^{116}_{HX/10^{-10}m}$	$\Delta^{X-H}_{CH_3-CH}$/ppm	$\Delta(2\beta_T - {}_T)^2_{CH_3-CH}$	Q (EXPERIMENTAL)	$Q(HATREE-FOCK)^{126}$
H	TETRAMETHYL-SILANE	2.40	$(\Delta\delta^{0}_{CH_3-CH} = 1.572$ ppm)	0.183	(1)	1
Cl	CARBON TETRACHLORIDE	3.00	$(\Delta\delta^{-0.022}_{CH_3-CH} = 1.550$ ppm)	0.128	6.5	10
F	DECAFLUORO-CYLCLOHEXENE	2.55	$(\Delta\delta^{-0.002}_{CH_3-CH} = 1.570$ ppm)	0.128	2.1	3.1
O	TETRANITRO-METHANE	2.60	$(\Delta\delta^{0.032}_{CH_3-CH} = 1.604$ ppm)	0.183	1.2	2.8*
H/O	1, 4 DIOXAN	2.44 (ave.)	$(\Delta\delta^{0.008}_{CH_3-CH} = 1.580$ ppm)	0.128	1.5	-
O					3.4	2.8*

cont'd....

H/Br	CARBONTETRA-BROMIDE (IN TETRAMETHYL-SILANE)	2.51 (Ave.)	($\Delta\delta_{CH_3\text{-}CH}^{0.004}$ = 1.576 ppm)	0.175 (Ave.)	1.3	-
Br					8.0	14

* Extrapolated on the basis of the number of electrons in the neutral atom.

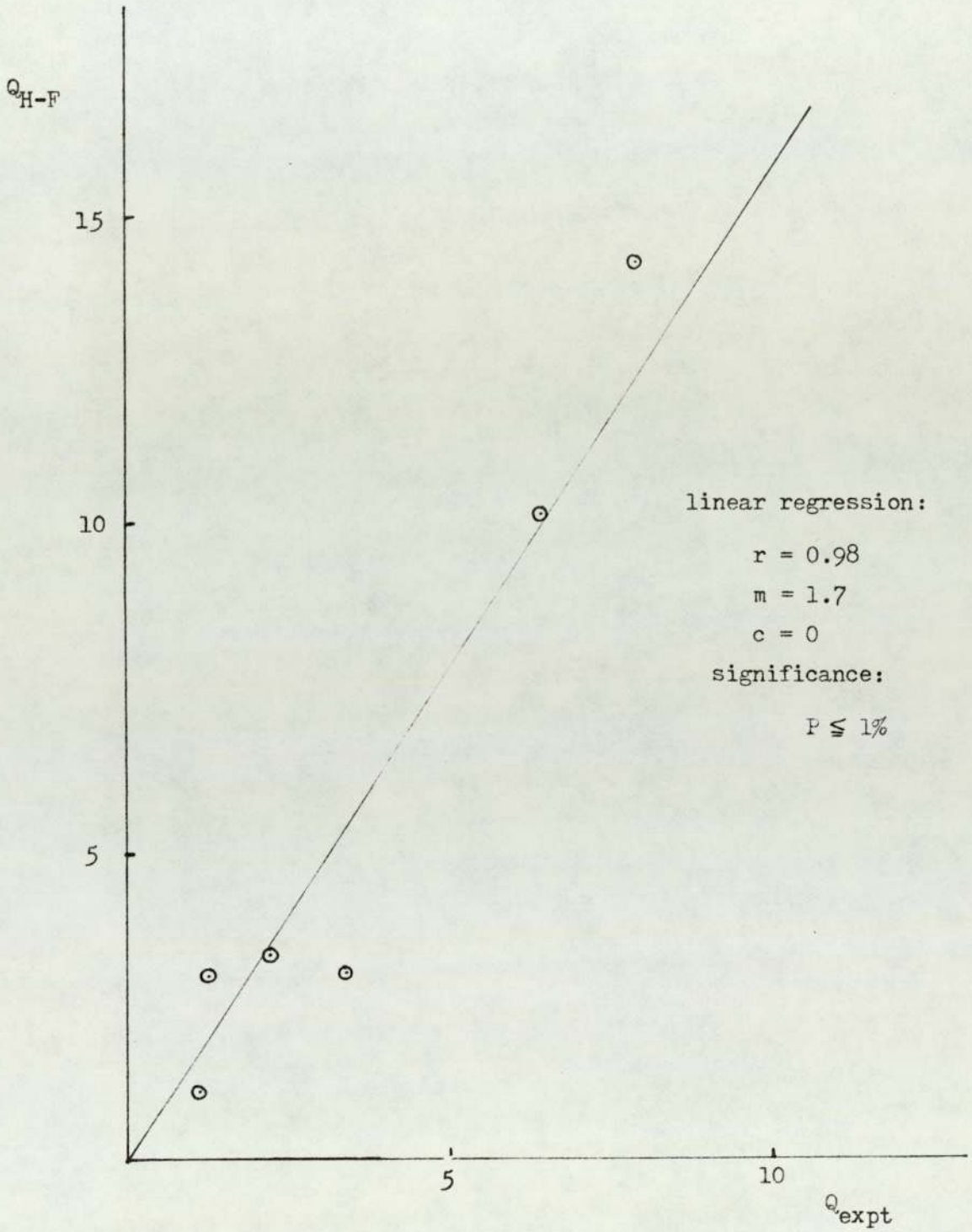

Fig. 5.6. Relationship between the Hartree-Fock calculated and experimental Q-values.

in the literature (section 3.7). The presence of an effect on σ_w due to steric effects is novel, although such steric effects on nuclear screening are not entirely new. It has been stated in connection with intramolecular nuclear screening[127] that

> "...Steric interaction causes deshielding only, since the effective shielding of the hydrogen nucleus is decreased on a symmetrical distortion of the electron cloud..."

and such an extension to intermolecular nuclear screening effects appears reasonable. However, certain limitations must be discussed before further evidence is presented to support the theory presented in this chapter, and indeed that in previous chapters.

The first observation must be in regard of the additivity of the square-field and thence nuclear screening terms. Whilst this is a well established fact,[35, 104-106] it is merely an approximation in the same way as the additivity of pair potential energies[70, 71, 115] but must be accepted if any progress is to be made. Also the overall approach uses equations for point dipoles in the sense that transient moments behave analogously to permanent moments. Such an approximation is probably not too bad in view of the results obtained so far.

The major criticism must come from the fact that no account is taken of the effect of molecular distortions away from the point of molecular encounter, since 'hard' molecular models are examined on a primarily hydrogen atom-hydrogen atom encounter situation. Also any repulsion effects have been ignored. Both the repulsion terms and molecular distortion terms would probably appear in other than square field terms and it is thought that such terms would only be of any significance when the molecule is in an excited electronic state. Therefore, because molecules are treated as being in the ground electronic state it is assumed

that the effect of molecular distortions and repulsion effects are negligible.

A more elegant derivation of the theory may be forthcoming by using a complete quantum-mechancial treatment rather than the essentially classical treatment used herein. However, the approximations inherent in any quantum treatment of molecular interactions involving more than one electron would probably be much greater or at least as great as those used in the present classical approach.

A drawback of the theory maybe that an entirely general formulation of β and ξ appears to be impossible and each molecular situation must be treated separately. It is not impossible, however, to envisage a $\beta$and ξ scale for particular functional group-solvent situations and will be discussed in the next chapter. Whatever the drawbacks of the approach presented herein it appears that it is definitely a step closer to a more complete characterization of the effects of van der Waals dispersion forces on nuclear screening and indeed (as will be demonstrated in the next two chapters) of some non-nmr effects.

CHAPTER 6

APPLICATION OF MOLECULAR ENCOUNTER THEORY TO N.M.R.

6:1 Introduction

Although the evaluation of K was a good absolute check on the theory presented in chapter 5, the rest of the results are really only self consistent and thus provide merely indirect evidence towards the general applicability of the theory.

It is now proposed to provide further evidence towards establishing the authenticity of the theory, especially in respect of σ_{BI}, by analysing more ^{1}H gas-to-liquid chemical shifts. Later some ^{19}F gas-to-liquid shifts will be analysed to demonstrate the extension of the theory to nuclei other than ^{1}H. From a more qualitative point of view and in an effort to demonstrate that the theory can be used with complex molecules the status of the linear reaction field in nuclear screening will be appraised. Finally a qualitative examination of some diastereotopic chemical shifts in various solvents will be conducted.

6:2 Gas-to-Solution ^{1}H Chemical Shifts in Relatively Simple Systems

6:2a The B-Value of Hydrogen in Methane

An indirect, though useful test of using equation 5.29, with K^H/r^6_{HH} set equal to 0.7133×10^{12} esu, is possible by analysing the gas-to-solution ^{1}H chemical shifts of CH_4 with $C(CH_3)_4$ and $Sn(CH_3)_4$ to obtain B for the hydrogen atom in CH_4 through the equation

$$\sigma_w = -B(\langle R_T^2 \rangle + \frac{K^H}{r^6_{HH}} (2\beta_T - \xi_T)^2) \qquad 6.1$$

For the two solvents $C(CH_3)_4$ and $Sn(CH_3)_4$ the respective experimental chemical shifts are -0.217 ppm[67] and -0.322 ppm[121] and $\langle R_T^2 \rangle$ is 0.186×10^{12} esu and 0.272×10^{12} esu (equation 4.18). The values of β and ξ are evaluated from a geometrical model

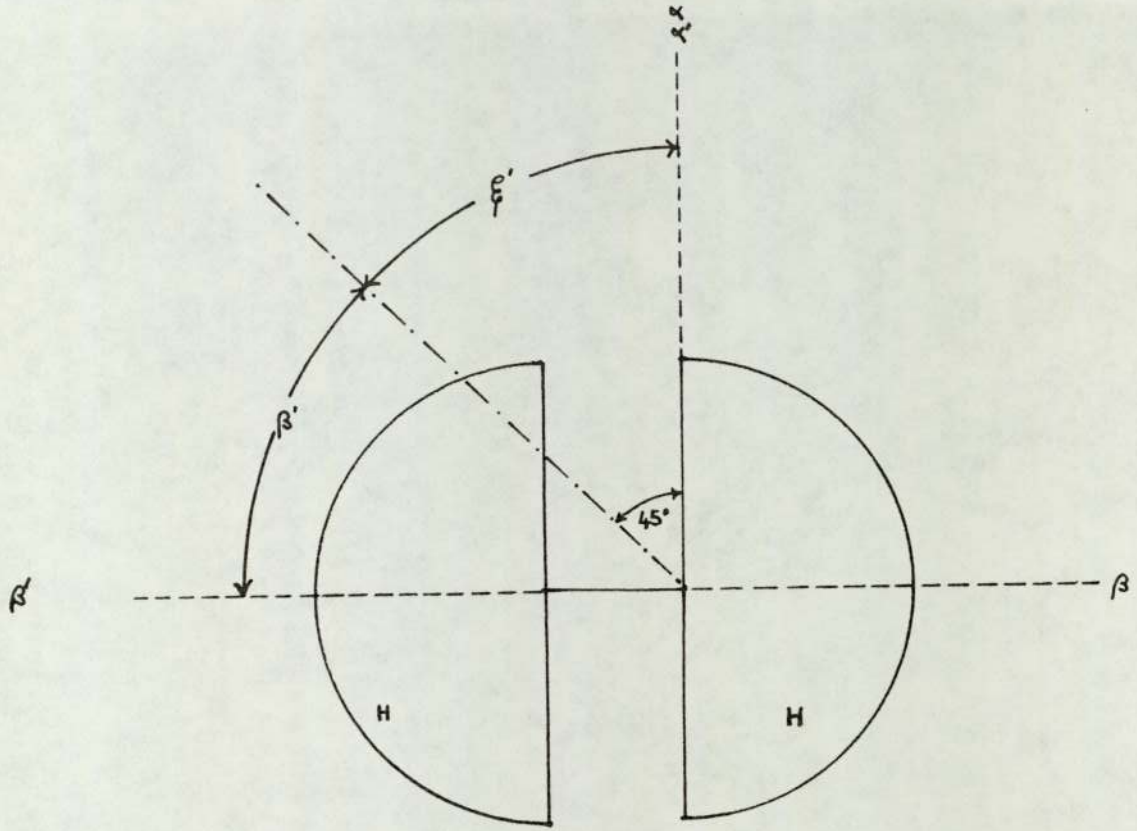

Fig. 6.1. Two dimensional representation of the hydrogen molecule.

similar to that depicted in figure 5.3 using the appropriate molecular data[67, 116]. For both solvents it was found that $\beta_T = 1$ and $\xi_T = 1.65$. B was evaluated (equation 6.1) as 0.79(3) x 10^{-18} esu from the $C(CH_3)_4$. It is not suprising that the average of these values (0.84(4) x 10^{-18} esu) is similar to the values of B determined for the group IVB tetramethyls (average 0.87 x 10^{-18} esu) because the hydrogen atoms are all contained in sp^3 hybridized bonds.

6:2b The Q-Values of Chlorine and Bromine

Knowing B for CH_4, values of Q for Cl and Br can be evaluated through equation 6.2 below:

$$\sigma_w = -B\left(\langle R_T^2\rangle + \frac{Q^X K^H}{r_{HX}^6}(2\beta_T - \xi_T)^2\right) \qquad 6.2$$

Taking σ_w as -0.410 ppm[67] and -0.567 ppm[35] for CH_4 with CCl_4 and CBr_4 respectively, the corresponding values of 0.355 x 10^{12} esu and 0.509 x 10^{12} esu for $\langle R_T^2\rangle$ and 0.096 and 0.090 for the geometrically measured values of $(2\beta - \xi_T)^2$ reveals that $Q^{Cl} = 7.2(9)$ and $Q^{Br} = 12.9(8)$. Whilst the former of these values is in excellent agreement with that given in table 5.3, the latter differs from the value given in table 5.3 by about 60%. This is due no doubt to the fact that the two experimental chemical shifts were obtained at quite different temperatures (30°C for 1, 3, 5 triisopropyl benzene and 100°C for CH_4).

6:2c σ_a of Cyclohexane and Benzene

Having validated the theoretical principles embodied in this thesis, they can now be put to further use. An important solvent screening that has eluded definitive experimental characterization is σ_a. The way now lies clear to deduce values of this for different anisotropic solvents using the formula:

$$\sigma_a = \sigma_w^{EXPT} - \sigma_w^{THEORY} \qquad 6.3$$

where σ_w^{THEORY} is calculated from equation 6.1. For convenience the solvents are assumed to be spherical in the calculation of β and ξ, with their molecular radii calculated from the molar volumes. The mean value of σ_a for C_6H_{12} is found to be 0.042 ppm (table 6.1) and is therefore between the values predicted by Raza and Raynes[92] (σ_a = o) and Homer[36] (σ_a = 0.1 ppm). The larger and consistently similar values for C_6H_6 (table 6.2), whose average value of σ_a is 0.500 ppm, show some dependence on the size of the solute molecule and numerically agree with generally accepted values[36].

6:2d The B-Value of Hydrogen in the Hydrogen Molecule

Any comments on the credibility of the values of B have been based on that deduced for the hydrogen atom[112]. Predictions have, however, been made for bound hydrogen in the H_2 molecule[128]. It is prudent, therefore, to compare the most recent prediction with values deduced using equations 4.24 and 5.21 or equation 6.2. The only suitable ^1H chemical shift data for H_2 are those given by Dayan and Widenlocher[129]. Unfortunately, in agreement with Rummens[82], it has to be concluded that all of the shifts reported by those authors[129] need another -0.3 ppm added to them (having been provided with the raw experimental data by Dr. Dayan it is difficult to see where the error arose). When the adjusted chemical shifts are further corrected by the appropriate values of σ_a, deduced earlier, and analysed using equation 6.2 the values of B given in table 6.3 (which contains the other necessary parameters) are obtained; it should be noted that H_2 is unique in that while $\beta_T = 1$ and $\xi_T = 2$ for the "buffetted" atom, so that for this

TABLE 6.1 σ_a VALUES FOR THE SOLVENT CYCLOHEXANE

SOLUTE	$B/_{10}{}^{-18}$ esu	$\sigma^{92}_{w/ppm}$	$\sigma_{RF/ppm}$	$(2\beta_T - \xi_T)^2$	$\sigma_{BI/ppm}$	$\sigma^{(eqn.\ 6.3)}_{a/ppm}$
CH_4	0.84	-0.277[129]*	-0.242	0.123	-0.074	0.039
CMe_4	0.81	-0.170	-0.126	0.230	-0.133	0.089
$SiMe_4$	0.87	-0.282	-0.128	0.270	-0.168	0.014
$SnMe_4$	0.92	-0.293	-0.130	0.285	-0.187	0.024

Mean σ_a = 0.042 ppm.
(S.D = $\pm$ 0.03 ppm)

TABLE 6.2 σ_a VALUES FOR THE SOLVENT BENZENE

SOLUTE	$B/10^{-18}$ esu	σ^{92}_{w}/ppm	σ_{RF}/ppm	$(2\beta_T - \xi_T)^2$	σ_{BI}/ppm	σ_a/ppm (eqn. 6.3)
CH_4	0.84	0.150[129]*	-0.332	0.123	-0.074	0.556
CMe_4	0.81	0.113	-0.184	0.230	-0.133	0.430
$SiMe_4$	0.87	0.133	-0.209	0.270	-0.168	0.510
$SnMe_4$	0.92	0.095	-0.212	0.285	-0.187	0.494

Mean σ_a = 0.500 ppm
(S.D. = $\pm$ 0.05 ppm)

TABLE 6.3 DATA FOR THE HYDROGEN MOLECULE SOLUTE

SOLVENT	σ^{129}_{w}/ppm	$\langle R_T^2 \rangle / 10^{12}$ esu	β' ($\beta_T = 1$; $\xi'_T = 2$)		σ_a/ppm	B/$_{10}$ esu	Q^x
C_6H_{12}	-0.300	0.1425	0.26	1.23	0.042	0.69 Mean 0.64	1
C_6H_6	0.167	0.2050	0.26	1.23	0.500	0.59	1
CCl_4	0.500	0.1919	0.34	1.34	-	0.64	7.2

σ_{BI} = 0 (equation 5.21), the same buffetting causes a finite value of σ_{BI} for the other atom because of the short distance involved.

The "buffetting" mechanism on the hydrogen molecule can be conveniently split into two parts. First, the normal contribution and secondly when the "buffetting" occurs in the four octants including the other hydrogen atom. Equation 5.21 may be rewritten as

$$\sigma_{BI} = \frac{-BQ^{K}K^{H}}{r_{HX}^{6}} \left\{ (2\beta_T - \xi_T)^2 + (2\beta'_T - \xi'_T)^2 \right\} \qquad 6.4$$

where β' and ξ' are the totally distance modulated values in the 'rear' four octants. As mentioned above, $\beta_T = 1$ and $\xi = 2$, and therefore the extra-octant contribution with $(2\beta'_T - \xi'_T)^2$ is the sole contribution to σ_{BI} for H_2. The molecular model for H_2 is shown in figure 6.1.

Whilst the average of the two values of B for hydrogen in H_2, 0.64×10^{-18} esu, is somewhat larger than predicted (0.285×10^{-18} esu)[128], it is important to note that both the value reported in the literature[128] and that found experimentally are less than for the hydrogen atom (0.74×10^{-18} esu)[112], or that found experimentally in section 4.5a (0.87×10^{-18} esu) for a hydrogen atom in an sp^3 hydridized bond to carbon. Furthermore, from the gas-to-solution chemical shift for H_2 in CCl_4[129] and the data given in table 6.3, a value of Q^{Cl} of 7.2 can be deduced, that is again in excellent agreement with the value given in table 5.3

6:2e Considerations of the Molecules $Si(OCH_3)_4$, $Si(OCH_2CH_3)_4$ and $Si(CH_2CH_3)_4$

The molecules used so far have been relatively simple and it is therefore prudent to examine some ^1H chemical shifts of solute molecules that are more complex. Some appropriate systems, that are still approximately isotropic, are $Si(CH_2CH_3)_4$ with $Si(CH_3)_4$,

$Si(OCH_3)_4$ with $Sn(CH_3)_4$ and $Si(OCH_2CH_3)_4$ with $Sn(CH_3)_4$. On account of the molecular complexity of the solutes, the errors in estimating β and ξ geometrically would be high and consequently it becomes convenient to evaluate $(2\beta_T - \xi_T)^2$ from each chemical shift and draw comparisons between the resulting values. It would be expected that the CH_3 and CH_2 groups of $Si(OCH_3)_4$ and $Si(OCH_2CH_3)_4$, respectively, should be in similar molecular environments. This is borne out by the similarity between the value of $(2\beta_T - \xi_T)^2$ given in table 6.4. The fact that the value of $(2\beta_T - \xi_T)^2$ for the CH_3 group of $Si(CH_2CH_3)_4$ is not similar suggests that differences between the bond angles and lengths in the Si-C-C and Si-O-C groupings enforces a small but detectable change in the steric environment of the relevent hydrogen atoms.

6:2f Solute Size and σ_a Using the Anomalous Solvent, $C(NO_2)_4$

The above-mentioned relatively complex molecules may be used to examine theories relating to the effect of solute size 130 on σ_a. It is believed that the solvent tetranitromethane, $C(NO_2)_4$ may be anisotropic[121]. By using equations 6.2 and 6.3, with the appropriate values of $(2\beta_T - \xi)^2$ estimated geometrically and the value of Q^o from table 5.3, the values of σ_a for the solvent $C(NO_2)_4$ containing various solutes may be evaluated. The appropriate analyses are shown in table 6.5 from which it appears that $C(NO_2)_4$ is indeed anisotropic with a mean value for σ_a of 0.350 ppm. The value of σ_a varies with the size of the solute molecule or the radial distance of the resonant nucleus from the centre of the molecule. The smaller solutes, or smaller distances of the ^1H from the molecular centre, gives rise to the larger values of σ_a in general. This is in agreement with previous findings using a somewhat different approach to the problem[130]. It is interesting to note that the value of σ_a for the CH_2 resonant ^1H in $Si(OCH_2CH_3)_4$

TABLE 6.4 DATA FOR THE SOLUTES $Si(OCH_3)_4$, $Si()CH_2CH_3)_4$ AND $Si(CH_2CH_3)_4$

SOLUTE	SOLVENT	$\sigma_{w/ppm}$	$\langle R_T^2 \rangle / 10^{12}$ esu	$(2\beta_T - \zeta_T)^2$
$Si(OCH_3)_4$	$SnMe_4$	-0.187^{92}	0.1203	0.132
$Si(O\underline{CH_2}CH_3)_4$	$SnMe_4$	-0.185^{92}	0.1081	0.146
$Si(OCH_2\underline{CH_3})_4$	$SnMe_4$	-0.205^{92}		0.179
$Si(\underline{CH_2}CH_3)_4$	$SiMe_4$	-0.145^{67}	0.0811	0.119
$Si(CH_2\underline{CH_3})_4$	$SiMe_4$	-0.178^{67}		0.172

TABLE 6.5 DATA FOR THE SYSTEMS INVOLVING $C(NO_2)_4$ AS THE SOLVENT

SOLUTE	σ^{121}_{w}/ppm	σ_{RF}/ppm	$(2\beta_T - \xi_T)^2$*	σ_a/ppm
$Si(O\underline{CH_2}CH_3)_4$	-0.053	-0.137	0.146	0.275
$Si(OCH_2\underline{CH_3})_4$	-0.045	-0.137	0.179	0.326
$Si(OCH_3)_4$	-0.042	-0.122	0.132	0.252
CMe_4	-0.028	-0.122	0.230	0.394
$SiMe_4$	-0.035	-0.122	0.270	0.439
$SnMe_4$	-0.072	-0.125	0.295	0.438
CH_4	-0.053	-0.247	0.090	0.311

Mean σ_a = 0.350 ppm (S.D. = 0.07 ppm)

* estimated from previous experience

Q^o = 3.4 from 1,4 dioxan point in section 5.5

B = 0.87×10^{-18} esu

and for the CH_3 in $Si(OCH_3)_4$ are in very close agreements supporting the idea expressed previously based on arguments involving $(2\beta_T - \xi_T)^2$, that these hydrogens are in very similar molecular environments.

In conclusion it has been demonstrated that experimental gas-to-liquid ^1H chemical shifts for 'simple' systems of isotropic molecules can be considered to arise from reaction field effects and a molecular "buffetting" due to pairwise encounters that are sterically controlled. The use of such an idea through the appropriate equations has provided an extensively consistent method of analysing experimental gas-to-liquid ^1H chemical shifts, as well as elucidating other interesting nmr parameters such as σ_a and ideas regarding molecular structure. However, ^1H chemical shifts are relatively small and it appears to be wise to turn attention to the larger solvent shifts found for ^{19}F.

6:3 Gas-to-Solution ^{19}F Chemical Shifts in Selected Systems

6:3a General

Although the theory has only been applied to ^1H nmr chemical shifts so far, there is no reason to believe that it should not be applicable to other resonant nuclei and in particular ^{19}F nmr chemical shifts. The method adopted here will be to use some ^{19}F gas-to-solution chemical shifts, σ_w, of isotropic systems and calculate the value of B for fluorine in different molecules from the expression:

$$\sigma_w = -B\left(\langle R_T^2\rangle + \frac{Q^X K^H}{r^6}\,(2\beta_T - \xi_T)^2\right) \qquad 6.5$$

The values of β_T and ξ_T are calculated geometrically in the same way as was done previously. However, the value of K^H/r^6 (0.7133×10^{12} esu) used previously for buffetting of the hydrogen atom has

to be modified to 0.4958×10^{12} esu to account for the difference between r_{HH} (2.4×10^{-8} cm) and r_{HF} (2.55×10^{-8} cm); further data relevant to the ensuing analyses are provided in table 4.6 and other tables specifically referring to the solute molecule under study.

6:3b B-Values of Fluorine in CF_4, SiF_4 and SF_6

Initially, the gas-to-solution chemical shifts of CF_4 in various solvents are analysed through equation 6.5 and using a model similar to the one depicted in figure 5.3. Although no value for the van der Waals radius of the CF_3 group could be found, its value was calculated as 2.34×10^{-8} cm from the known bond lengths of C-F and C-H, l(C-F) and l(C-H), and van der Waals radii, r_w, of F, H and CH_3, using the formula

$$r_w(CF_3) = r_w(CH_3) \quad \frac{r_w(F) + l(C\text{-}F)}{r_w(H) + l(C\text{-}H)}$$

The results of the analysis on CF_4 is given in table 6.6. It is evident that there is some variation in B, as was found by Mohanty and Bernstein[32], although the mean value ($30.8(5) \times 10^{-18}$ esu) compares well with that of 26×10^{-18} esu deduced from gas phase studies[32].

Other relevant and suitable gas-to-solution chemical shift data are available for the molecules SiF_4 and SF_6. The geometrical models for these are depicted in figures 5.3 and 6.2 respectively; the van der Waals radii of the SiF_3 group (2.54×10^{-8} cm) and SF_5 group (2.4×10^{-8}cm) are found in the way described for the CF_3 group. It should be noted that the model for SF_6 is an extension of figure 5.3, but with account being taken of the extra number of atoms peripheral to the SF_5 group. The relevant analyses are given in tables 6.7 and 6.8. Again there is some degree of

TABLE 6.6 DATA AND RESULTS FOR THE SOLUTE CF_4

SOLVENT	$\sigma_{w/ppm}^{120}$	ξ_T ($\beta_T = 1$)	$\langle R_T^2 \rangle / 10^{12}$ esu	$\bar{E}^2 / 10^{12}$ esu	$B / 10^{-18}$ esu
$SnMe_4$	-6.82	1.68	0.1235	0.0508	39.1(3)
$SiEt_4$	-6.00	1.62	0.1039	0.0716	34.1(9)
$SnEt_4$	-6.26	1.61	0.1242	0.0754	31.3(6)
C_6H_{12}	-6.00[132]	1.69	0.1565	0.0476	29.3(9)
C_6H_6*	-7.11[82]	1.70	0.2381	0.0446	26.9(2)
CCl_4*	-7.60	1.71	0.2261	0.0763	25.1(3)
$SiCl_4$*	-6.85	1.71	0.1534	0.0763	29.8(2)

$$\left(\bar{E}^2 = \frac{Q^X K^H}{r_{FX}^6} (2\beta_T - \xi_T)^2 \right)$$

Mean B = 30.8(5) $\times 10^{-18}$ esu
(S.D. = $\pm$ 4.3 $\times 10^{-18}$ esu)

* anisotropy of 0.5 ppm included in calculation

* $Q^{Cl} = 6.5$

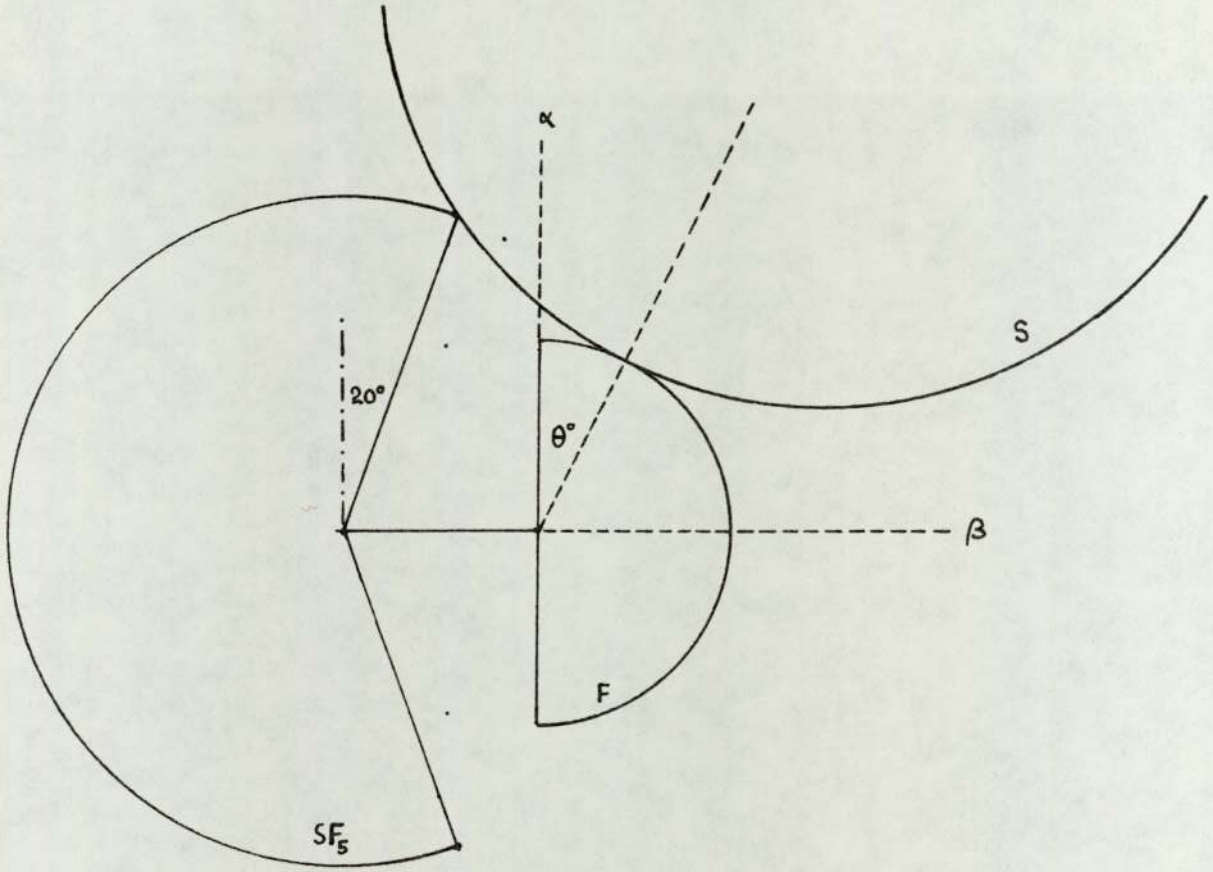

Fig. 6.2. Two dimensional representation of a sulphur hexafluoride molecule (fluorine F and rest of molecule SF_5) encountered by an isotropic solvent molecule(S).

TABLE 6.7 DATA AND RESULTS FOR THE SOLUTE SiF_4

SOLVENT	σ^{120}_{w}/ppm	ξ_T ($\beta_T = 1$)	$\langle R_T^2 \rangle / 10^{12}$ esu	$E^2/10^{12}$ esu	$B/10^{-8}$ esu
$SnMe_4$	-10.05	1.62	0.1402	0.0716	47.4(5)
$SiEt_4$	-9.82	1.58	0.1201	0.0875	47.3(1)
$SnEt_4$	-9.12	1.56	0.1437	0.0960	38.0(5)
CCl_4*	-11.15	1.69	0.2410	0.0872	33.9(8)
$SiCl_4$*	-10.10	1.69	0.1674	0.0876	39.6(7)

$$\left(\bar{E}^2 = \frac{Q^X K^H}{r_{FX}^6} \; (2\beta_T - \xi_T)^2 \right)$$

Mean B = 41.2(9) $\times 10^{-18}$ esu
SD = $\pm$ 5.3 $\times 10^{-18}$ esu

* $Q^{Cl} = 6.5$

TABLE 6.8 DATA AND RESULTS FOR THE SOLUTE SF_6

SOLVENT	σ^{120}_{w}/ppm	ξ_T ($\beta_T = 1$)	$\langle R^2 \rangle / 10^{12}$ esu	$\bar{E}^2 / 10^{12}$ esu	$B / 10^{-18}$ esu
$SnMe_4$	-7.05	1.33	0.1484	0.2226	19.0(0)
$SiEt_4$	-6.35	1.28	0.1266	0.2570	15.9(5)
$SnEt_4$	-6.70	1.27	0.1512	0.2642	16.1(3)
CCl_4*	-7.98	1.40	0.2601	0.3265	13.6(0)
$SiCl_4$*	-7.03	1.40	0.1792	0.3265	13.9(0)

$$\left(\bar{E}^2 = \frac{Q^X K^H}{r_{FX}^6} (2\beta_T - \xi_T)^2 \right)$$

Mean B = 15.7(2) x 10^{-18} esu
(SD = ± 1.9 x 10^{-18} esu)

* $Q^{Cl} = 6.5$

variation in the B values tabulated. This is more so in the case of SiF_4, as was also shown by Mohanty and Bernstein[32]. The average of the B values evaluated for fluorine in SiF_4 and SF_6 are $41.2(9) \times 10^{-18}$ esu and $15.7(2) \times 10^{-18}$ esu respectively. This is compared to the respective values[32] of 43×10^{-18} esu and 45×10^{-18} esu from gas phase studies. It would appear that whilst agreement is good in the case of SiF_4 it is not so good in the case of SF_6. The situation is not improved significantly by considering the values of B for fluorine in CF_4, SiF_4 and SF_6 reported earlier by Petrakis and Bernstein[31] to be 16.4×10^{-18} esu, 43.5×10^{-18} esu and 29.5×10^{-18} esu respectively; in any event there is some indication that these values may be inferior to the later values given by Mohanty and Bernstein[32]. It has been inferred[31] that B values for X-H bonds in ^1H nmr should decrease as bond contraction or double bond character increases but the B values for X-F bonds in ^{19}F nmr should increase with increased double bond character. If it is possible to quantify double bond character directly in terms of bond contraction, viz. the difference in the calculated bond length and the observed bond length, then it is evident that double bond character changes as C-F < S-F < Si-F. Thence, it may be expected that B(C-F) < B(S-F) < B(Si - F) in accordance with the findings of Petrakis and Bernstein[31] but not with Mohanty and Bernstein[32], who found B(C-F) < B(Si - F) $\lesssim$ B(S-F). Although the findings herein show that B(S-F) < B(Si-F), the absolute value of B(S-F) appears to be anomalously low. It is possible that the SF_6 molecular model is at fault or the "buffetting" equation must be redefined on account of the resonant fluorine atom having a different site symmetry than any previously considered ones. In general for tetrahedrally disposed atoms in spherical molecules the site

symmetry[131] of the resonant nucleus is C_{3v} (this is probably a reasonable assumption even in the case of the hydrogens of the group IVB tetramethyls) whereas the site symmetry[131] of the fluorine atom in SF_6 is C_{4v}. Because the question of symmetry was never considered during the development of the theory (chapter 5) it is not known how the "buffetting" equation may be altered by a change in symmetry. However, accepting the fact that there may be a deficiency in the theoretical make-up regarding SF_6 it must also be accepted that the presently proposed value of B for fluorine in SF_6 is as good has has been previously proposed[31, 32].

6:3c The B-Value of Fluorine in C_6F_6

A final examination of ^{19}F nmr chemical shifts is undertaken with the molecule C_6F_6 - hexafluorobenzene. The geometrical model was considered in two parts (figures 6.3 and 6.4); the molecule viewed to the side of the benzene ring as shown in fig. 6.3 and to the plane of the benzene ring as shown in fig. 6.4. The time probability of a solvent molecule encountering the C_6F_6 solute molecule may be considered on the basis of relative areas of the parts of the molecule being approached. It is easily shown that the ratio of the areas of the C_6F_6 molecule viewed from the side of the benzene ring (fig. 6.2) to the plane of the benzene ring (fig. 6.3) is approximately equal to unity. It would appear therefore, that the encounter probability should be the same from the side of the ring as from the plane of the ring. With this premise, the values of B are evaluated through equation 6.5 and presented in table 6.9, along with other appropriate data. The mean value of B for fluorine in C_6F_6 is $15.8(7) \times 10^{-18}$ esu which is lower than found in CF_4 ($\simeq 30 \times 10^{-18}$ esu). Although no

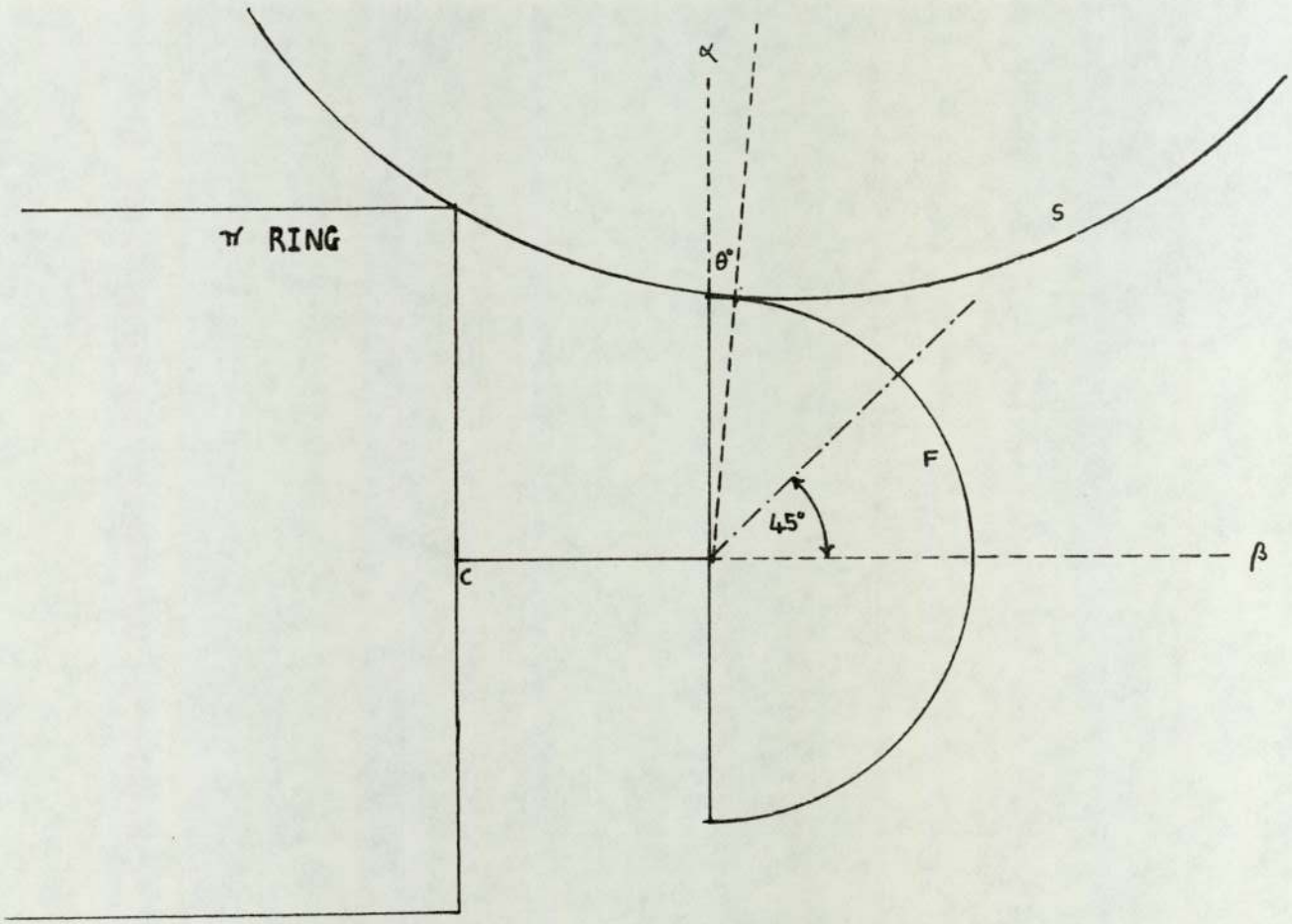

Fig. 6.3. Two dimensional representation of a hexafluorobenzene molecule (fluorine F) encountered by an isotropic solvent molecule(S)-I.

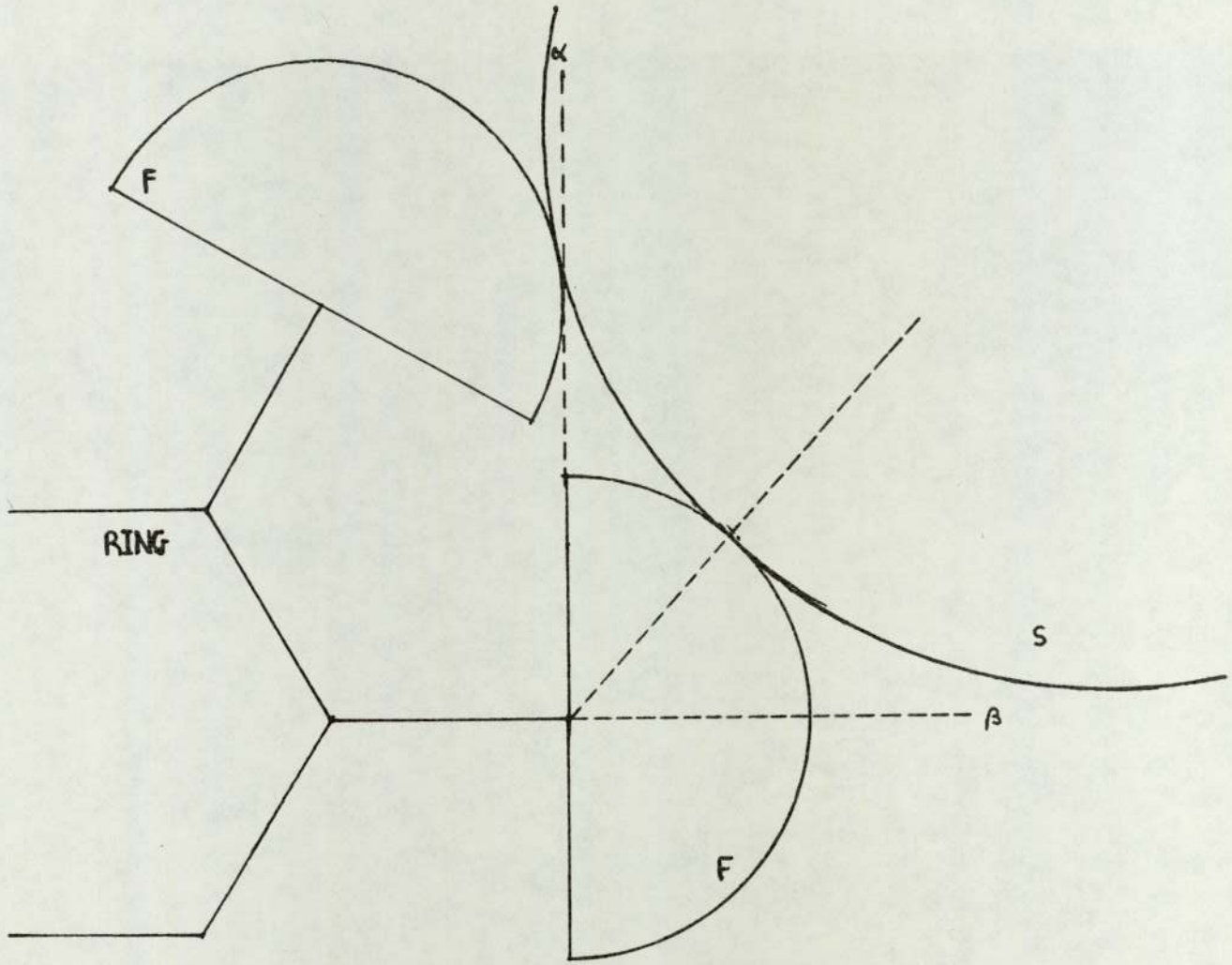

Fig. 6.4. Two dimensional representation of a hexafluorobenzene molecule (fluorine F) encountered by an isotropic solvent molecule(S)-II.

TABLE 6.9 DATA AND ANALYSES FOR THE SOLUTE C_6F_6

SOLVENT	CONTACT $\theta_{I/O}$	ξ_I^C	ξ_I^D	ξ_{II}^D	ξ_T	$\langle R_T^2 \rangle / 10^{12}$ esu	$\bar{E}^2 / 10^{12}$ esu	$\sigma_{w/ppm}^{120}$	$B / 10^{-18}$ esu
$SnMe_4$	38	0.844	0.115	0.266	1.23	0.1208	0.2940	-7.89	19.0(2)
$SiEt_4$	37.5	0.833	0.124	0.206	1.22	0.0955	0.3014	-7.16	18.0(4)
$SnEt_4$	37.	0.822	0.131	0.266	1.22	0.1157	0.3014	-7.21	17.2(9)
C_6H_{12}	39	0.867	0.098	0.266	1.22	0.1664	0.2940	-7.70^{132}	16.7(2)
CCl_4*	39.5	0.878	0.095	0.271	1.24	0.2554	0.5242	-8.81	11.3(0)
$SiCl_4$*	39.5	0.878	0.095	0.271	1.24	0.1643	0.5242	-8.85	12.8(5)

Mean $B = 15.8(7) \times 10^{-18}$ esu
(S.D. $= 3 \times 10^{-18}$ esu)

$$\left(\text{CONTACT } \theta_{II} = 45^\circ;\ \beta_T = 1;\ \xi_{II}^C = 0;\ E^2 = \frac{Q^X K^H}{r_{FX}^6} (2\beta_T - \xi_T)^2 \right)$$

* $Q^{Cl} = 6.5$

literature value can be found to make a comparison, it is interesting to note that wherever the site symmetry of the resonant nucleus is other than C_{3v} (or differs from a sp^3 bonding situation) the value of B appears to have been reduced. For example the B value of F in SF_6 is found to be lower than in CF_4 and in SiF_4, and in the case of B values of H the value is lower in the case of H_2 compared to CH_4.

It appears that the theory is applicable to ^{19}F gas-to-solution chemical shifts as well as ^1H shifts. Because of the relatively large values of ^{19}F chemical shifts compared to the anisotropy screening, σ_a, which is independent of the resonant nucleus, any inherent anisotropies of the solvents chosen in the aforegone studies will not be of any great detriment to the analysis, however approximate the σ_a correction. In the above ^{19}F shift analyses σ_a for C_6H_{12} was ignored and σ_a for C_6H_6 taken as 0.5 ppm.

6:4 Some ^1H Chemical Shifts of Spheroidal Molecules

Spheroidal molecules (oblate and prolate) have been studied from the point of view of linear reaction field screening[99, 100, 133, 134]. However if the spheroidal molecule is non-polar only the mean square reaction field need be considered and to a first approximation it is possible to treat spheroidal molecules as spherical.

6:4a ^1H Chemical Shift Analysis of Benzene

Gas-to-solution chemical shift data is available for benzene with four 'protic' isotropic solvents. It is reasonable to assume that the nuclear screening due to molecular "buffetting" is the same in all four solvents and therefore a linear regression analysis of σ_w on $\langle R_T^2 \rangle$ is possible. With the solvent C_6H_{12} the value of σ_a was varied between 0 and 0.1 ppm until the best straight line was found. The value of σ_a was not allowed to exceed 0.1 ppm

TABLE 6.10 LINEAR REGRESSION ANALYSIS FOR BENZENE

SOLVENT	$\sigma_{w/ppm}^{67}$	$\langle R_T^2 \rangle / 10^{12}$ esu
CMe_4	-0.268	0.103
SiMe	-0.243	0.101
$SnMe_4$	-0.277^{92}	0.146
C_6H_{12}	-0.203	0.183

Regression analysis of σ_w on $\langle R_T^2 \rangle$:

$\sigma_a(C_6H_{12})$/ppm	correlation coefficient	$B/10^{-18}$ esu	
0.	-0.61	-	
0.05	0.25	0.100	
0.10	0.92	0.586	(intercept = -0.195 ppm)
neglect C_6H_{12} point	0.73	0.546	(intercept = -0.200 ppm)

SOLVENT	$\sigma_{w/ppm}^{92}$	$\langle R_T^2 \rangle / 10^{12}$ esu
CCl_4	-0.443	0.265

use B = 0.58(6) x 10^{-14} esu; Q^{Cl} found as 5.68

because this is the generally accepted[36, 121] upper limit of σ_a for C_6H_{12}. The relevant analyses are shown in table 6.10 where the best straight line (correlation coefficient = 0.92) is when σ_a = 0.1 ppm. The value of B is given as 0.58(6) x 10^{-18} esu. If cyclohexane is removed from the regression analysis the value of B is shown to be 0.54(6) x 10^{-18} esu (correlation coefficient = 0.73), although there are only three points in the regression analysis. The value of B for hydrogen in an sp^2 hybridized bond will be taken as 0.58(6) x 10^{-18} esu. It is interesting to note that the ratio of hydrogen (bonded to carbon) B values in an sp^2 bond to an sp^3 bond is 0.68 and the ratio of fluorine (bonded to carbon) B values in an sp^2 bond to an sp^3 bond is 0.51, indicating that the effect of hybridization on both ^1H and ^{19}F chemical shifts may stem from a similar cause.

If the reaction field screening calculated from equation 4.22 is taken from each gas-to-solution shift of benzene (table 6.10), the appropriate value of $(2\beta_T - \xi_T)^2$ can be evaluated for each system using equation 5.21. Furthermore, the values of β_T and ξ_T are evaluated geometrically using figures 6.3 and 6.4 of the appropriate dimensions. The encounters of the hydrogen atoms in benzene is divided into two modes, as was the case with C_6F_6. Based on the encounter probability towards the plane of the ring being equal to the probability of encounters towards the side of the ring (on the basis that the relative surface areas are about equal) β was found to be 1 and ξ approximately 1. It can be seen from table 6.11 that this is not in accord with the experimentally expected value of ξ_T. It is possible that the time probability of solvent encounters towards the benzene ring cannot be defined precisely on the simple basis of relative surface areas. It may

be speculated that because of the electron rich area on the plane of the benzene ring, the solvent may spend a greater time in this position that at the relatively electron deficient side of the ring. This could be due to a specific type of complexation occurring between the π-electrons of the benzene ring and the solvent on a transient though continuous basis. It is indicated in table 6.11 that a better agreement is found between the experimental and geometrical ξ_T value if the encounter probability of the solvent to the atom containing the resonant nucleus is greater towards the plane of the ring than towards the side of the ring. The analysis in table 6.11 indicates that solvent encounters towards the plane of the ring should take place for between 2/3 and 3/4 of all time.

Returning to the C_6F_6 molecule (section 6:3c) where equal solvent encounter probabilities towards the plane and the side of the ring gave a B value of about 16×10^{-18} esu (table 6.9). If encounter time probabilities of a solvent molecule towards the plane of the C_6F_6 ring is taken to be 2/3 of all time, this renders a value of B for fluorine, B_{sp^2} (C-F), at about 25×10^{-18} esu ($\beta_T = 1$ and $\xi_T = 1.4(5)$) and then the ratio of B_{sp^2} (C-F) to B_{sp^3} (C-F) as about 0.8, closer to the ratio found for hydrogen B values (0.68).

6:4b Analysis of Some Other Spheroidal Molecules

Some further gas-to-solution chemical shift data of selected spheroidal molecules in different solvents with the appropriate analyses and results are given in table 6.12. The values of β_T and ξ_T have not been determined geometrically but it has been assumed that in each case the ratio of $(2\beta_T - \xi_T)^2$ for a group IVB tetramethyl solvent to CCl_4 as solvent is 1.2. This number arises from the ratio of the $(2\beta_T - \xi_T)^2$ value for CH_4 with a

TABLE 6.11 DETAILED β AND ξ ANALYSES OF BENZENE

SOLVENT	(β = 1) EXPT. ξ	(β = 1; refer to figs. 6.3 and 6.4) GEOMETRICAL VALUES OF ξ WITH TIME WEIGHTINGS (I : II) $^1/_2 : ^1/_2$	$^2/_3 : ^1/_3$	$^3/_4 : ^1/_4$
CMe_4	1.2(9)			
$SiMe_4$	1.3(4)			
$SnMe_4$	1.3(2)	1.0(1)	1.2(4)	1.3(5)
C_6H_{12}	1.3(2)			

(σ_a = 0.1 ppm)

($B = 0.58(6) \times 10^{-18}$ esu)

TABLE 6.12 DATA AND RESULTS FOR SOME SPHEROIDAL SOLUTES

SOLUTE	SOLVENT	$-\sigma_w^{92}$/ppm	$\langle R_T^2 \rangle / 10^{12}$ esu	$B/10^{-18}$ esu	CALC. Q	σ_a/ppm
1, 3, 5 $\underline{Me}_3$ C_6H_3	$SnMe_4$	-0.278	0.131	0.87	-	-
1, 3, 5 $\underline{Me}_3$ C_6H_3	CCl_4	-0.417	0.277	0.87	7.1(0)	-
1, 3, 5 Me_3 $C_6\underline{H}_3$	$SnMe_4$	-0.205	0.131	0.59	-	-
1, 3, 5 Me_3 $C_6\underline{H}_3$	CCl_4	-0.292	0.277	0.59	6.5(0)	-
MeC≡CMe	$SnMe_4$	-0.288	0.139	0.87	-	-
MeC≡CMe	CCl_4	-0.477	0.249	0.87	7.1(3)	-
MeC≡CMe	C_6H_{12}	-0.270	0.172	0.87	-	0.017
MeC≡CMe	C_6H_6	+0.210	0.263	0.87	-	0.606
$Me_2C=CMe_2$	$SnMe_4$	-0.230	0.123	0.87	-	-
$Me_2C=CMe_2$	CCl_4	-0.340	0.257	0.87	4.3(0)	-
$Me_2C=CMe_2$	C_6H_{12}	-0.217	0.169	0.87	-	0.053
$Me_2C=CMe_2$	C_6H_6	+0.175	0.271	0.87	-	0.534

cont'd....

C_2H_6	CCl_4	-0.310[67]	0.322	0.87	(6.5)*	-
C_2H_6	C_6H_{12}	-0.173[67]	0.251	0.87	-	0.063
C_2H_6	C_6H_6	+0.233[67]	0.322	0.87	-	0.531
C_2H_4	CMe_4	-0.230[67]	0.158	0.59	-	-
C_2H_4	CCl_4	-0.358[67]	0.320	0.59	5.6(5)	-
C_2H_4	C_6H_{12}	-0.212[67]	0.250	0.59	-	0.073
C_2H_4	C_6H_6	+0.200[67]	0.342	0.59	-	0.538

† $\sigma_a = \sigma_w^{EXPT} - \sigma_{RF} - \sigma_{BI}^{Gp.\overline{\overline{IV}}B}$; $\sigma_{BI}^{Gp\overline{\overline{IV}}B} = \sigma_{HH}^{BI}$ of $Gp\overline{\overline{IV}}BMe_4$

* σ_{HH}^{BI} calcd. from CCl_4 value using $Q^{Cl} = 6.5$

group IVB tetramethyl solvent to that with CCl_4 as solvent. Although this may not be exactly the case in all instances it serves the purposes of giving some semi-quantitative value to the analyses. It is evident from table 6.12 that the Q^{Cl} values compare very favourably with the ones derived previously in this thesis. The values of σ_a for C_6H_{12} and C_6H_6 as solvents are also close to the ones derived previously, both in this thesis and elsewhere[36].

6:5 An Examination of the Linear Reaction Field

Laszlo and Musher[96] examined quantitatively the linear reaction field concept using nmr screening constants for ^1H's in two molecules (I & II). Their conclusions were that the reaction field must assume different values at different points in the molecule, especially complex molecules. Moreover, the magnitude and direction of the linear reaction field at a given molecular position given by the equation for a spherical cavity[94] or spheroidal cavity[133] does not adequately describe the experimental reaction field dependence on ϵ :

$$\vec{R} = \frac{(n^2 - 1)}{3\alpha} \frac{(\epsilon - 1)}{(\epsilon + (n^2/_2))} \vec{\mu} \qquad 6.6$$

The linear electric field (or reaction field) effect on ^1H shielding is well accepted[94, 135, 136] and for a given ^1H in a chemical bond, in the absence of electric saturation[69], is given by

$$\Delta\sigma^i = -AE_z^i \qquad 6.7$$

where E_z^i is the electric field component along the bond directed towards the ^1H. A is accepted to be reasonably constant bonded to carbon and quoted at about 2×10^{-12} esu.

The solute molecules considered were cis - 2, 6 - dibromo - 4, 4-diphenylcyclohexanone(I) and 2-bromo-4, 4 diphenylcyclohexanone

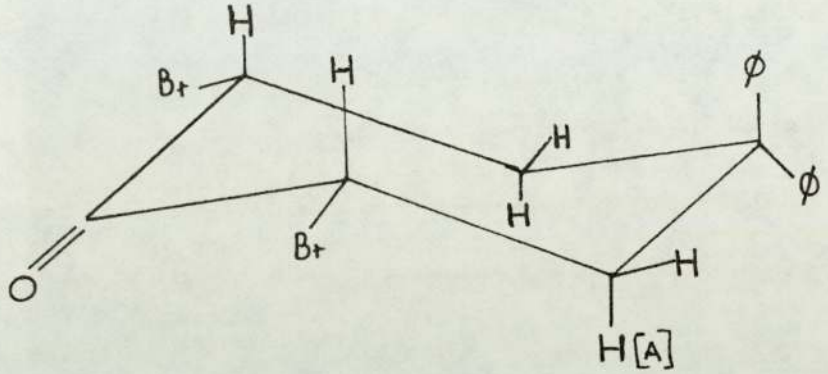

I. cis-2,6-dibromo-4,4-diphenylcyclohexanone.

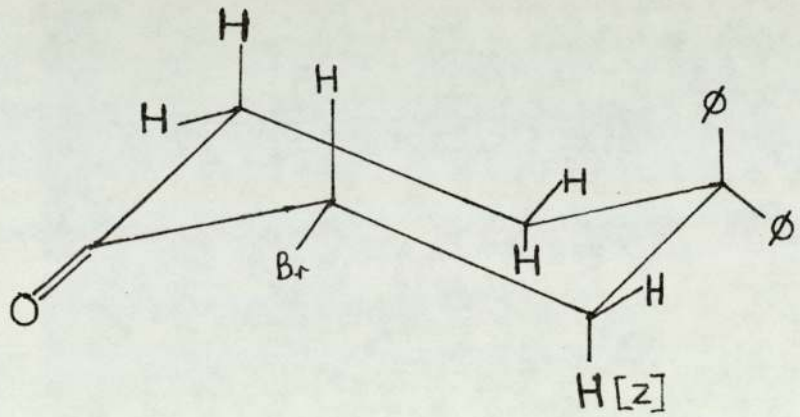

II. 2-bromo-4,4-diphenylcyclohexanone.

(II). Examination of a molecular model of each of these molecules indicates that the nuclei A and Z in molecule I and II respectively are in similar steric positions the bromine atom not being in a position to affect nucleus A in molecule I to any significant degree. Without any justification of any particular steric effect on nuclear screening, the difference in screening between nucleus A and nucleus Z should leave the linear reaction field only. Examination of table 6.13 shows that with the limited data available it would appear that whilst the reaction field difference $\Delta R(A-Z)$ (calculated using equation 6.6 and data in reference 96) varies in a systematic fashion, the difference in screening $\Delta\sigma(A-Z)$ is effectively constant. The only conclusion that can be drawn from this is that the linear reaction field effect on nuclear screening is unimportant and close to zero. This could go some way towards explaining the quandary left by Laszlo and Musher[96] as was indicated above. It is not suprising to find that linear electric reaction field effects are very small since they are analagous to the paramagnetic nuclear screening (section 1:9b) which is an effect that depends on the mixing of ground and exited states of the atom in the presence of B_o. This effect is small for ^{1}H chemical shifts but very much more significant for ^{19}F chemical shifts.

It appears that without any specific reference to the molecular encounter theory, or "buffetting" theory, a conclusion has been reached regarding the status of the linear reaction field. Furthermore it appears that it may be valid to examine the theory in this thesis using polar solute molecules, provided the solvent is suitably non-polar.

6:6 Solvent Effects on Diastereoisotopic Chemical Shifts in Sulphinyl Chloride Compounds

Magnetic non-equivalence of the alpha gem-dimethyl groups of

TABLE 6.13 NUCLEAR SCREENING DIFFERENCES AND LINEAR REACTION FIELD DIFFERENCES FOR THE ^{1}H NUCLEI A AND Z IN MOLECULES I AND II RESPECTIVELY[96]

$-\Delta\sigma(A-Z)$/ppm	$-\Delta R(A-Z)/10^{4}$ esu	SOLVENT ϵ
0.150	0.47	15.70
0.169	0.45	12.67
0.153	0.43	9.67
0.153	0.40	6.78

isopropyl-β-ketosulphinyl chlorides ($RCOC(CH_3)_2SOCl$) has been observed and has been shown to be solvent dependent[137]. This is probably due to the different steric environments of the hydrogen atoms in the methyl groups relative to the rest of the molecule. However the original choice of solvent was not as judicious as it might have been in the light of the evidence presented so far in this thesis. Consequently a series of these isopropyl-β-ketosulphinyl chlorides have been studied at low concentration (< 5 mol %) in the solvents tetramethyl silane and carbon tetrachloride using a Perkin-Elmer R12B NMR spectrometer operating at 60 MHz. The intramolecular difference in the methyl group ^1H nuclear screening were thus observed in a 'protic' and 'chloric' solvent. The results are presented in table 6.14.

It was observed that the methyl groups generally showed a different diasterotopic shift in the two solvents. The screening difference between the methyl groups (A and B) in the two solvents may be given by:

$$\Delta\sigma^{A-B}_{CCl_4-TMS} = \frac{-BK^H}{r^6_{HH}}\left[Q^{Cl}\left(\frac{r_{HH}}{r_{HCl}}\right)^6 (2\beta-\xi)^2_{CCl_4} - (2\beta-\xi)^2_{TMS}\right] \qquad 6.8$$

The square reaction field effects of course cancel by difference. Specific effects of self-association are expected to be eliminated by using a low concentration of solute and it is expected that linear reaction effects can be neglected (section 6:2c). Thus, the difference $\Delta\sigma^{A-B}_{CCl_4-TMS}$ may be considered to depend on the solvent size, the nature of the peripheral atoms on the solvent and the nature of the R-group in the solute together with its steric hindrance of the methyl groups of interest (A & B).

The most spectacular change is where the R-groups are phenyl and β-naphthyl, going from a screening difference, $\Delta\sigma^{A-B}_{SOLVENT}$,

TABLE 6.14 NUCLEAR SCREENING DIFFERENCES (in Hz at 60 MHz) OF ALPHA GEM-DIMETHYL GROUPS IN SULPHINYL CHLORIDES

CH_3 [A]
RCOC-SOCl
CH_3[B]

$\Delta \sigma^{A-B}_{SOLVENT}$

R-group	TMS	CCl_4
Methyl	5.4(2)	5.4(2)
n-butyl	5.1(7)	4.3(3)
1,methylethyl	6.2(5)	6.6(7)
1,methylpropyl	6.6(6)	6.7(0)
cyclohexyl	6.6(7)	5.2(7)
phenyl	2.8(3)	0
β-naphthyl	2.3(4)	0
α-naphthyl	0	0

Note: $\Delta\sigma^{A-B}_{SOLVENT}$ is measured with respect to calibrated chart paper over 5 ppm and are stated as the average of at least five measurements with standard deviations of less than 0.05 H_z.

of 0 when the solvent is carbon tetrachloride to 2.3 and 2.8 Hz when the solvent is tetramethylsilane. Although no quantitative value can be given, it is evident that the phenyl group and β-naphthyl group display a similar steric role in the compounds being studied. It is interesting to note that when the R-group is changed to an α-naphthyl group the value of $\Delta\sigma^{A-B}_{SOLVENT}$ is 0 for both carbontetrachloride and tetramethylsilane. This may have been predicted to some extent, especially when the solvent was carbon-tetrachloride, from the results on the phenyl group and β-naphthyl group. However, it is evident that the α-naphthyl and β-naphthyl groups display different steric effects in the compounds being studied.

Furthermore, it may be expected that n-butyl will have a greater steric effect on $\Delta\sigma^{A-B}_{SOLVENT}$ than the methyl group. This is reflected in the results given in table 6.14. Also it is evident that the 1 methylethyl and 1 methylpropyl groups, although of differing steric effects with respect to solvent encounters in an absolute sense, are susceptible to similar changes in $\Delta\sigma^{A-B}_{SOLVENT}$ when the solvent is changed from tetramethylsilane to carbon tetrachloride. This should not be too surprising in view of the similar molecular shape of 1 methylethyl and methylpropyl groups. Although no quantitative value can be given to the above results it is evident that there is a definite solvent dependent steric effect on the diastereotopic chemical shifts in the sulphinyl chloride compounds studied. As an aside, it was interesting to note that the coupling constant of the methyl and methine hydrogens in the isopropyl group of the molecule $Me_2CHCOCMe_2SOCl$ is observed to change from 6.2(5) to 5.6(7) Hz upon changing the solvent from tetramethylsilane to carbon tetrachloride.

The solute $MeCOCMe_2SOCl$ was studied in more detail because

the screening difference $\Delta\sigma^{A-B}_{SOLVENT}$ is the same in both tetramethylsilane and carbon tetrachloride. It would have been desirable to have a gas phase spectrum of this solute and observe the intrinsic screening difference betweeen the methyl groups A and B. However this was impractical on account of its low vapour pressure[138] (b.pt. 80° (@ 2 torr). The extensive solvent measurements, made in finer detail, are shown in table 6.15. It is observed that there is a change in $\Delta\sigma^{A-B}_{SOLVENT}$ generally, although some of this may be due to specific or anisotropic effect, especially in the case of hexafluorocylohexane and benzene. The fact that benzene gives a different $\Delta\sigma^{A-B}_{SOLVENT}$ to tetramethylsilane, both being 'protic' solvents, indicates that the two methyls A and B are in different magnetic and possibly steric positions. The equality of the $\Delta\sigma^{A-B}_{SOLVENT}$ values for tetramethylsilane and carbon tetrachloride is possibly a volume effect on the β and ξ values that more or less outweighs the difference in "buffetting" strength of the chlorine atom relative to the hydrogen atom. It appears however that there is a solvent effect on diastereotopic chemical shifts, possibly of the type described in chapter 5.

6:7 Conclusions

It would appear that gas-to-solution nmr chemical shifts of van der Waals origin can be analysed precisely when they are treated as arising from two effects; the first being due to the reaction field effects of the solvent continuum (chapter 4) and the second due to short range non-continuum molecular "buffetting" (chapter 5). The former effect is formulated using an extended Onsager type approach and the latter by a novel semi-classical

TABLE 6.15 NUCLEAR SCREENING DIFFERENCES (IN Hz AT 60 MHz) OF THE ALPHA GEM-DIMETHYL GROUPS IN THE SULPHINYL CHLORIDE, Me-C(=O)-C(Me)(Me)-SOCl

SOLVENT	$\Delta\sigma^{A-B}_{SOLVENT}$ (measured over 100 Hz range)
T.M.S.	5.2(0)
CCl_4	5.2(4)
CBr_4 (saturated solution in CCl_4)	5.0(4)
C_6F_{10}	5.8(3)
C_6H_6	5.0(4)

dipolar electric field approach. Whilst the emphasis has been on the analysis of nmr chemical shifts through equations 4.22 and 5.21, it is evident (chapter 4) that the overall approach may be applied to some non-nmr problems. Such problems will be dealt with in chapter 7.

Probably the most promising aspect of the work is the recognition of the "buffetting" interaction and the characterization of the corresponding nuclear screening, σ_{BI} (equation 5.21). Whilst this depends on both the solute and solvent molecules, it also depends, through β_T and ξ_T on the steric accessibility of the solvent molecule to the solute molecule containing the resonant nucleus. It would appear that repulsion forces can be neglected because of the favourable comparison between the experimental and 'hard' atom calculated values of β_T and ξ_T.

With a knowledge of the appropriate, and apparently universal, fundamental constants it follows that equation 5.21 may emerge as a means of determining local features of molecular structure and thus facilitate the elucidation of molecular structures.

CHAPTER 7

SOME NON-N.M.R. ASPECTS OF MOLECULAR ENCOUNTER THEORY

7:1 Van der Waals a-Values

In section 4:7b the van der Waals a-value was predicted for pure liquids using a relationship of the form

$$a^{RF} = \frac{3}{8} \angle \alpha \langle R_1^2 \rangle \; V_m \qquad 7.1$$

By comparing the predicted and accepted values of a it is contended that there should be a contribution to the van der Waals a-value from what may be the "buffetting" effect. It is expected that the "buffetting" square field will give rise to a similar form of energy dependence as that due to reaction fields, but with some steric control.

Inherent in the theory of molecular "buffetting" is that only pairwise atom-atom encounters are considered. The parameters β and ξ describe the total effective accessibility of the solvent to the solute atom as a result of many pairwise interactions, considered to operate successively; successive pairwise encounters need not involve the same solute atom or even the same solvent molecule. If this model is correct, the contribution of the "buffetting" effect to intermolecular forces can be considered to arise from the square field implicit in equation 5.19, which in turn can be considered to be operative for any one of the solute peripheral atoms:

$$E_{BI}^2 = \frac{K}{r^6} (2\beta - \xi)^2 \qquad 7.2$$

By analogy with the reaction field energy considerations, the van der Waals constant a^{BI}, due to molecular "buffetting" may be written:

$$a^{BI} = \frac{1}{2} \angle \alpha_B \bar{E}_{BI}^2 \; V_m \qquad 7.3$$

However, the following assumptions must be made, with the reasons given:

(1) α_B is the polarizability of the bond containing the resonsant atom since it is this part of the molecule that is distorted most in transmitting the force through the molecule, i.e. the "buffetting" contribution originates locally at the periphery of the solute molecule.

(2) V_m is the molar volume of the entire molecule because the entire molecule experiences the force.

(3) $\bar{E}^2_{BI}$ is the same at the surface of the liquid as in the bulk of the liquid since the force required is the total force from one encounter which may be considered to be maintained through successive collisions. There is one exception to this however - the case of the H_2 molecule. In this case, whatever the orientation of the H_2 molecule in the surface, it is uncertain how the "buffetting" may be determined. For convenience $\bar{E}^2_{BI}$ will be taken to be zero at the surface of the liquid for H_2.

In keeping with the reference[116] stating van der Waals a-values in units of l^2 atm mol^{-2} the values of a^{BI} will be calculated and stated in these units also. Rewriting equation 7.3 therefore, leads to:

$$a^{BI} \ (l^2 \text{ atm mol}^{-2}) = 2.972 \times 10^{} \ \alpha_B \ \bar{E}^2_{BI} \ V_m \qquad 7.4$$

with α_B in cm^3 $bond^{-1}$, $\bar{E}^2_{BI}$ in cgs esu, V_m in cm^3 mol^{-1}. A complete table is presented (table 7.1) with a^{CRIT}, a^{ONS}, a^{RF}, a^{BI} and a^{CALC} (= $a^{RF} + a^{BI}$) set out. Whilst fundamental data

TABLE 7.1 VAN DER WAALS a-VALUES - II

Approx. $(2\beta - \xi)^2$	SPECIES	$a^{ONS}/l^2atmmol^{-2}$	$a^{RF}/l^2atmmol^{-2}$	$a^{BI}/l^2atmmol^{-2}$	$a^{CALC}/l^2atmmol$	$a^{CRIT}/l^2atmmol$ [116]
-	Ar	0.26	0.77	-	0.77	1.345
-	Kr	0.41	1.23	-	1.23	2.3
-	Xe	1.33	3.99	-	3.99	4.194
0.09(G)	CH_4	0.95	2.56	0.37	2.93	2.253
0.23(G)	CMe_4	2.72	8.16	3.95	12.11	16.49
0.27(G)	$SiMe_4$	3.35	10.05	5.20	15.25	18.07
0.25*	C_6H_{12}	5.01	15.03	3.75	18.78	22.81
0.19 (E, Ave.)	1, 3, 5 $(CH_3)_3$-C_6H_3	8.95	26.95	3.65	30.60	34.39
0.47 (E)	C_6H_6	5.88	17.64	5.78	23.42	18
0.06*	C_2H_2	0.86	2.58	0.36	2.94	4.39
0.14 (E)	C_2H_4	2.47	7.42	0.77	8.19	4.472

cont'd....

0.03 (E)	C_2H_6	2.64	7.92	0.15	8.07	5.489
-	H_2	0.02	0.05	-	0.05	0.244
0.09 (G) (Q_F = 2.1)	SiF_4	0.40	1.21	1.03	2.24	4.195
0.09 (G) (Q_{Cl} = 6.5)	CCl_4	6.56	20.57	2.78	23.35	20.39

(G) - Geometrically derived

(E) - Experimentally derived

* - taken to be like a group IVB tetramethyl.

∓ - estimated on a crude geometrical basis.

are given elsewhere in this thesis (table 4.6) bond polarizibilities[119] are taken to be;

$$\alpha_B\ (C\text{-}H) = 0.65 \times 10^{-24}\ cm^3$$

$$\alpha_B\ (C\text{-}Cl) = 2.63 \times 10^{-24}\ cm^3$$

$$\alpha_B\ (Si\text{-}F) = 0.83 \times 10^{-24}\ cm^3$$

and $(2\beta_T - \xi_T)^2$ is either calculated geometrically as explained in section 5:3 or derived from nmr experimental data presented in previous sections of this thesis. It can be seen from fig. 7.1 that, despite the approximate nature of the calculations, the agreement between the classically based and presently calculated total values for a is quite satisfactory and appears to be significant; the correlation reveals the expected slope of unity with a zero intercept.

The foregoing justification of the theoretical interpretations proposed in this thesis from a non-nmr point of view provides the stimulus for following a more extensive use and assessment of the theory. To this end, the work on heats of vaporization initiated in chapter 4 will be extended.

7:2 Heats of Vaporization

In section 4:7c the heat of vaporization was determined for various liquids using a reaction field relationship of the form

$$\Delta H^{VAP} = \alpha \angle \langle R^2_{SUR} \rangle /2 + LkT \qquad 7.5$$

It is contended that there is a "buffetting" contribution to the heat of vaporization when treated on an electric field basis, in much the same way as with the van der Waals a-value. Equation 7.5 may be completed by including the "buffetting" field contribution to the energy. It is proposed that ΔH^{VAP} can be fully described through the following equation:

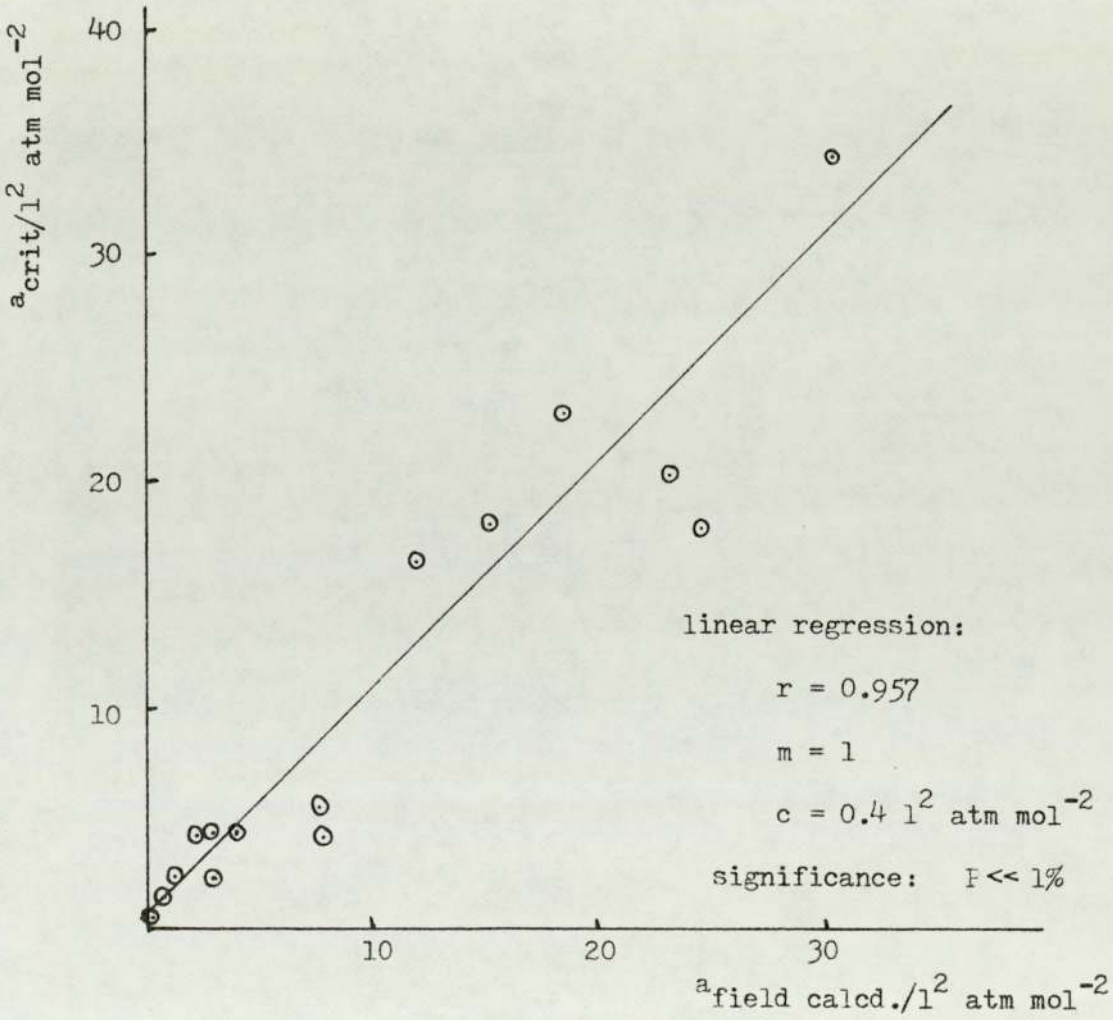

Fig. 7.1. Relationship between critical and field calculated Van der Waals a-values.

$$\Delta H^{VAP} = \alpha L \langle R_{SUR}^2 \rangle / 2 + \alpha_B L \bar{E}_{BI}^2 + LkT \qquad 7.6$$

It can be seen from table 7.2 and fig. 7.2, along with the statistical analyses, that the relationship between the literature[116] and calculated heats of vaporization is significant with a good correlation. By no means is the relationship perfect but it must be remembered that no account has been taken of the effect of temperature on the electric fields concerned whereas the ΔH^{VAP} literature values are quoted over a temperature range. The most dissatisfying aspect of this work is the significant size of the intercept, but this may be due to the assumptions made in section 4:7c concerning the equivalence of the interaction potential and the negative energy of vaporization. It has been argued[73] that the interaction potential is a free energy function whereas the energy of vaporization is an energy function in the thermodynamic sense. Nevertheless, the versatility of "buffetting" and reaction field theory away from nmr chemical shifts has once again been demonstrated.

7:3 An Investigation of Some Vibrational and Electronic Spectral Line Intensities

It may be expected that a solvent will perturb the energy levels of a solute molecule in solution relative to when it is in the gas phase at low pressure. Evidently, this can affect the vibrational and electronic spectrum of the solute molecule in the same way that the nmr spectrum is changed in going from the gas phase to the liquid phase. The solvent effect in vibrational and electronic spectroscopy may manifest itself as frequency shifts, line width changes and line intensity changes. Because of the abundance of data, the relatively simpler theoretical background and the size of the effect[139] it is proposed to investigate, from a semi-quantitative point of view, line intensity changes

TABLE 7.2 HEATS OF VAPORIZATION - II

SPECIES	ΔH^{VAP}_{EXP} (kJ mol^{-1})[116]	ΔH_{RF} -LkT (kJ mol^{-1})	ΔH^{*}_{BI} (kJ mol^{-1})	ΔH^{VAP}_{CALC} (Ave.)* (kJ mol^{-1})
Ne	2.047	0.11	-	0.36
Ar	7.273	2.85	-	3.70
Kr	10.283	3.30	-	4.47
Xe	15.843	8.79	-	9.91
CH_4	8.898	9.95	1.26	12.27
CMe_4	23.611	6.84	3.21	12.53
$SiMe_4$	26.916	7.53	3.78	13.97
$SnMe_4$	33.013	13.57	4.12	20.07
$PbMe_4$	36.967	24.35	4.19	31.15
C_6H_{12}	32.733	14.48	3.50	21.13
C_6H_6	34.052	20.75	6.56	30.63
CCl_4	31.888	22.17	2.14	27.52
C_2H_2	19.503	6.36	0.87	9.47
C_2H_4	14.436	19.37	1.95	22.93
C_2H_6	15.631	19.24	0.35	21.30
1, 3, 5-$(CH_3)_3C_6H_5$	43.960	20.28	2.65	26.13
SiF_4	22.113	2.02	1.83	5.43
H_2	1.048	0.16	-	0.33

* - $(2\beta - \xi)^2$ as in table 7.1

ǂ - ΔH^{VAP}_{CALC} (Ave) from equation 7.6 with LkT taken as the average over the temperature range quoted with ΔH^{VAP}_{EXP} in ref. 116.

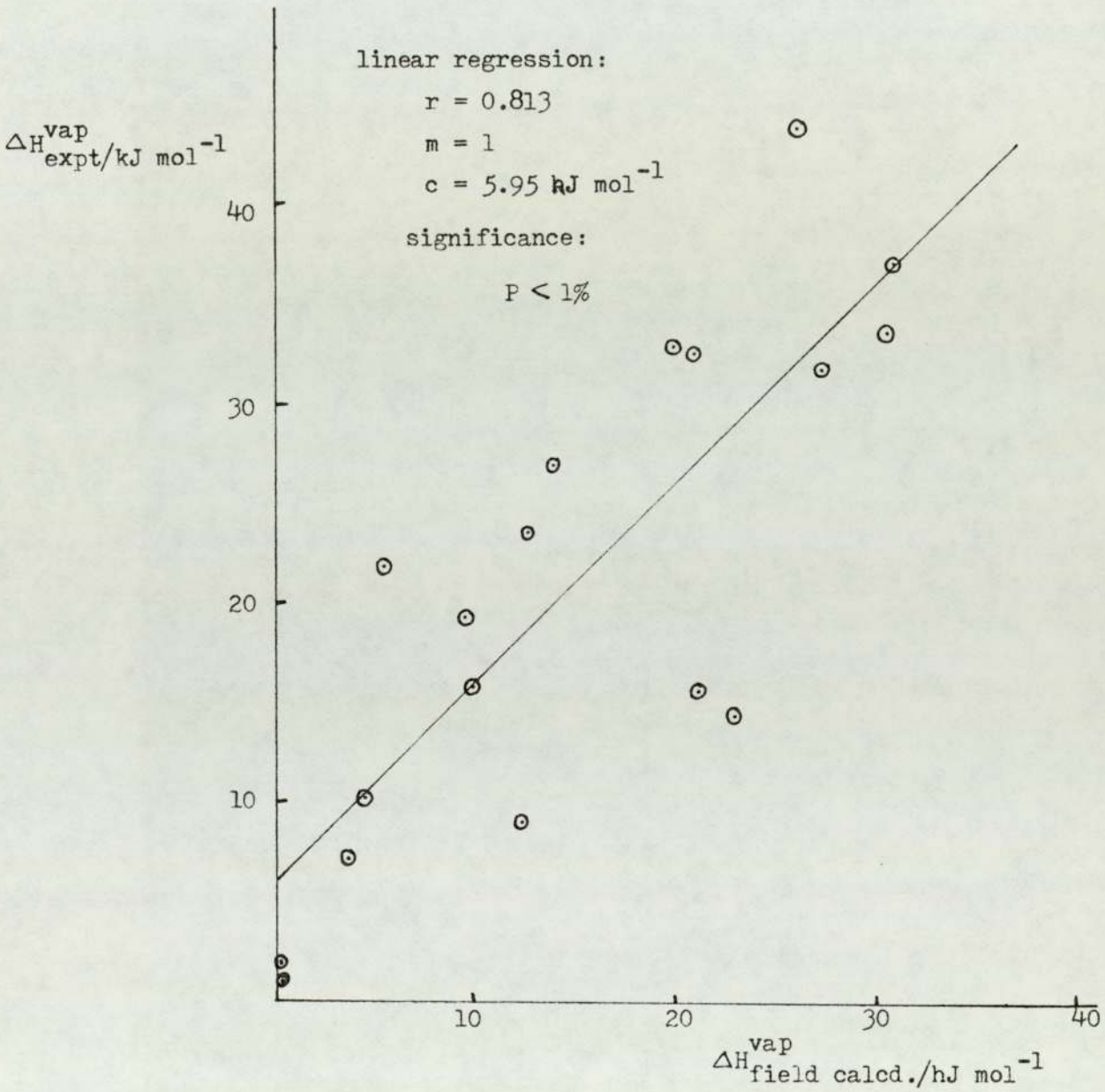

Fig. 7.2. Relationship between experimental and field calculated heats of vaporization.

in the spectrum of a molecule in going from the gas phase to the liquid phase.

7:3a Basic Theory

In the case of vibrational and electronic spectroscopy the spectrum is produced as a consequence of electric dipole moment changes caused by the external electric field of the electromagnetic irradiation. It is therefore necessary to imagine that there is an external electric field operative when considering the reaction field. No such field was necessary from the nmr viewpoint.

Following the work of Onsager[68], the cavity electric field may be written as

$$\bar{F} = \bar{G} + \bar{R} \qquad 7.7$$

where the internal field $\vec{G}$ is given by

$$\bar{G} = \frac{3\epsilon_2}{(2\epsilon_2 + 1)} \bar{E} \qquad 7.8$$

and the reaction field $\bar{R}$ is given by

$$\bar{R} = g\bar{\mu} + \alpha g \bar{F} \qquad 7.9$$

Because the time taken for an electric dipole transition is short compared with the time taken for $\bar{\mu}$ to cause molecular reorientations, $\bar{R}$ may be rewritten[68, 140, 141] from equation 7.9 as

$$\bar{R} = \frac{2(\epsilon_2 - 1)}{(2\epsilon_2 + 1)} \quad \frac{(n^2 - 1)}{(n_1^2 + 2)} \vec{F} \qquad 7.10$$

where the explicit expressions for g and α/a^3 are used in terms of dielectric sonstants and refractive indices. From equations 7.8 and 7.10 $\bar{F}$ may be written

$$F = \frac{\epsilon_2 (n_1^2 + 2)}{(2\epsilon_2 + n_1^2)} \bar{E} \qquad 7.11$$

and thence

$$F^2/E^2 = n_2^4 (n_1^2 + 2)^2 / (2n_2^2 + n_1^2)^2 \qquad 7.12$$

where ϵ_2 is replaced by n_2^2. Extending the idea of reaction field 'overspills' from neighbouring solvent molecules into the solute cavity (chapter 4) it is proposed that the overall ratio of the square fields, F^2/E^2, may be given by

$$F^2/E^2 = n_2^4 (n_1^2 + 2)^2/(2n_2^2 + n_1^2)^2 + f((n_2^2 + 2)/3)^2 \qquad 7.13$$

for a dilute solution, or for a pure liquid

$$F^2/E^2 \simeq 3((n^2 + 2)/3)^2 \qquad 7.14$$

This is in keeping with previous expressions[140, 141] for F^2/E^2 for a pure liquid whose values are about three times less that of equation 7.14. The change in spectral intensity for a molecule in the liquid phase relative to the gas phase is given[140] by the ratio F^2/E_o^2, where E_o is the applied electric field in vacuo. If A_l is the line intensity in the liquid phase and A_g the line intensity in the gas phase at low pressure then the ratio of these is given by

$$A_l/A_g = F^2/E_o^2 \qquad 7.15$$

As[140] $E_o^2 = n_2 E^2$, for a dilute solution

$$A_l/A_g = n_2^3 (n_1^2 + 2)^2/(2n_2^2 + n_1^2)^2 + f((n_2^2 + 2)/3)^2 \qquad 7.16$$

and for a pure liquid

$$A_l/A_g \simeq 3((n^2 + 2)/3)^2/n \qquad 7.17$$

Before examining the validity of equations 7.16 and 7.17, some gas phase data for methane in foreign gases at different pressures[142] will be considered. It can be seen from figure 7.3 that there is an excellent linear relationship between the ratio A_M/A_p (ratio of the line intensity in the mixture (M) to the pure gas (p) and the gas density (ρ), or, more precisely, ρ/M. It appears that a reaction field equation, such as equation 7.16, can not be used in this case, even when the density is relatively high. The linearity suggests that the interactions of importance

TABLE 7.3 SOME GAS PHASE VALUES OF $(A\rho_1/A\rho_2)$ FOR METHANE AT VARIOUS PRESSURES IN He, Ar AND N_2 [142]

a) ν_3 - BAND OF CH_4 IN He

ρ/M	Am/Ap
1	1.000
100	1.015
200	1.029
300	1.044
400	1.059

b) ν_3 - BAND OF CH_4 IN Ar

ρ/M	Am/Ap
1	1.000
100	1.040
200	1.081
300	1.120
400	1.160

c) ν_3 - BAND OF CH_4 IN N_2

ρ/M	Am/Ap
1	1.000
100	1.054
200	1.107
300	1.162
400	1.216

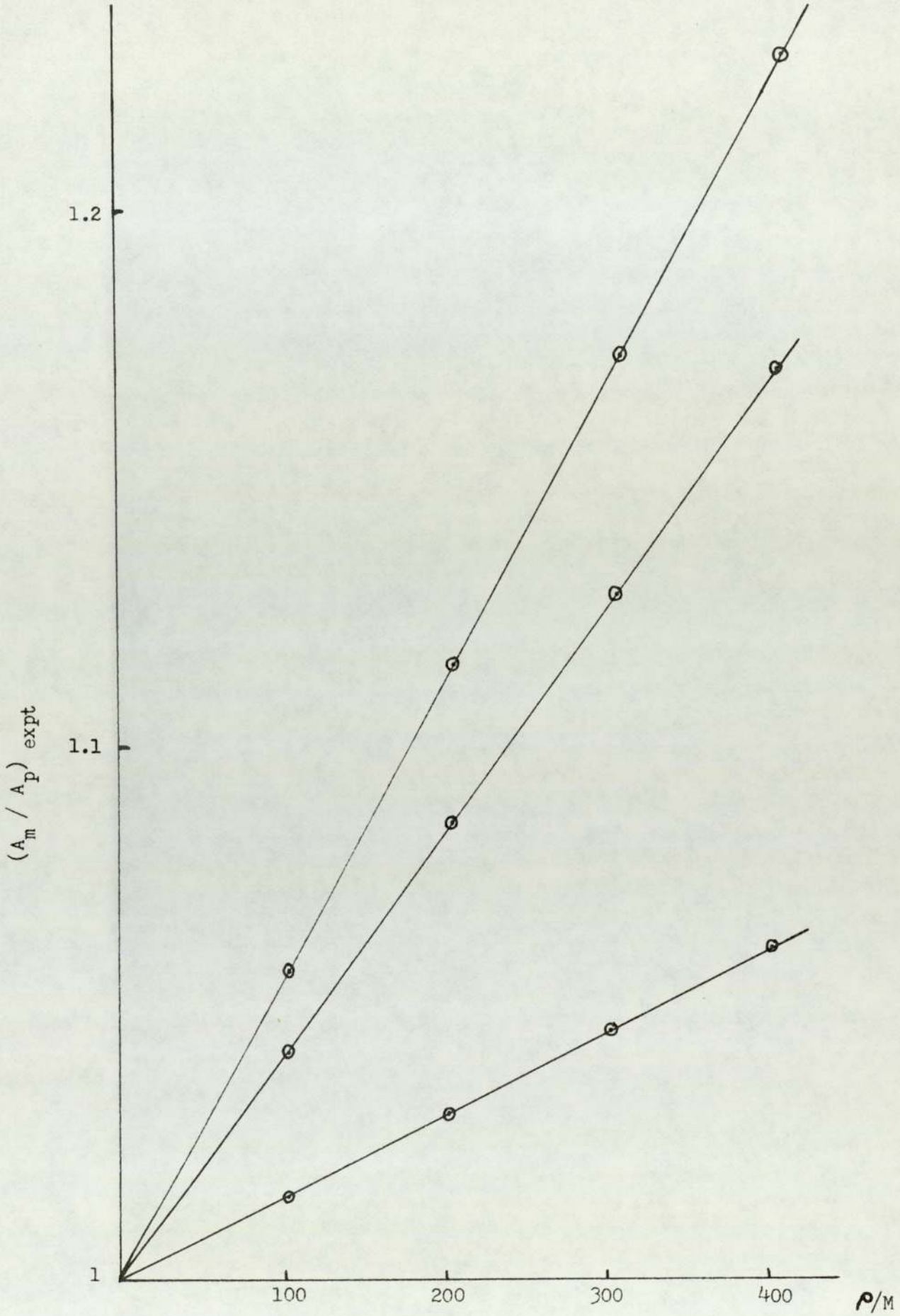

Fig. 7.3. Relationship between $(A_m/A_p)_{expt}$ and ρ/M for the ν_3-band of methane.

are due to simple encounters, not attributable therefore to reaction fields. Furthermore, it may be postulated that the A_m/A_p measurements can be characterized in terms of a molecular interaction that has some analogy with the buffetting concept (chapter 5). The fact that the gradients of the lines (fig. 7.3) are different indicates that the interaction depends on the perturbing solvent and the ratio of the gradients may be in the ratio of the Hartree-Fock scaling factors, Q^X, (section 5.5) for He, Ar and N_2. The ratio of the gradients is found to be He:Ar:N_2 1:2.7:3.7. Nevertheless it would be difficult to interpret this ratio quantitatively.

The gas-to-solution intensity changes for n-hexane[142] (3μ-band) were reported to be well accounted for using the traditional formula for a pure liquid. However this may be fortuitous because if the traditional or extended formula (equation 7.16) for a dilute solution is used the calculated values of (A_I/Ag) are not in so good agreement with experiment (Table 7.4a). There is evidently something missing from the field equation leading to A_I/Ag (equation 7.15). If it can be imagined that an extra square field term is added to F^2 (equation 7.13) of the order $6E^2$, a good agreement is found between calculated and experimental (Al/Ag)'s (Table 7.5). From previous nmr experience it is evident that the distance modulated Hartree-Fock factor (section 5.5) for fluorine is not too different to that of chlorine and will probably be not too different to that of sulphur. So, to a first approximation, it is assumed that the "buffetting" effect of the solvents CS_2, CCl_4 and CnFm is the same.

From the gas-to-pure liquid intensity change of cyclohexane[143]

TABLE 7.4 SOME VALUES OF A_I/Ag FOR CERTAIN SYSTEMS

a. VIBRATIONAL 3 μ-BAND OF n-HEXANE (n = 1.375)[142]

n	SOLVENT	(A_I/Ag) rel. EXPTAL.	CALC. R/F (TRADITIONAL)	CALC. R/F (EXTENDED)
1.630	CS_2	1	1	1
1.463	CCl_4	0.91	0.98	0.75
1.329	CnFm	0.82	0.96	0.60

b. VIBRATIONAL 9.85 μ-BAND OF CYCLOHEXANONE AT DIFFERENT TEMPERATURES[143]

T/°C	n	(A_I/Ag) rel. EXPTAL.	CALC. R/F (TRADITIONAL AND EXTENDED)
35	1.445	1	1
65	1.430	0.96	0.99
90	1.420	0.87	0.98
125	1.405	0.77	0.97

cont'd....

c. VIBRATIONAL 852cm^{-1}/1394cm^{-1} - BANDS OF BENZENE AT DIFFERENT TEMPERATURES[143]

T/°C	n	(A^1_T/A^1_{90}) rel. EXPTAL. 852 cm^{-1}	EXPTAL. 1394 cm^{-1}	CALC. R/F (TRADITIONAL AND EXTENDED)
26	1.498	1	1	1
77	1.450	0.96	0.94	0.96
141	1.391	0.90	0.91	0.93
(90	1.439	-	-	-)

d. ELECTRONIC BANDS FOR THE SOLUTIONS SHOWN[144, 145]

SOLUTE	SOLVENT	n_1	n_2	(A1/Ag) rel. EXPTAL.	CALC. R/F (TRAD.)	CALC. R/F (EXT.)
CYCLOPENTADIENE	n-HEXANE	1.464	1.375	0.80	0.98	0.95
CYCLOHEXADIENE	n-HEXANE	1.475	1.375	1	1	1
ISOPRENE	n-HEPTANE	1.422	1.388	0.99	0.99	0.99
CIS-PIPERYLENE	n-HEPTANE	1.430	1.388	1	1	1
TRANS-PIPERYLENE	n-HEPTANE	1.430	1.388	0.68		

TABLE 7.5 A CONTINUATION OF THE RESULTS FROM TABLE 7.4

a. VIBRATIONAL 3 μ-BAND OF N-HEXANE[143]

SOLVENT	$(F^2 + 6E^2)/E_0^2$ (rel.) (eqn. 7.13 extd.)	(Al/Ag) EXPTAL
CS_2	1	1
CCl_4	0.89	0.91
CnFm	0.84	0.82

b. VIBRATIONAL 9.85 μ-BAND OF CYCLOHEXANONE AT VARIOUS TEMPERATURES[143]

T/oC	$(F^2 + qE^2)/E_0^2$ (rel.) (eqn. 7.14 extd.)	q/E^2	(Al/Ag) EXPTAL.
35	1	1.45	1
60	0.96	1.20	0.96
90	0.87	0.65	0.87
120	0.77	0	0.77

c. VIBRATIONAL 852 /1394 cm^{-1} - BANDS OF BENZENE AT VARIOUS TEMPERATURES[143]

T/oC	$(F^2 + qE^2)/F_{90}^2$ (rel.) (eqn. 7.14 extd.)		$(A_1^T / A_1^{90})_{EXPTAL}$	
	$q/E^2 = 0.1$	$q/E^2 = 0.2$	852 cm^{-1}	1394 cm^{-1}
26	1	1	1	1
77	0.95	0.94	0.96	0.94
141	0.91	0.90	0.90	0.91

at different temperature the calculated (A_1/Ag) values are not in agreement with the experimental (A_1/Ag) values (table 7.4b). Again it appears that there is something missing, although at first sight it may appear that there is something extra accounted for in the reaction field treatment. Since the measurements were taken at different temperatures, it may be imagined that the cavity size may increase with increase in temperature. Because "buffetting" originates with the polarization of solute peripheral atoms by R_2 (chapter 4), then the larger the cavity it may be expected that the "buffetting" probability will be smaller. It is therefore necessary to add a different amount to the reaction-field-type F (equation 7.14) for a pure liquid at different temperatures; less added at the higher temperatures. The results are illustrated in table 7.5b where it can be seen that by adding various amounts of E^2 to F^2 to account for "buffetting", excellent agreement can be demonstrated between experimental and calculated (A_1/Ag). It is interesting to note that nothing is added at 120°C implying an extremely large cavity or zero "buffetting". Because the boiling point of cyclohexamone is $\simeq$155°C it is possible that this has a significant effect on the situation.

Similar arguments apply to the gas-to-pure liquid measurements on benzene[143] where (A_1^T/A_1^{90}) -values are reported (table 7.5c). Following this idea an extra amount of field is added to the benzene value at 26°C only (boiling point of benzene $\sim$80°C). It is possible in the case of vibrational spectroscopy that the "buffetting" effect may be different for different vibrational modes.

With the extension to electronic spectroscopy[144, 145] it can be seen (table 7.4d) that the reaction-field type analyses (equation 7.13) by no means explains the experimental intensity

changes (more correctly oscillator strength changes). It may be expected that in electronic spectroscopy no simple reaction field type theory can account for this adequately. Certainly changes in molecular shape in electronic and vibrational spectroscopy would necessitate a different approach to the theoretical treatment of the molecular encounter or "buffetting" theory.

Perhaps the most interesting observation is with cis- and trans-piperylene where the reaction type field will probably be the same but the "buffetting" will be different. This is reflected in the experimental results shown in table 7.4d.

Whilst little has been deduced about the nature of the reaction and cavity field as presented in this section, or whether the traditional or extended approach is valid, it has been demonstrated that there is another effect operative, that is possibly of a steric nature. The results are by no means extensive or entirely conclusive, but the internal consistency of each set a data is a good indication that there may be an additional effect operative just as there appears to be in the nmr screening equation for σ_w.

7:4 Conclusions

Based on a theory using an extended reaction field continuum approach along with an essentially pairwise non-continuum "buffetting" interaction, that was designed to account for the van der Waals nuclear screening constant, several non-nmr parameters have been accounted for with a reasonable degree of precision. This was possible by an adaptation of the electric fields derived for use in the nuclear screening equation.

It has been possible to describe quantitatively the van der Waals a-values, as used in the van der Waals equation of state, and heats of vaporization of non-polar liquids. Although exact agreement between the values derived in this work and values

derived elsewhere was not apparent in every case there was a significant correlation between the values. Furthermore, it has been possible to analyse some non-nmr spectral line intensity changes in going from gas to liquid, albeit on a somewhat empirical basis. The general success of the entire approach regarding nmr and non-nmr problems that reflect van der Waals dispersion forces indicates that further and more complex problems may be open to explanation. A long standing problem that has eluded satisfactory interpretation is the mechanism of interaction of the lanthanide shift reagent with certain molecules and the way that it affects the chemical shift. It is possible that the application of the theory in this thesis may provide the answer. Also a method of quantifying steric effects with respect to reaction mechanisms and molecular conformations may be afforded by an extension or adaptation of the theory regarding molecular encounters. This would have fundamental implications in the field of polymer chemistry and biochemistry where an understanding of the intimacies of molecular interactions is of great importance. Thus there is scope for further work from a fundamental and applications point of view regarding the work in this thesis.

REFERENCES

1. W. Pauli, Naturwiss, 12, 741 (1924)
2. O. Stern, Z. Phys., 7, 249 (1921)
3. I. I. Rabi, S. Hillman, P. Kusch and J. R. Zacharias, Phys. Rev., 55, 526 (1939)
4. N. F. Ramsey, 'Molecular Beams', Oxford University Press (1956)
5. F. Bloch, W. W. Hansen and M. E. Packard, Phys. Rev., 69, 127 (1946)
6. E. M. Purcell, H. C. Torrey and R. V. Pound, Phys. Rev., 69, 37 (1946)
7. J. A. Pople, W. G. Schneider and H. J. Bernstein, 'High Resolution Nuclear Magnetic Resonance Spectroscopy', McGraw-Hill Book Co., (1959)
8. J. W. Emsley, J. Feeney and L.H. Sutcliffe, 'High Resolution Nuclear Magnetic Resonance Spectroscopy - Vols. I and II, Pergamon Press, (1965)
9. C. P. Slichter, 'Principles of Magnetic Resonance' 2nd Edition, Springer-Verlag, (1978)
10. A Einstein, Physik. Z, 18, 121 (1917)
11. E. M. Purcell, Phys. Rev., 69 681 (1946)
12. W. A. Anderson, Phys. Rev., 104, 850 (1956)
13. J. I. Kaplan and S. Meiboom, Phys. Rev., 106, 499 (1957)
14. F. Bloch, Phys. Rev., 70, 460 (1946)
15. F. Bloch, Phys. Rev., 102, 104 (1956)
16. R. K. Wagsness and F. Bloch, Phys. Rev., 89, 728 (1953)
17. G.V.D. Tiers, J. Phys. Chem., 65, 1916 (1961)
18. W. D. Knight, Phys. Rev., 76, 1259 (1949)
19. W. G. Proctor and F. C. Yu, Phys. Rev., 77, 717 (1950)
20. W. C. Dickinson, Phys. Rev., 77, 736 (1950)
21. G.V.D. Tiers, J. Phys. Chem., 62, 1151 (1958)
22. G. Filipovich and G.V.D. Tiers, J. Phys. Chem., 63, 761 (1959)
23. A. C. Chapman, J. Homer, D. J. Mowthorpe and R. T. Jones, J.C.S. Chem. Communs, 121 (1965)
24. C. P. Nash and G. E. Maciel, J. Phys. Chem., 68, 832 (1964)
25. G.V.D. Tiers, J. Phys. Chem., 63,1379 (1959)

26. J. Homer, Tetrahedron, 23, 4065 (1967)

27. P. Laszlo, A. Speert, R. Ottinger and J. Reisse, J. Chem. Phys., 48, 1732 (1968)

28. S. Gordon and B.P. Dailey, J. Chem. Phys., 34, 1084 (1961)

29. W. T. Raynes, A. D. Buckingham and H. J. Bernstein, J. Chem. Phys., 36, 3481 (1962)

30. L. Petrakis and H. J. Bernstein, J. Chem. Phys., 37, 273 (1962)

31. L. Petrakis and H. J. Bernstein, J. Chem. Phys., 38, 1562 (1965)

32. S. Mohanty and H. J. Bernstein, J. Chem. Phys., 54, 2254 (1971)

33. A. Saika and C. P. Slichter, J. Chem. Phys., 22, 26 (1954)

34. N. F. Ramsey, Phys. Rev., 77, 567 (1950); 78, 699 (1950); 83, 540 (1951); 86, 243 (1952)

35. A. D. Buckingham, T. Schaefer and W. G. Schneider, J. Chem. Phys., 32, 1227 (1960)

36. J. Homer, Appld. Spectroscopy Revs., 45, 1 (1975)

37. W. C. Dickinson, Phys. Rev., 81, 717 (1951)

38. C. Lussan, J. Chim. Phys., 61, 462 (1964)

39. J. R. Zimmerman and M. R. Foster, J. Phys. Chem., 61, 282 (1957)

40. P. Laszlo, Progress in N.M.R. Spectroscopy, 3, 241 (1967)

41. D. J. Frost and G. E. Hall, Mol-Phys., 10, 191 (1966)

42. H. H. Landolt and R. Bornstein, Zahlenwerte und Funktionen, Band II, Teil 10 Springer-Verlag (1966)

43. J. Homer, M. H. Everdell, E. J. Hartland and C. J. Jackson, J.C.S., A, 1111 (1970)

44. J. K. Beconsall, Mol-Phys. 15, 129 (1968)

45. J. K. Beconsall, G. D. Davies and W. R. Anderson, J. Amer. Chem. Soc., 92, 430 (1970)

46. W. G. Proctor and F. C. Yu, Phys. Rev., 81, 20 (1951)

47. H. S. Gutowsky and D. W. McCall, Phys. Rev., 82, 748 (1951)

48. W. T. Dixon, 'Theory and Interpretation of Magnetic Resonance Spectra', Plenum Press (1972)

49. E. R. Andrew, 'Nuclear Magnetic Resonance', Cambridge University Press (1953)

50. J. J. Arnold, Phys. Rev., 122, 136 (1956)

51. W. McFarlane and R.F.M. White, 'Techniques of High Resolution Nuclear Magnetic Resonance Spectroscopy', Butterworths (1973)

52. E. L. Hahn, Phys. Rev., 80, 580 (1950)

53. H. Y. Carr and E. M. Purcell, Phys. Rev., 94, 630 (1954)

54. R. R. Ernst and W. A. Anderson, Rev. Sci. Instruments, 37, 93 (1966)

55. T. C. Farrar, Analytical Chemistry 42A, 109 (1970)

56. J. K. Beconsall and M.C. McIvor, Chem. in Britain, 5, 147 (1969)

57. A. L. Bloom and M. E. Packard, Science, 122, 738 (1955)

58. B. A. Evans and R. E. Richards, J. Sci. Instruments, 37, 353 (1960)

59. A. P. McCann, F. Smith, J.A.S. Smith and J. D. Thwaites, J. Sci. Instruments, 39, 349 (1962)

60. H. Prinnas and H. H. Gunthard, Rev. Sci. Instruments, 28, 510 (1957)

61. M. E. Packard, Rev. Sci. Instruments, 19, 435 (1948)

62. E. B. Baker and L. W. Bard, Rev. Sci. Instruments, 28, 313 (1957)

63. Varian Associates HAIOOD Model N.M.R. Spectrometer Handbook.

64. A. R. Dudley, Ph. D. Thesis, University of Aston in Birmingham (1975)

65. A. Coupland, Ph. D. Thesis, University of Aston in Birmingham (1978)

66. Perkin-Elmer R12B Model N.M.R. Spectrometer and Double Resonance Accessory Handbooks.

67. F.H.A. Rummens, W. T. Raynes and H. J. Bernstein, J. Phys. Chem., 72, 2111 (1968)

68. L. Onsager, J. Amer. Chem. Soc., 58, 1068 (1936)

69. C.J.F. Böttcher, 'Theory of Electric Polarization: Vol. I - Dielectrics in Static Fields', 2nd Edition, (revised by O.C. Van Belle, P. Bordewijk and A. Rip.), Elsevier Scientific Publishing Co., (1973); H. Frölich, 'Theory of Dielectrics', Oxford University Press (1958)

70. R. Eisenshitz and F. London, Z. Phys., 60, 491 (1930); F. London, Z. Phys., 63, 245 (1930)

71. F. London, Trans. Faraday Soc., 33, 8 (1937)

72. B. B. Howard, B. Linder and M. T. Emerson, J. Chem. Phys., 36, 485 (1962)

73. B. Linder, J. Chem. Phys., 33, 668 (1960); 35, 371 (1961)

74. N. Lumbroso, T. K. Wu and B.P. Dailey, J. Phys. Chem., 67, 2469 (1963)

75. B. Fontaine, M-T. Chenon and N. Lumbroso-Bader, J. Chim. Phys. 62, 1075 (1965)

76. Ph. deMontgolfier, C. R. Acad. Sci. Paris, 263C, 505 (1966)

77. Ph. deMontgolfier, J. Chim. Phys., 64, 639 (1967)

78. Ph. deMontgolfier, J. Chim. Phys., 65, 1618 (1968)

79. Ph. deMontgolfier, J. Chim. Phys., 66, 685 (1969)

80. F.H.A. Rummens, Chem. Phys. Lett., 31, 596 (1975)

81. F.H.A. Rummens, J. Chim. Phys., 72 448 (1975)

82. F.H.A. Rummens, N.M.R. Principles and Progress, 10, (1975)

83. F.H.A. Rummens, Can. J. Chem., 54, 254 (1976)

84. R. P. Bell, Trans. Faraday Soc., 27, 797 (1931)

85. F.H.A. Rummens and H. J. Bernstein, J. Chem. Phys., 43, 2971 (1965)

86. F.H.A. Rummens, Mol. Phys., 19, 423 (1970)

87. H. B. Dwight, 'Tables of Integrals and Other Mathematical Data', Macmillan and Co. Ltd. (1969)

88. M. I. Foreman, N.M.R. Specialist Periodical Reports (C.S.) 6, 233 (1975)

89. J. G. Kirkwood, J. Chem. Phys., 7, 911 (1939)

90. A. Prock and G. McConkey, 'Topics in Chemical Physics', Elsevier Scientific Publishing Co., (1962)

91. Proceedings of the International Congress of Quantum Chemistry, 1st, Menton (France), 1973: 'The World of Quantum Chemistry', (editors R. Daudel and B. Pullman), Reidel (1974)

92. M. A. Raza and W. T. Raynes, Mol. Phys., 19, 199 (1970)

93. M. R. Bacon and G. B. Maciel, J. Amer. Chem. Soc., 95, 2413 (1973)

94. A. D. Buckingham,. J. Chem. Phys., 38, 300 (1960)

95. N. Lumbroso-Bader, M.-T. Chenon and J. Bouquant, J. Chim. Phys., 67, 1829 (1970)

96. P. Laszlo and J. I. Musher, J. Chem. Phys., 41, 3906 (1964)

97. C. A. Coulson, Proc. Roy. Soc., 225A, 69 (1960)

98. A. R. Martin, Phil. Mag. (7th), 8, 547 (1929)

99. A. J. Dekker, Physica, 12, 209 (1946)

100. T. G. Scholte, Physica, 15, 437 (1949)

101. C.J.F. Böttcher, Physica, 5, 635 (1938)

102. B. Linder, Adv. Chem. Phys., 12, 225 (1967)

103. W. B. Bonner, Trans. Faraday Soc., 47, 1143 (1951)

104. M. Born, 'Atomic Physics', 8th Edition, Blackie (1969)

105. H. C. Longuet-Higgins, J. Chim. Phys., 61, 13 (1964)

106. W. T. Raynes, J. Chem. Phys., 51, 3138 (1969)

107. J. C. Slater, Phys. Rev., 36, 57 (1930)

108. J. H. Van Vleck, 'Electric and Magnetic Susceptibilities' Oxford University Press (1932)

109. J. G. Kirkwood, Physik Z., 33, 57 (1932)

110. K. Pitzer, Adv. Chem. Phys., 2, 57 (1959)

111. R. Langley, 'Practical Statistics', Pan Books Ltd. (1970)

112. T. W. Marshall and J. A. Pople, Mol. Phys., 1, 199 (1958)

113. A. A. Bothner-By, J. Mol. Spectroscopy, 5, 52 (1960)

114. S. Glasstone, 'Textbook of Physical Chemistry', Macmillan and Co. Ltd. (1951)

115. D. L. Goodstein, 'States of Matter', Prentice-Hall Inc. (1975)

116. 'Handbook of Chemistry and Physics', 53rd Edition. (edited by R.Weast), Chemical Rubber Co. Ltd. (1972/3)

117. J. H. Hildebrand and R. C. Scott, 'The Solubility of Non-Electrolytes', 3rd Edition, Dover, New York (1964)

118. J. C. Slater, 'Introduction to Chemical Physics', McGraw-Hill Publishing Ltd. (1939)

119. C. G. LeFèvre and R.J.W. LeFèvre, Revs. of Pure and Applied Chem., 5, 261 (1955)

120. W. T. Raynes and M. A. Raze, Mol. Phys., 20, 555 (1971)

121. W. T. Raynes and M. A. Raza, Mol. Phys., 17, 157 (1969)

122. R. R. Yadava, Ph. D. Thesis, University of Aston in Birmingham (1972)

123. N. J. Trappeniers and J. G. Oldenziel, Physica, 824, 581 (1976)

124. G. Barrow, 'Physical Chemistry', McGraw-Hill Kogakushu Ltd. (1973)

125. J. I. Musher, J. Chem. Phys., 41, 2671 (1964)

126. T. Yonemoto, Can. J. Chem., 44, 223 (1966)

127. D. Williams and I. Fleming, 'Spectroscopic Methods in Organic Chemistry', McGraw-Hill Publishing Ltd. (1973)

128. A. J. Sadlej and W. T. Raynes, Mol. Phys., 35, 101 (1978)

129. E. Dayan and G. Widenlocher, C. R. Acad. Sci. Paris, 263B, 1346 (1966)

130. J. Homer and D. L. Redhead, J.C.S. Faraday II, 68, 1049 (1972)

131. F. A. Cotton, 'Chemical Applications of Group Theory', Interscience (1970)

132. R. J. Abraham, D. F. Wileman and C. R. Bedford, J.C.S. Perkin II, 1027 (1973)

133. P. Diehl and R. Freeman, Mol. Phys., 4, 39 (1961)

134. I. G. Ross and R. A. Sack, Proc. Roy. Soc. London, 63B, 893 (1950)

135. P. Laszlo, Bull. Soc. Chim. (France), 85 (1964)

136. J. I. Musher, J. Chem. Phys. 37, 34 (1962)

137. R. P. Gupta, J. S. Pizey and K. Symeonides, Tetrahedron, 32, 1917 (1976)

138. J. S. Pizey and K. Symeonides, Phosphorus and Sulphur, 1 , 41 (1976)

139. L. A. Gribov, 'Intensity Theory for Infrared Spectra of Polyatomic Molecules', C.B.E. Inc. (1964)

140. S. R. Polo and M. K. Wilson, J. Chem. Phys., 23, 2376 (1955)

141. R. Mecke, Disc. Faraday Soc. 9, 161 (1950)

142. J. H. Jaffe and S. Kimel, J. Chem. Phys., 25, 374 (1956)

143. W. B. Person, J. Chem. Phys., 28, 319 (1958)

144. L. W. Picket, E. Paddock and E. Sackter, J. Amer. Chem. Soc., 63, 1073 (1941)

145. J. R. Platt, J. Chem. Phys., 16, 1137 (1948)